Cultural Heritage and Modern Technologies **2023**, no.1, 1-68

Cultural Heritage & Modern Technologies

www.aaatec.org ***ISSN** 2837-0759*

DOI: 10.24412/2837-0759-2023-1168
UDC: 904:621

Reconstructing the Antikythera Mechanism lost eclipse events applying the Draconic gearing - the impact of gear error

Aristeidis Voulgaris[1], Christophoros Mouratidis[2], Andreas Vossinakis[3]

Abstract

We present new observations concerning the procedure for the reconstruction of the lost eclipse events engraved in the Saros spiral cells of the Antikythera Mechanism. For the reconstructed eclipse events we applied the necessary, albeit missing, Draconic gearing of the Antikythera Mechanism [using the Fragment D(raconic) – gear r1], which was probably a part of the Mechanism's gearing, representing the fourth lunar motion, the Draconic cycle. The Draconic gearing is very critical for the eclipse prediction and defines whether an eclipse will occur. For our research we created a program which presents the phase of the four lunar cycles - including the position of the Draconic pointer relative to the ecliptic limits. After calibrating the program according to the preserved eclipse events, the lost eclipse events of the Saros spiral were calculated and discussed. The procedure for the calculation of the events' times by using solely the Mechanism based on the pin&slot configuration, is also presented. The eccentricity error of a gear which is preserved on the ancient prototype is analyzed. An experimental setup facilitated the analysis of the mechanical errors of the gears and the study of the motion transmission between gears with triangular teeth. The experimental study of the gears errors revealed the strong impact the Antikythera Mechanism pointers' position has on the results.

Keywords: Antikythera Mechanism Saros spiral, Draconic gearing, Nodes, Ecliptic limits, gear errors, gear eccentricity, eclipse events.

Introduction

The Antikythera Mechanism was a unique geared device of the Hellenistic era and was constructed in order to make calculations/predictions of astronomical events of the near future based on the time measuring. These mechanical calculations were made by a large number of engaged gears. The results were presented by a number of pointers, which rotated on their measurement scales. The results were read by the user, who just had to observe the relative position of each pointer rotating on its corresponding measuring scale which also had subdivisions.

[1] City of Thessaloniki, Directorate Culture and Tourism, Thessaloniki, GR-54625, Greece;
e-mail: arisvoulgaris@gmail.com (corresponding author)
[2] Merchant Marine Academy of Syros, GR-84100, Greece
[3] Thessaloniki Astronomy Club, Thessaloniki, GR-54646, Greece

The Mechanism could predict the phases of the Moon, the position of the Sun on the ecliptic versus time, the starting date of the athletic Games and the astronomical events of solar and lunar eclipses (Freeth et al. 2006, 2008), which are still very important today (Pasachoff 2018). On the lower half of the Back plate of the Mechanism there was the Saros spiral in which the sequence of the eclipse events was engraved. Today the Saros spiral is preserved by about 30%, in 3 parts: Fragment A2, F and E.

The Saros spiral consisted by four full spiral turns, divided in 223 sectors/cells representing the 223 synodic months of a Saros period (Ptolemy in refers to this cycle as ΠΕΡΙΟΔΙΚΟΣ/Periodikos, ed. Heiberg 1898, p. 270; ed. Toomer 1984, p. 175; Voulgaris et al. 2021). After 223 synodic months, equal to 18^{y} 11^{d} 8^{h}, the eclipse events sequence is repeated in the same order, with a delay of 8 hours. After a Sar period (half Saros, Voulgaris et al. 2021), from a solar eclipse, a lunar eclipse occurs at the same Node, but in reversed distance from the Earth (Apogee/Perigee) (Fig. A.79-A.83). After three Saros periods, equal to 54^{y} 33^{d}, named Exeligmos, the eclipse events are visible from about the same observing place, at about the same time (Neugebauer 1975, p. 310). We say '*about*' rather than '*exactly*', because the equality in integer number of cycles is an approximation; actually 223 synodic months = 241.998703 draconic months = 238.99195 Anomalistic months for Era of 1 AD (see Appendix A to the text Section 11 (Fig. A.85-A.89)). This means that the repeated eclipse path per each Exeligmos changes through time, as the Node slightly shifts by about 0.46° (≈ one lunar diameter) per Saros cycle. After 3 Exeligmos cycles (starting with New Moon at a Node) the New Moon will be located about 4.3° far away from a Node, either to the North or to the South. The repeated *Saros* sequence finishes with a last partial solar eclipse (only visible from one of the Earth's poles) or a penumbral lunar eclipse. As the Earth and Moon perpetual rotate around the Sun and around each other, new Saros series begin starting from one of the poles with a partial eclipse. Note that the 181 Saros series presented by F. Espenak in NASA eclipse web page '*Index to catalog of Saros series of solar eclipses*' (https://eclipse.gsfc.nasa.gov/SEsaros/SEsaroscat.html) start with the Moon on the (Northern/Southern) ecliptic limit; on the contrary, the Antikythera Mechanism Saros eclipse events starting by the Moon just on the Node (Voulgaris et al. 2023a).

Object of Study

a) The eclipse events on the Antikythera Mechanism Saros spiral

The solar and lunar eclipse events sequence of the Antikythera Mechanism was presented on the Saros spiral. On some of the cells, information related to the eclipse events (whether it was solar or lunar and the time it occurred) was engraved. The letter H, ΗΛΙΟΣ (Helios-Sun) meant that a solar eclipse would occur, whereas the letter Σ, ΣΕΛΗΝΗ (Selene-Moon) meant that a lunar eclipse would occur (Anastasiou et al. 2016; Freeth et al. 2006, 2008). There are also preserved cells with both letters engraved, meaning a lunar and a solar eclipse will occur in this month.

Following the calibration of the Mechanism pointers, using the very important astronomical and religious date of 22/23 December 178BC as a starting point (Voulgaris et al. 2023a), additional astronomical information could be extracted, i.e. the position of the Moon and the Sun in the sky/Zodiac constellation and the corresponding day of the Egyptian calendar. Moreover, if a Lunar eclipse occurred on the constellation of Leo or Virgo, then by checking whether the Games pointer aims at the ΛΑ-ΟΛΥΜΠΙΑ (Olympiad) quadrant (Freeth et al. 2008) the user could be informed if the Olympiad would start during the Lunar eclipse (Mommsen (ed.) 1864;

Perrotet 2004; Robertson 2010; Vaughan 2002 https://www.onereed.com/articles/vvf/olympics.html).

b) Lunar cycles represented on the Antikythera Mechanism gearing trains

The ancient Greek astronomers of the Hellenistic era (the Babylonians and Egyptians too) studied the motions of the Moon and Sun by applying their periodicities equations resulting from a long time of observations. The sync of the three lunar cycles, Synodic, Draconic and Anomalistic, into a period that contains an integer number of each creates a composite cycle named Saros. This contains 223 Synodic months, 239 Anomalistic months and 242 Draconic months (also 241.029 Sidereal months).

From the currently preserved fragments of the Mechanism it is concluded that the Mechanism gearings represent three out the four known lunar cycles that were known and extensively used by the astronomers of the Hellenistic Era. The three preserved lunar cycles of the Mechanism - Sidereal, Synodic and Anomalistic - can be detected on the gearing of the Mechanism:

a) The Sidereal cycle, one rotation of the Moon relative to the 'fixed' stars, is represented as one full rotation of the Lunar disc-pointer around the Zodiac (constellation) month ring. For example, the lunar pointer starts at the zodiac Sign of Capricorn constellation and after one rotation aims again at the same zodiac Sign.

b) The Synodic cycle, the time it takes the Moon to return to the same lunar phase, is represented by re-alignment of the Lunar pointer with the Golden sphere-Sun pointer (Bitsakis & Jones 2016), i.e. from New Moon to the next New Moon. At the same time the little lunar sphere located on the Lunar disc of the Mechanism, presents the same phase (black hemisphere), Voulgaris et al. 2018b; Wright 2006. The Synodic cycle is the main measuring unit of the Mechanism. The units of the Saros (also Exeligmos), Metonic and Games scales are based on the Synodic month. The Antikythera Mechanism was a time machine calculator based on the Luni(solar) calendar, mostly using units of the lunar synodic month.

c) The Anomalistic cycle of the Moon presents the periodically variable angular velocity of the Moon as it travels in the sky. According to Geminus' description in *Introduction to the Phenomena*, chap. 18 *About Exeligmos*, the Moon crosses the zodiac sky in a variable angular velocity: initially it moves with its minimum angular velocity (i.e. the Moon located at Apogee) and through time increases its velocity. Afterwards, it gradually decreases its maximum angular velocity (the Moon located at Perigee) down to the initial smallest value. The Anomalistic cycle starts when the Moon is located at Apogee position (Voulgaris et al. 2023a).

The Anomalistic cycle is also represented on the Antikythera Mechanism gearing: the ancient manufacturer introduced the unique idea of the conversion of a constant angular velocity into a periodically variable angular velocity introducing the *pin&slot* gearing design:
Two gears in a common, but eccentric modified axis so that their centers do not coincide (Freeth et al. 2006; Voulgaris et al. 2018b, 2019a). This system of the two gears k1/k2 and their k-axis is on-board of the large gear e3. The variable angular velocity of this unique design system represents the Anomalistic lunar cycle of the Antikythera Mechanism.

The fourth lunar cycle, the Draconic cycle, also known as nodal or nodical month, is based on the periodic transits of the Moon through the Ecliptic. The name '*Draconic*' or '*Draconitic*' relates to the Dragon (ΔΡΑΚΩΝ in Greek) which eats the Sun or the Moon, as believed in the Middle Ages (see Kircher 1646, p. 410). The ancient Greek astronomers used the phrase ΑΠΟΚΑΤΑΣΤΑΣΙΣ ΚΑΤΑ (ΕΚΛΕΙΠΤΙΚΟΝ) ΠΛΑΤΟΣ (restitution in Ecliptic latitude) or, alternatively the phrase ΠΛΑΤΙΚΑΙ ΑΠΟΚΑΤΑΣΤΑΣΕΙΣ (Jones 1990). The lunar orbit crosses

periodically, the Ecliptic in two points, named ΑΝΑΒΙΒΑΖΩΝ ΣΥΝΔΕΣΜΟΣ/Ascending Node and ΚΑΤΑΒΙΒΑΖΩΝ ΣΥΝΔΕΣΜΟΣ/Descending Node. The Greek word ΕΚΛΕΙΠΤΙΚΗ (Ecliptic) derives from the word ΕΚΛΕΙΨΗ (Eclipse), which makes sense, since on this zone took place the solar and lunar eclipses. The Ecliptic is referred to in the Antikythera Mechanism inscription as ΕΓΛΕΙΠΤΙΚΗ (see Bitsakis & Jones 2016) and is represented with the Zodiac month dial ring (Voulgaris et al., 2018a).

The relation between the Synodic phase and the Draconic phase determines the occurrence of an eclipse: when a New Moon coincides with the beginning or the middle of the Draconic cycle, a solar eclipse will occur (Voulgaris et al. 2022). When a Full Moon coincides with the beginning or the middle of the Draconic cycle, a lunar eclipse will occur. This, very important lunar cycle, was known and used by the astronomers of the Hellenistic era.

Today, the important Draconic cycle/Draconic gearing is not represented on the Antikythera Mechanism or is not preserved. As the four lunar cycles were extensively used during the Hellenistic Astronomy, the assumption of the Draconic gearing on the AM is not far-fetched. In addition, by engaging the preserved Fragment D-gear r1 with the shaft of gear a1 (a1 gear is engaged to the b1 gear and the shaft of a1presents an unknown mechanical output) it could become part of the Draconic gearing of the AM (regarding the Input of the Mechanism see Voulgaris et al. 2022 p. 116). If the Antikythera Mechanism included the Draconic gearing, then the eclipse sequence information engraved on the Saros cells could be calculated without any additional external information and the eclipse events sequence would be an actual prediction by a pure mechanical procedure.

As the three gears (b1, a1, r1) out of four (s1 gear - hypothetical/lost) are preserved today, we believe that the Draconic gearing of the Mechanism was most probably included in the Mechanism as an important and crucial part, as it directly related to the eclipse prediction (Voulgaris et al. 2022).

In this work we consider the Draconic gearing as included in the Mechanism and its existence gives answers to a number of critical questions.

By applying the Draconic gearing we will show that the specific eclipse event sequence was a result of the Draconic gearing of the Mechanism and the eclipse sequence was calculated through a mechanical procedure, without any additional external information, as also the hour of the eclipse events occur.

We will also show that the omitted eclipses (Anastasiou et al. 2016; Carman & Evans 2014; Freeth 2014, 2019; Iversen & Jones 2019) resulted from the mechanical errors of the gears, especially the error of eccentricity (pointer or gear or both of them).

The Draconic cycle/gearing presents the position of the Moon relative to the Ecliptic. The Draconic pointer (the output of the Draconic gearing) was rotated around the Draconic scale. The Draconic scale consisted of a circle, representing the lunar orbit, and an engraved line-diameter, parallel to the plane which is defined by the Zodiac month ring located on the Front dial. This line represented the Line of Nodes, the Nodes marking the ends of this line. Out of this line, the Draconic pointer showed that the Moon is above or below the Ecliptic plane. Two arcs, each containing a Node, define the ecliptic limits (see below, *Reconstructing the lost eclipse events applying the Draconic gearing on the Antikythera Mechanism. The ecliptic limits of the Draconic scale* and (Fig. 13)).

The inclusion of the Draconic gearing, scale and pointer in the Antikythera Mechanism allowed real eclipse prediction via a pure mechanical procedure: By checking the relative positions of the two pointers, Lunar pointer aiming at the Golden Sphere, i.e. New Moon (or, in

opposite position, Full Moon), and the Draconic pointer aiming (or not) at/close to the Ecliptic plane, the ancient Manufacturer could know if a solar (or lunar) eclipse will be occur (Fig. 15) (Voulgaris et al. 2022, Fig. 17). The Moon phase and position in relation to the Ecliptic was the key for the eclipse events engravings on the Saros cells. This way, the ancient Manufacturer did not need any additional information in order to calculate the eclipse events sequence; he only needed the initial starting date, which defined the starting position of the Mechanism's pointers, i.e. the positions of the Sun in the zodiac sky, the Moon relative to the Sun, the anomalistic phase (position of the pin inside the slot) (Voulgaris et al. 2023a) and the Moon position relative to a Node.

c) Ecliptic Limits and eclipses

Due to the sizes of the Earth's and the Moon's shadows, for an eclipse to occur the geometrical centers of the Sun, the Earth and the Moon need not lie on a straight line.

The ecliptic limits define the maximum angular distance (measured from the Earth) by which the Moon can deviate from the straight line connecting the Earth's center and a Node of the Moon's orbit still allowing for an eclipse occurrence. When the full disc of the New Moon/Full Moon is located between the Ecliptic Limits, either a total or annular solar eclipse/a total lunar eclipse is bound to be visible somewhere on the Earth.

If the Earth had a bigger diameter, then the possibility of the lunar shadow projection on the Earth's surface (solar eclipse) would be greater and also its shadow would have been larger, increasing the probability and the duration of a lunar eclipse. On planet Saturn, solar and moon eclipses often are visible from somewhere on Saturn's surface (atmosphere).

The ecliptic limits have not fixed values because the Sun-Moon-Earth system is dynamically variable: the distances between them as well as the angular dimension of their shadows vary with time (Green 1985, p. 444; Kennard 1923; Smart 1949, p. 378).

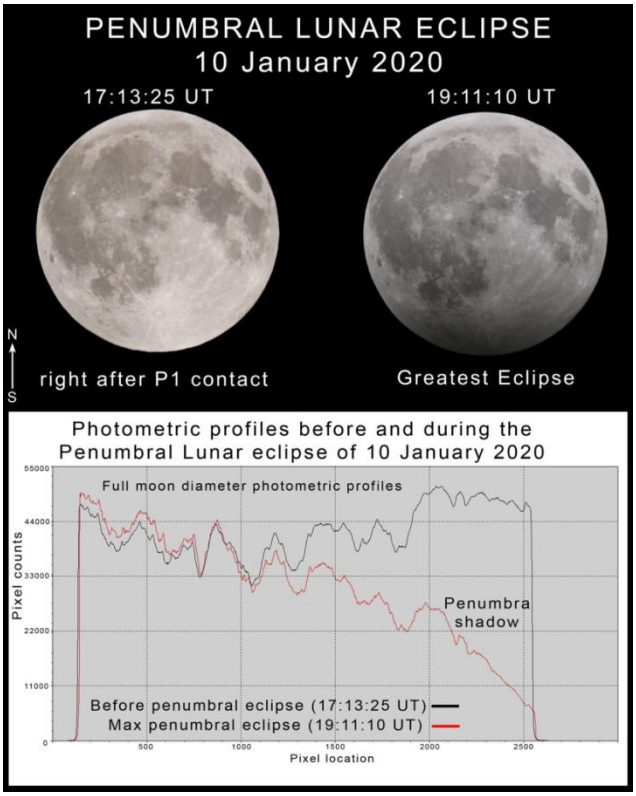

Figure 1. The Full Moon before (left) and during (right) the Penumbral eclipse of January 10, 2020, observed and captured by the Aristeidis Voulgaris from Thessaloniki, Greece

(https://eclipse.gsfc.nasa.gov/LEplot/LEplot2001/LE2020Jan10N.pdf). For the capturing, an apochromatic refractor, 127 mm diameter, 920 mm focal length, was used. The exposure time was the same for both images. Note that the brightness of the upper parts of the lunar disc remained constant during the max of the penumbral eclipse. The Moon brightness at Greatest Eclipse is about 0.787 of the brightness of the Full Moon before P1 contact, yielding a brightness drop by 0.26 mag, as it resulted by their corresponding photometric profiles (cut-through in vertical Lunar diameter). This small difference in the brightness of the Moon in duration of about 2 hours it is difficult to be easily perceived by the naked eye of an observer.

Ptolemy in Almagest (ed. Heiberg 1898, p. 485-498; ed. Toomer 1984, p. 287-288) calculates and presents the ecliptic limits:

- For any kind of a solar eclipse, the ecliptic limits are 20.683° to the north of a Node and 11.36° to the south.
- For a (partial) lunar eclipse, the ecliptic limits are ±15.2° off a Node.

There are two characteristic patterns when three eclipses occur in two successive synodic months:

- If a total lunar eclipse occurs too close to the Node, then one fortnight before and after this date, two partial Solar Eclipses will be visible alternately from the Earth's poles (Espenak & Meeus 2008).
- If a total/annular solar eclipse occurs too close to the Node, then one fortnight (half synodic month) before and after this date a Lunar penumbral eclipse will occur (Espenak & Meeus 2008).

During a Penumbral Lunar Eclipse, the brightness of the Moon is slowly decreasing in a time span of about 2 hours (Fig. 1). Even though the lunar disc enters on the penumbra shadow of the Earth, only a small part of the lunar disc is gradated and darkened. Most of the penumbral eclipses are not detectable by the eye because the darkening happens too slowly and gradually for the eye to notice. Even if this decreased brightness is detectable by some observer, they might as well assume that it is due to a thin cloud passing in front of the lunar disc. Therefore, the Penumbral lunar eclipse is difficult to be detected without any prior information regarding this event.

On the Saros spiral eclipse events, two successive events H-Σ in two successive cells or Σ-H in one cell, is preserved. As already mentioned, the penumbral lunar eclipses are difficult to detect and the partial solar eclipses only visible from the Earth's poles are also difficult to catch for an observer living around the Mediterranean Sea, because the percentage of covering is relatively small.

This is the reason why on the Antikythera Mechanism there should not be three eclipse events within two successive cells (synodic months), i.e. the eclipse event pattern

Cell (x)=Σ+H and Cell (x+1)=Σ (*Lunar-Solar-Lunar*) or

Cell (y)=H and Cell (y+1)=Σ+H (*Solar-Lunar-Solar*).

d) Reconstructing the lost eclipse events applying the Draconic gearing on the Antikythera Mechanism. The ecliptic limits of the Draconic scale.

In order to represent the phase correlation of the three lunar cycles (Synodic, Draconic, Anomalistic), we implemented a simulation created in *Python* programming language code. The simulation, which will be referred as *DracoNod* program, reproduces the position of the Moon phase in relation to the Apogee/Perigee, to the Nodes, (and to the constellations of the Ecliptic-

Sidereal cycle, which is not presented in this work) versus time, applying the equation 1 Saros cycle = 223 Synodic cycles = 242 Draconic cycles = 239 Anomalistic cycles (= 241.029 Sidereal cycles). For the calculation of the lunar phase anomaly we applied the approximation that derives from the *pin&slot* gear system as calculated in Voulgaris et al. 2018b, and not the robust one that derives from Kepler's laws. The simulation was transformed into a graphic environment, where we used the *GeoGebra* software (https://www.geogebra.org) for the user's convenience. The lunar cycles are represented by three independent circles – the Synodic, the Draconic and the Anomalistic – with their characteristic points or arcs that represent: New Moon-Full Moon, Node A-Node B with their ecliptic limits, and Apogee-Perigee respectively (Fig. 2).

As the initial starting position (Saros begin-Cell 1) of the three lunar cycles the New Moon phase at Apogee and at Node-A was selected (Voulgaris et al. 2023a) and the Moon was set at the zodiac Sign-Day 1 of Capricorn, even though initially the sidereal cycle was not necessary for the lost eclipse events calculation.

In this position of the Moon, a solar eclipse occurred (Moon at Node-A), which was a long duration annular eclipse (Moon at Apogee).

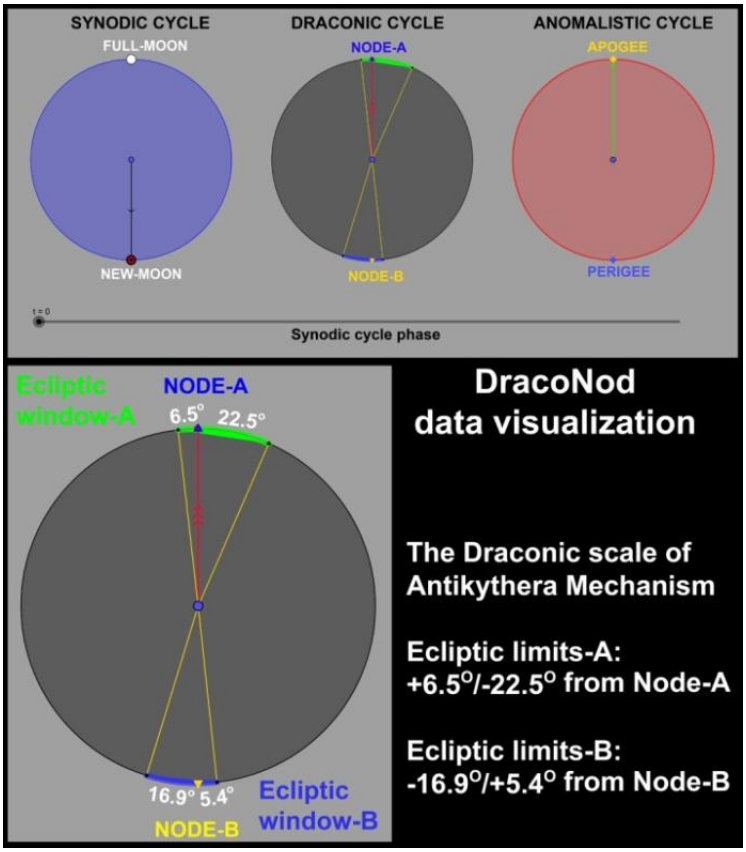

Figure 2. Data calculated by the program *DracoNod* were visualized using *GeoGebra* software. The phases of the three lunar cycles during the beginning of Saros period/Saros spiral (end of cell-01) are presented: New Moon at Node-A and at Apogee (Voulgaris et al. 2023a). The two ecliptic windows are presented in green and blue arcs. The ecliptic limits are defined by the yellow lines. Each of the circle's orbital radiuses rotates with the period of the corresponding lunar cycle. An eclipse event occurs when the orbital radius of the Draconic cycle (red color) is located inside the ecliptic window during the phase of New Moon or Full Moon. The third cycle (Anomalistic) defines the kind of the eclipse (total, annular or hybrid).

On the Draconic circle we firstly applied the ecliptic limits described in Ptolemy's Almagest (ed. Toomer 1984, p. 287-288):

20.683° South/North of Node A/B – 11.366° North/South of Node A/B for a solar eclipse, and 15.2° North/South of Nodes for a lunar eclipse.

Then, we ran the *DracoNod* and we recorded the solar and lunar eclipses on their corresponding cells.

By applying the limits referred by Ptolemy, the calculated eclipse events sequence was not in agreement with the preserved events of the Mechanism. For example, the *DracoNod* program calculated events Σ+H for cell-13 and no event for cell-12. Moreover, it calculated three eclipse events in two successive synodic months. This mismatch is a result of the wrong values of the ecliptic limits introduced to the program: Ptolemy's ecliptic limits were different than the limits adopted by the ancient Manufacturer of the Mechanism.

So, we re-calibrated the ecliptic limits of our program, in order to achieve the best correlation to the Saros spiral preserved events.

According to this calibration, the proper ecliptic limits which present the best correlation with the preserved eclipse events are common for the solar and the lunar eclipses:

For the Ecliptic Window-A: **–22.5°** (Southern of Node-A) and **+6.5°** (Northern of Node-A) and for the Ecliptic Window-B: **–16.9°** (Northern of Node-B) and **+5.4°** (Southern of Node-B).

These non-symmetrical ecliptic limit values might be considered as unusual and unjustified, but we present a satisfactory explanation in the next sections and in Appendix A to the text Section 10 (Fig. A.84).

On **Table 1**, the missing eclipse events calculated by the *DracoNod* program and on **Table 2** the summary of the results are presented (see Appendix A to the text for further analysis each of the Events).

Table 1. Prediction of the lost eclipse events of the Saros spiral using the Authors' program *DracoNod*. The new numbering of the Saros cells was applied according to Voulgaris et al. 2021, 2023a (preserved events in bold, Iversen & Jones 2019). Out of the hooked A (Ⱥ) for A3 index number event (Iversen & Jones 2019), a second symbol ß was introduced as the index number (B3) for the last events of the sequence, on cell 218. Summary, results and comments on **Table 2** and in Appendix A to the text (Fig. A.4-A.72).

Event Number	**Figure in Appendix A (Lunar cycles phase position: Synodic, Draconic, Anomalistic)**	**Event index letter**	**New cell numbering (*Voulgaris et al. 2021*)**	**Preserved Eclipse events of Saros cells**	**Reconstructed eclipse events sequence, applying the Draconic gearing. Calculated by *DracoNod* program**	**Comments/ Moon position relative to the Node/ecliptic limit**
1, (2?)	A.4 A.72	[A1]	Cell-1 (Cell-224)		Sun ***The longest duration of the annular eclipse***	**Saros cycle begins.** **New Moon at *Apogee and at Node-A.*** *(probably no lunar eclipse event in accordance to*

						cell-112 - Sar period)
2, 3	A.5 A6	**B1**	**Cell-7**	**Moon, Sun**	**Moon, Sun**	
4	A.7	**Γ1**	**Cell-12**	**Sun**	**Sun**	New Moon close to the ecliptic limit
5	A.8	Δ1	Cell-13		Moon	
6	A.9	**E1**	**Cell-19**	**Moon**	**Moon**	
7	A.10	**Z1**	**Cell-24**	**Sun**	**Sun**	
8	A.11	**H1**	**Cell-25**	**Moon**	**Moon**	Full Moon at *Node-B*
9	A.12	Θ1	Cell-30		Sun	
10	A.13	I1	Cell-31		Moon	Full Moon close to the ecliptic limit
11	A.14	K1	Cell-36		Sun	
12, 13	A.15 A.16	Λ1	Cell-42		Moon Sun	New Moon close to Node-B
14, 15	A.17 A.18	M1	Cell-48		Moon Sun	New Moon close to Node-A
16, 17	A.19 A.20	N1	Cell-54		Moon Sun	New Moon on the ecliptic limit
18	A.21	Ξ1	Cell-59		Sun	
19	A.22	[O1]	**Cell-60**	**Moon**	**Moon**	
Omitted event-1	A.23		Cell-65	Event not exists	Sun	New Moon just right on the ecliptic limit. Indeterminacy or eccentricity error
20	A.24	**Π1**	**Cell-66**	**Moon**	**Moon**	Full Moon close to the ecliptic limit
21	A.25	**P1**	**Cell-71**	**Sun**	**Sun**	
22	A.26	[Σ1]	**Cell-72**		Moon	Full Moon close to Node-B
23	A.27	**T1**	**Cell-77**	**Sun**	**Sun**	
24	A.28	**Y1**	**Cell-78**	**Moon**	**Moon**	Full Moon just right on the ecliptic limit
25	A.29	[Φ1]	Cell-83		Sun	
26, 27	A.30 A.31	[X1]	Cell-89		Moon Sun	New Moon close to Node-B
28, 29	A.32 A.33	[Ψ1]	Cell-95		Moon Sun	
30	A.34	[GƆ1]	Cell-101		Moon	
31	A.35	[A2]	Cell-106		Sun	

32	A.36	[B2]	Cell-107		Moon	
Omitted event-2	A.37		Cell-112	Event not exists	Sun	New Moon approaches the ecliptic limit. Error of eccentricity? or tooth un-uniformity of gear s2?/ Draconic pointer. Same position of the pointer in the beginning of cell-01
33	A.38	**Γ2**	**Cell-113 Middle of *Saros Cycle*, A new Sar period begins**	**Moon**	**Moon** ***Total lunar eclipse (shortest duration)***	**At the middle of Cell-113, Full Moon at *Perigee* and at *Node-A*.**
34	A.39	**Δ2**	**Cell-118**	**Sun**	**Sun**	
35	A.40	**E2**	**Cell-119**	**Moon**	**Moon**	
36, 37	A.41 A.42	**Z2**	**Cell-124**	**Moon, Sun**	**Moon, Sun**	Full Moon on the ecliptic limit
Additional event-1: 38, 39	A.43 A.44	**H2**	**Cell-130**	**Moon, Sun**	**Sun** (Moon was not predicted)	Full Moon just out of the ecliptic limit. Error of eccentricity
40, 41	A.45 A.46	**Θ2**	**Cell-136**	**Moon, Sun**	**Moon, Sun**	*New Moon at Node-B*
42, 43	A.47 A.48	[I2]	Cell-142		Moon Sun	New Moon close to the ecliptic limit
44	A.49	[K2]	Cell-148		Moon	
45	A.50	[Λ2]	Cell-153		Sun	
46	A.51	[M2]	Cell-154		Moon	
47	A.52	[N2]	Cell-159		Sun	
48	A.53	[Ξ2]	Cell-160		Moon	Full Moon close to Node-A
49	A.54	[O2]	Cell-165		Sun	
Omitted event-3	A.55		Cell-166	Event not exists	Moon	Full Moon just on the ecliptic limit. Error of eccentricity or indeterminacy.
50, 51	A.56 A.57	**Π2**	**Cell-171**	**Moon, Sun**	**Moon, Sun**	

52, 53	A.58 A.59	**P2**	**Cell-177**	**Moon, Sun**	**Moon, Sun**	Full Moon just right on the ecliptic limit. New Moon at Node-A
54, 55	A.60 A.61	**Σ2**	**Cell-183**	**Moon Sun**	**Moon, Sun**	
56 Plus Omitted event-3	A.62 A.63	**T2**	**Cell-189**	**Moon**	**Moon** and Sun (prediction of one additional event)	New Moon just on the ecliptic limit. Error of eccentricity or indeterminacy
57	A.64	[Y2]	Cell-195		Moon	
58	A.65	[Φ2]	Cell-200		Sun	
59	A.66	[X2]	Cell-201		Moon	Full Moon at Node-B
60	A.67	[Ψ2]	Cell-206		Sun	
61	A.68	ϬƆ2	Cell-207		Moon	
62	A.69	[2̂] (A3)	Cell-212		Sun	
63, 64	A.70 A.71	[ß] (B3)	Cell-218		Moon Sun	

DracoNod predicted all the preserved solar eclipses plus three additional eclipses (Draconic pointer just on the limit) which are non-engraved events and present high indeterminacy.

Was predicted all the preserved lunar eclipses out of one which is also presents high indeterminacy. The predicted lunar eclipse on cell-01 is doubtful if finally it was real engraved (comparing to Cell-112). See all the eclipse events visualization in Appendix A to the text and the presentation of the omitted/additional events (I-V and 38) (Fig. A.73-A.78).

Table 2. Summary and comments of the predicted events via *DracoNod* program (see also Appendix A to the text).

***DracoNod* eclipse events prediction**	
Solar eclipse events on Cell:	**Lunar eclipse events on Cell:**
1, 7, 12, 24, 30, 36, 42, 48, 54, 59, 71, 77, 83, 89, 95, 106, 118, 124, 130, 136, 142, 153, 159, 165, 171, 177, 183, 200, 206, 212, 218 **(31 events)**	7, 13, 19, 25, 31, 42, 48, 54, 60, 66, 72, 78, 89, 95, 101, 107, 113, 119, 124, 130, 136, 142, 148, 154, 160, 171, 177, 183, 189, 195, 201, 207, 218 **(33 events)**
Lunar and Solar eclipse events in Cell:	
1(?), 7, 42, 48, 54, 89, 95, 101, 124, 130, 136, 142, 171, 177, 183, 189, 218	
Additional/Omitted eclipse events	
Omitted event: Cell-65 non engraved event-predicted H, Pointer at the limit (indeterminacy or gearing error)	Additional event, Cell-130 Σ, engraved-not predicted, Pointer just out of limit (indeterminacy? or gearing error)
Omitted event: Cell-112 non engraved-predicted H, Pointer close to the limit (gearing error?)	Omitted event: Cell-166 predicted Σ at limit (indeterminacy or gearing error), based on the preserved index numbering this event is not exists
Omitted Cell-189 non engraved-predicted H,	Omitted event (?) Cell-01/(‘Cell-224’)

Pointer at the limit (indeterminacy or gearing error)	predicted Σ. It could be exist or not exist

The Draconic pointer position for all of the Omitted/Additional events is located on or too close to the ecliptic limits. Taking into account that in a geared device there have to be mechanical errors, the omitted/additional eclipse events could be a result of mechanical errors in the Antikythera Mechanism gearings, (Draconic gears and pointer/Golden Sphere-Sun gearing, or it could be an error of reading or a result of indeterminacy (discussed below).

Methods and Calculations

a) Errors in time measurements using a geared measuring device

In his '*Introduction to the Phenomena*', chap. 18, About Exeligmos, Geminus (ed. Manitius 1898, p. 206; ed. Spandagos 2002, p. 123/231) describes the variable lunar angular velocity calculation using an angle measuring instrument and writes: …ΛΟΙΠΑ ΑΡΑ ΕΣΤΙ ΤΑ ΕΚΦΥΓΟΝΤΑ ΤΗΝ ΤΩΝ ΦΑΙΝΟΜΕΝΩΝ ΔΙΑ ΤΩΝ ΟΡΓΑΝΩΝ ΠΑΡΑΤΗΡΗΣΙΝ (…these angle measurements are lost as a result of the instrument's measuring errors).

When using a measuring instrument, measuring errors appear and affect every measurement. These errors are an inherent problem of the *instrument-user* system.

There are many types of measuring errors (Herrmann 1922; Muffly 1923). Some of the errors are owed to the instrument and some errors to the user of the instrument.

In this work we present and discuss the errors that can be directly related to the Antikythera Mechanism operation.

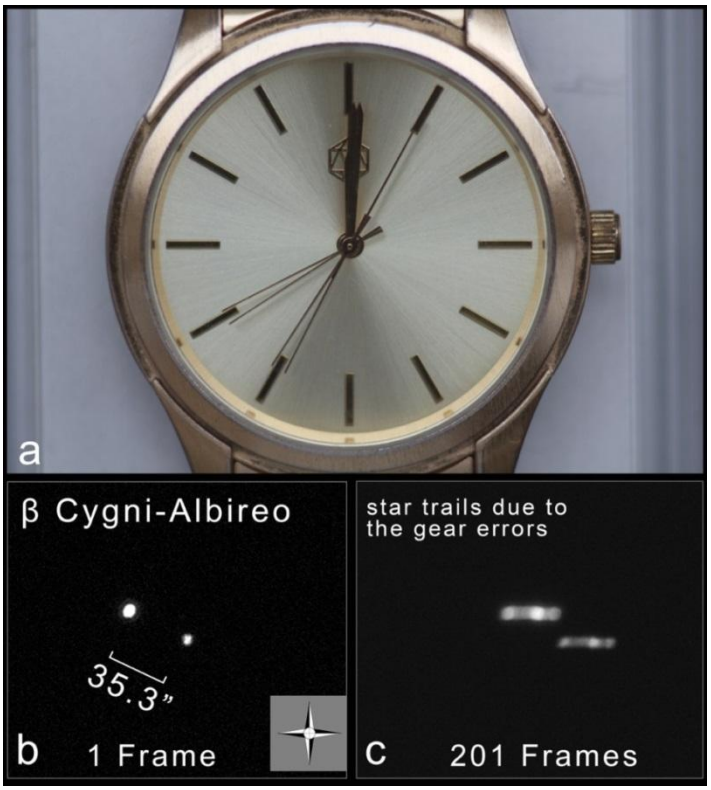

Figure 3. The gear errors affect the pointers' position of a clock and the stars' position on the telescope's field (telescope adapted on an equatorial mount). **a –** the pointer of the seconds aims at the dial subdivision (subdivision 1). In the opposite position, the pointer of the seconds should aim on the subdivision '7' for the 35th sec and on '8' for the 40th sec. Because of the pointer's (or

dial's) eccentricity, the 35th sec is located after the subdivision '7' and the 40th sec is located after the subdivision '8'. This effect is characteristic of the geared devices, as a result of a gear or axis or measuring scale eccentricity. If, now, we consider the dial line '7'=35th sec as the first ecliptic boundary limit of the Draconic scale, this means that the Draconic pointer aiming either out of the ecliptic limits, meaning that-no eclipse event occurs although it actually does, or within the ecliptic limits, meaning that an eclipse event occurs although it actually does not. Watch suffering from eccentricity, from first author's collection; **b –** a single photograph via a Maksutov telescope (diameter 150 mm, Focal length 1500 mm) of the double star β-Cygni, named Albireo; **c –** multi-combined image of 201 single images of 1 sec exposure. As a result of the gears' eccentricity of the equatorial mount, the two stars are continuously recorded in different position (pixels) on the CCD camera and the stars' shift to east-west direction is evident. Images by Aristeidis Voulgaris.

The most common error owed to the user is the reading error. For example, the reading error with an old analog voltmeter/ampere meter is the parallax effect between the user's eye and the indication needle, which moves to indicate the measurement results. The reading error becomes extremely critical when the measurement results concern the *on*/*off* selection: For a measurement just right at the limit, the user must decide for a procedure that is '*on*' or '*off*' situation.

Measurements which are too close to the *on-off* limit, or just right *on* the limit, have high uncertainty: the user cannot judge which side of the limit the measuring needle lies on (resolution error) and the indeterminacy of the measurement rises (see Appendix A to the text, Section 3).

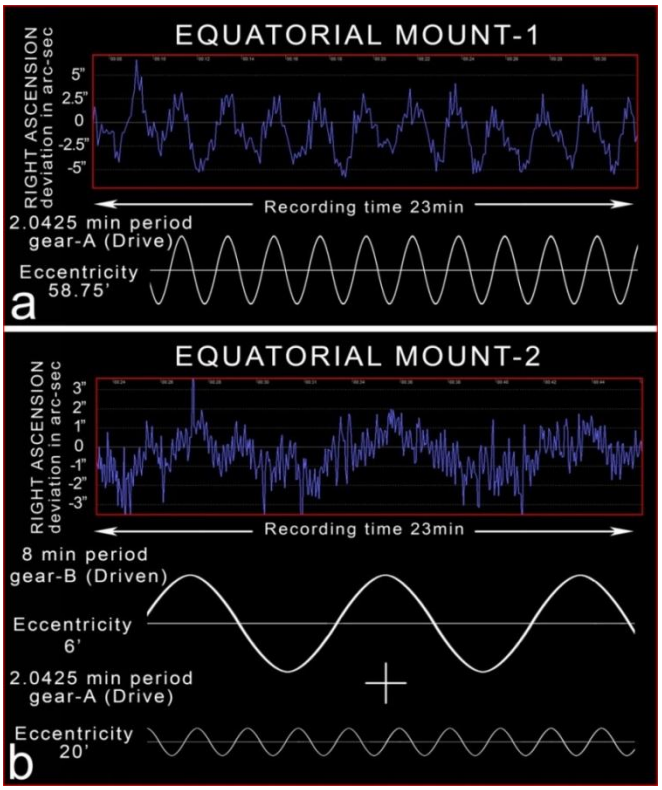

Figure 4. The periodic errors detected in two equatorial mounts, as result of the eccentricity of the gear(s): **a** and **b –** periodic errors measurements (via a guiding software-*PHD2* Guiding Project and *PHD2 Log Viewer*) were detected in both of first author's equatorial mounts 1 and 2, which are constructed by the same factory and they have about the same mechanical design. The graphs represent the periodically varying position of a star (as it is focused on a CCD camera, via

a telescope), through time (both graphs 23 min recording). Both mounts have the same design of the clock drive but different number of teeth on their drive/driven gears. The two graphs differ because the error of the eccentricity on the top graph concerns only one gear (drive gear-A with 9 teeth) and on the bottom graph the error of eccentricity appears in two gears (drive gear-A with 12 teeth and driven gear-B with 47 teeth). If the gears were perfect constructions, the graph should have appeared as a horizontal straight line coinciding with the x-axis, i.e. deviation '0' in Right Ascension, representing a constant angular velocity of the gear. The high frequency variations (9 picks per period of gear-A/Equatorial mount-1 and 12 picks per period of gear-A/Equatorial mount-2) is the variation in the transmission motion *tooth by tooth* from gear-A to gear-B. Even the two gears constructed with the involute teeth profile, the non-perfect transmission is visible on the graph (Fig. 7).

As regards geared measuring instruments used for time measurement, such as clocks, equatorial mounts for telescopes, heliostats etc., there are mechanical errors that affect the results of an instrument's operation, precision and measurements.

The most common mechanical errors of a geared device are the gear/axes/shafts eccentricities (Fig. 3, 4), the axes/pointers eccentricities or precession, the gear teeth non-uniformity, and the imperfect transmission rotation between the gear teeth (the triangular shape of the gear teeth of the Antikythera Mechanism makes this problem even worse, (see further below and in Figure 7).

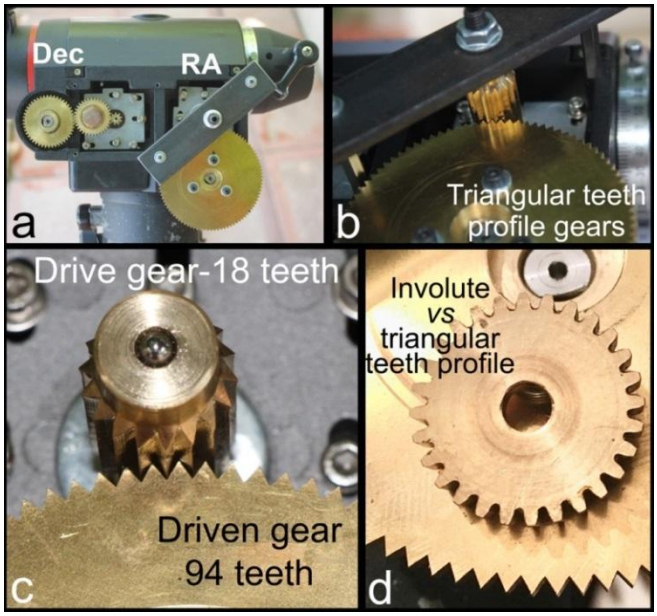

Figure 5. Replacement of the (Right Ascension axis - RA) modern gears (with involute tooth shape) with the Antikythera Mechanism style gears (triangular tooth shape) on the Equatorial mount-1: **a –** on the Equatorial mount-1, the two gears of the clock drive were replaced by gears with triangular tooth profile, as are the gears of the Antikythera Mechanism. The gears of the Declination axis (Dec) were not replaced; **b –** a bar with a screw; **c –** a bearing ball was placed in order to avoid the precession of the drive gear axis during its rotation. By applying a fast rotation of the input gear, the triangular teeth engagement produces a characteristic sound like a '*gun machine rattle*' (https://www.youtube.com/watch?v=h-qpXYK3bls); **d –** the difference between the involute and the triangular teeth profile. Bronze parts construction and image by Aristeidis Voulgaris.

For time measuring by using geared devices, the error of eccentricity and the gear teeth non-uniformity, create mismatches between the true time and the calculated time:

The eccentricity is defined as the difference between the axis of rotation and the axis of symmetry. On a gear which suffers from eccentricity, the central hole of the gear does not coincide with the center of the circle defined by the teeth peaks, known as *addendum circle*, or with the center of the circle defined by the valleys, known as *dedendum circle*. An axis/shaft eccentricity appears when the mechanical center of axis/shaft's rotation does not coincide to the geometrical center of its cross section.

A gear (or an axis) eccentricity is an inherent and permanent mechanical problem of the equatorial mounts made for telescopes (also in heliostats/coelostats, also in clocks). These mounts are geared devices having a well-timed axis rotation. The equatorial mount compensates the Earth's rotation by only using one axis of rotation called *polar axis*. The polar axis rotates at the same (and constant) angular velocity as the celestial objects (sidereal for the stars, solar for the Sun etc.), about 1 turn/24h. The geared system (motor and gears) that rotates the polar axis is called clock drive.

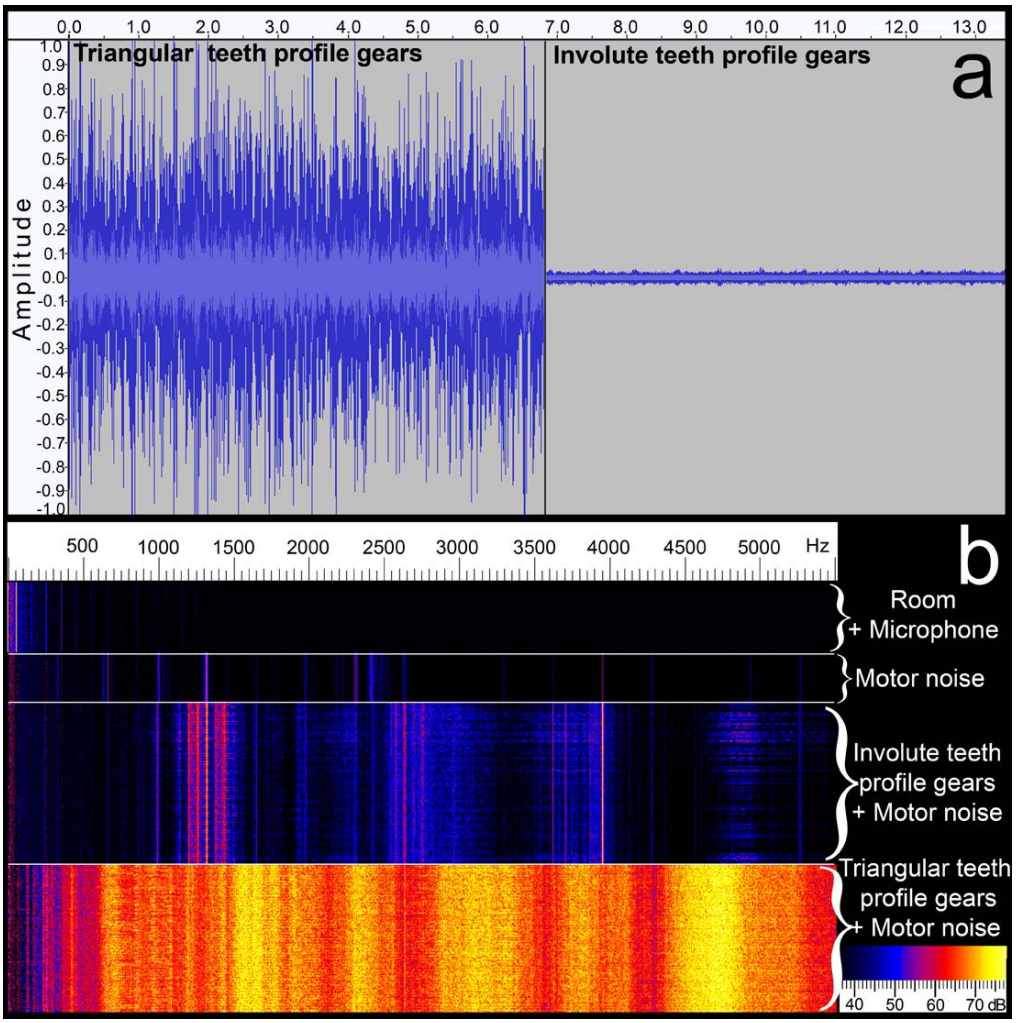

Figure 6. A comparative sound analysis (amplitude and frequency) during the operation of the modern and the Antikythera Mechanism style gears: **a –** the sound amplitude difference between the operation of gears with triangular teeth profile (left graph) and the gears with the involute teeth profile (right graph). The sound graph of the gears with triangular teeth profile is equal to the sound graph produced by a '*gun machine rattle*'; **b –** the sound spectrum analysis between 0-6000 Hz. First spectral strip: the spectrum of noise from the recording room and the

self-noise of the microphone (Average intensity ≈27 dB). Second strip: the spectrum of the motor sound without engaged gears. Third strip: the sound spectrum during the rotation of the gears with involute teeth profile and the sound of the motor operation. The room and the microphone noise were subtracted (Average intensity ≈53 dB). Fourth strip: the spectrum of the gears with triangular teeth profile and the sound of the motor operation. The spectral band concerns the full spectrum in average intensity ≈74 dB and resulted from the strikes between the teeth of the engaged gears, because they are not in constant contact during their engagement (Fig. 7). On the contrary, the sound spectrum produced by the gears with involute teeth has much lower intensity and presents broadband gaps.

As the equatorial mount compensates for the Earth's rotation, a celestial object, e.g. a star, when observed through the eyepiece of a telescope, should appear fixed on the center of field of view. Due to the eccentricity errors in the clock drive gears, the fixing of a star in the field of view is not perfect: The star periodically drifts back and forth (east-west) relative to a central point. This effect is continuously repeated during all of the time of observation (Fig. 3, 4). The motor of the clock drive rotates at a constant angular velocity (i.e. x-steps/time = constant). The eccentricity(ies) of the gears transform the constant velocity of the motor to a periodically variable velocity, resulting in the linear drifting of the star in the field of view.

There is no mechanical solution to fix the problem of eccentricity, but there is a solution via electronics and software: The PEC (*Periodic Error Correction*) procedure: via an educated algorithm, the motor is not rotated at constant velocity, but at variable (inversed) velocity, in order to compensate for the error of eccentricity (see Appendix A to the text, Section 5).

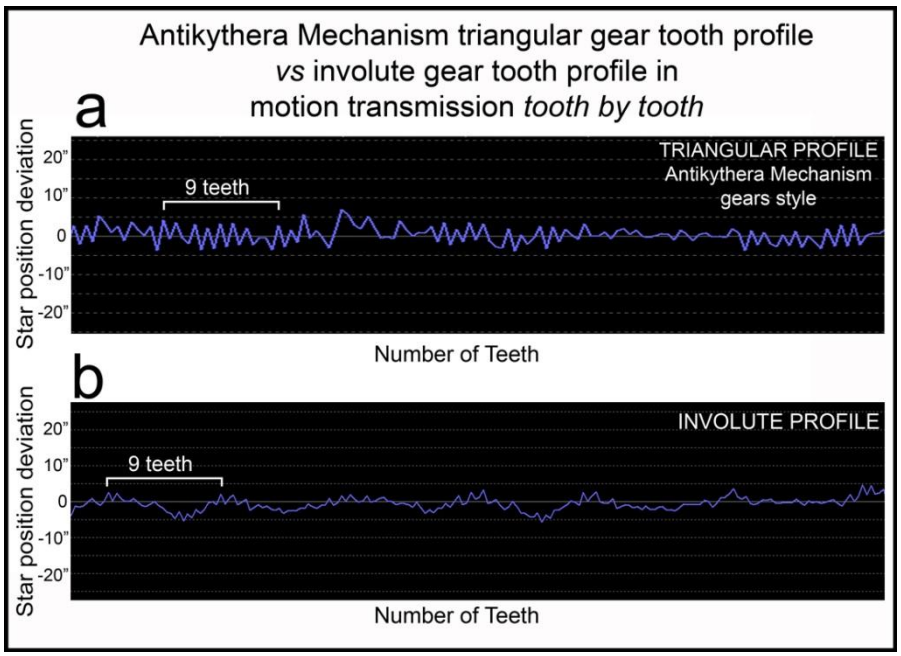

Figure 7. The graphs present the *star position deviation vs number of the (successive) gear teeth*: **a –** the motion transmission by adaptation of gears with triangular teeth profile on the clock drive of the Equatorial mount-1; **b –** the motion transmission of the original gears with involute teeth profile. The motion transmission *tooth by tooth* in the gears with triangular tooth shape profile is much worse than the modern gears, about two times. If the motion transmission was perfect, the graph should be a smooth line without picks (constant value 0). Note that the modern gear-A (Drive) presents the error of eccentricity.

An additional error in the gearings is the transmission error in *tooth by tooth* engagement. The involute tooth profile offers the best uniformity of motion transmission between the engaged gears. As the Earth rotates with a fixed period, the gears adaptation on an equatorial mount can be used for the quality evaluation of the gears' construction and their errors detection: In order to examine the motion transmission (*tooth by tooth*) of gears with triangular tooth profile, the two gears (with involute profile) of the clock drive/Equatorial mount-1 (A=9 teeth and B=47 teeth) have been replaced by two gears constructed with triangular tooth profile and having the same ratio of teeth numbers (drive gear *a*=18 teeth and driven gear *b*=94 teeth) (Fig. 5, https://www.youtube.com/watch?v=h-qpXYK3bls). Both of gears were designed, constructed, adapted and tested by Aristeidis Voulgaris.

During the rotation of the gears (at the fast rotation) we recorded the sound, by stabilizing a microphone on the Equatorial mount-1. The evaluation in the gears' errors and the transmission motion can be achieved applying the acoustic analysis (Gaylard et al. 1995; Korpel 1968; van Riesen et al. 2006; Tavner 2008). The signals were digitized via an ADC sound card and afterwards were processed by the software *Audacity*, *Spectrum Lab* and *Radio Sky Pipe*. The amplitude and the sound spectrum graph analysis, show the strong noisy sound during the rotation of the gears with triangular teeth profile in comparison to the rotation of the gears with involute teeth profile **(**Fig. 6).

The graphs of Figure 7 show that the triangular tooth shape does not offer a smooth motion during the gears' rotation. The *tooth by tooth* motion appears more as intermittent motion: the aimed star is not immobilized but it seems to constantly make 'little jumps'.

b) The error of eccentricity in the Antikythera Mechanism gear(s)

By studying the AMRP radiography of Fragment A we found that the ancient Manufacturer fitted a thin copper sheet (thickness 0.1÷0.2 mm) into the central hole of the m2-gear: the Manufacturer probably made the central square hole of the gear by accident a bit larger (a mistake also made by Aristeidis Voulgaris during the gear construction) and then he adapted the copper sheet in order to stabilize the gear on its shaft (Fig. 8).

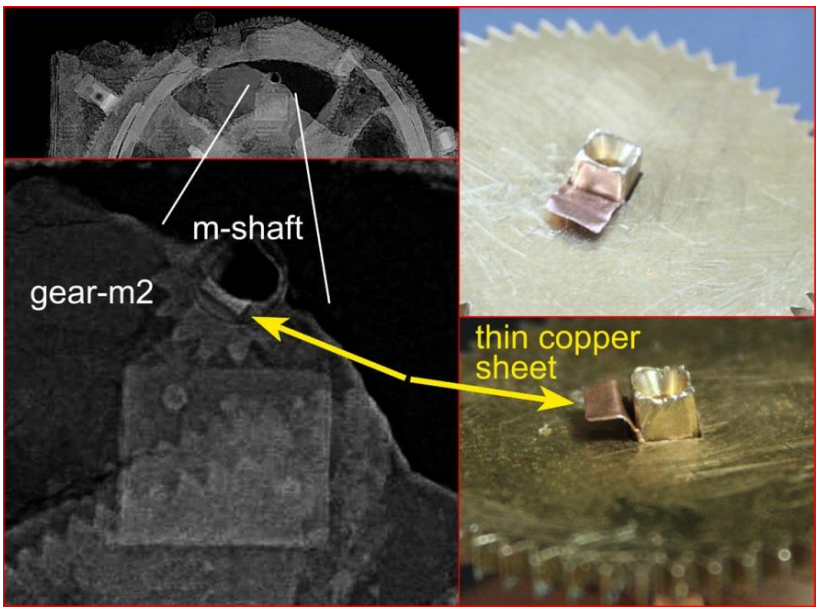

Figure 8. AMRP radiography of Fragment A and bronze reconstructions. In the radiography of Fragment A (processed by the authors), a thin part adapted on the square hole of gear m2 is visible. This thin copper sheet was in contact with the square shaft of m2 gear (which is poorly

preserved). A reproduction of this observation is presented in the visual images by Aristeidis Voulgaris. The copper sheet stabilizes (tightens) the gear to its axis.

The ancient Manufacturer may also have detected a high eccentricity in this gear (the hole of this gear was not exactly centered to the gear's geometrical center) and he tried to eliminate it, by enlarging the hole and fitting this copper sheet into it. Both of these justifications for the copper sheet fitting related to the existence of the eccentricity errors in some of the Mechanism's gears. As aforementioned, the eccentricity of the gears is an inherent mechanical error of the geared devices and it is mostly created during the construction of the gears.

The error of Eccentricity makes the ratio '*epicenter angle φ/teeth*', which otherwise would be constant, a variate:

When a shaft rotates at a constant angular velocity and the gear with eccentricity is adapted on the shaft, then the gear presents during its rotation a variable linear velocity (measured at the perimeter of the gear/teeth), because the radius of the gear differs. Therefore, the ratio '*tooth/time*' is not constant. This means that half of the teeth are moved faster and the other half of the teeth (located opposite) are moved slower.

A gear with radius R_0 = 4.2 mm and 15 teeth (m2-gear), having eccentricity e = 0.2 mm (the copper sheet thickness), presents a max angle difference $\Delta\varphi$ relative to the ideal gear (Fig. 9):

$$\tan(\varphi) = e/R_0 \rightarrow \tan(\varphi) = 0.2/4.2 \rightarrow \Delta\varphi = 2.79°, \quad (1)$$

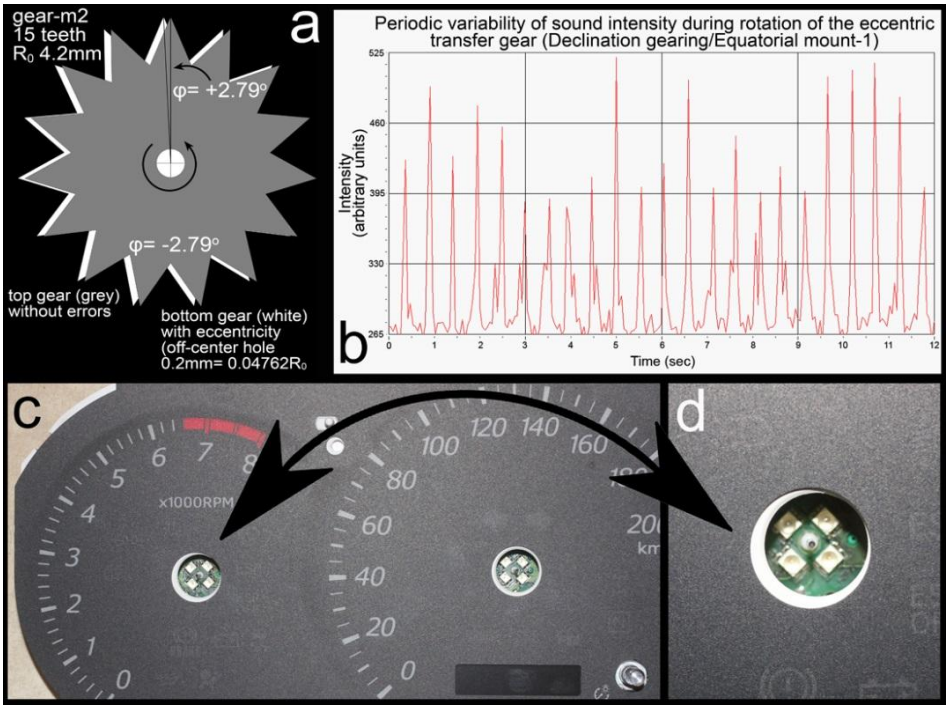

Figure 9. The Effects of the gear(s)/axis Eccentricity on the positioning and the sound: **a** – Two same gear scheme (m2 gear), in grey the (top) gear without errors and in white the (bottom) gear with eccentricity of 0.2 mm. The centers of the gears coincide and the positioning difference of the gear teeth is visible; **b** – the periodic variability graph of the sound intensity (via *Radio Sky Pipe* software), during the operation of the Declination gearing (Equatorial mount-1). The sound intensity variability is due to the eccentricity of the transfer gear (Fig. 5); **c** and **d** – many measuring circular scales present the common error of eccentricity: On the instrument panel of a car, the geometrical center of the Speed Dial scale is not coincided to the pointer's axis and the measuring error is appeared. Image by Aristeidis Voulgaris.

Discussion of Results

a) The error of the gear eccentricity impacts the Antikythera Mechanism pointers' position

When gear A has an error of eccentricity and is engaged to gear B (with same teeth number and without errors), the periodically variable angular velocity of gear A is transmitted to gear B. If we stabilize a pointer on gear B, the pointer will be periodically rotated faster (for the first half period) and then slower (for the second half period), even though the input of the gearing is rotated at a constant angular velocity (see also Edmunds 2011).

Gear m2 is engaged to the (lost) gear n1 (53 teeth), which rotates the Metonic pointer (see gearing scheme Freeth et al. 2006 and Voulgaris et al. 2018b). The variable angular velocity of gear m2 (as result of the eccentricity) is transmitted to the gear n1, suppressed by the gearing reduction: $2.79°\cdot(15/53) \rightarrow \Delta\varphi \approx 0.79°$ on the Metonic pointer (see eq. 1). Taking into account that each Metonic cell corresponds to ≈ 7.66°, the eccentricity phase of ±0.79° is not critical.

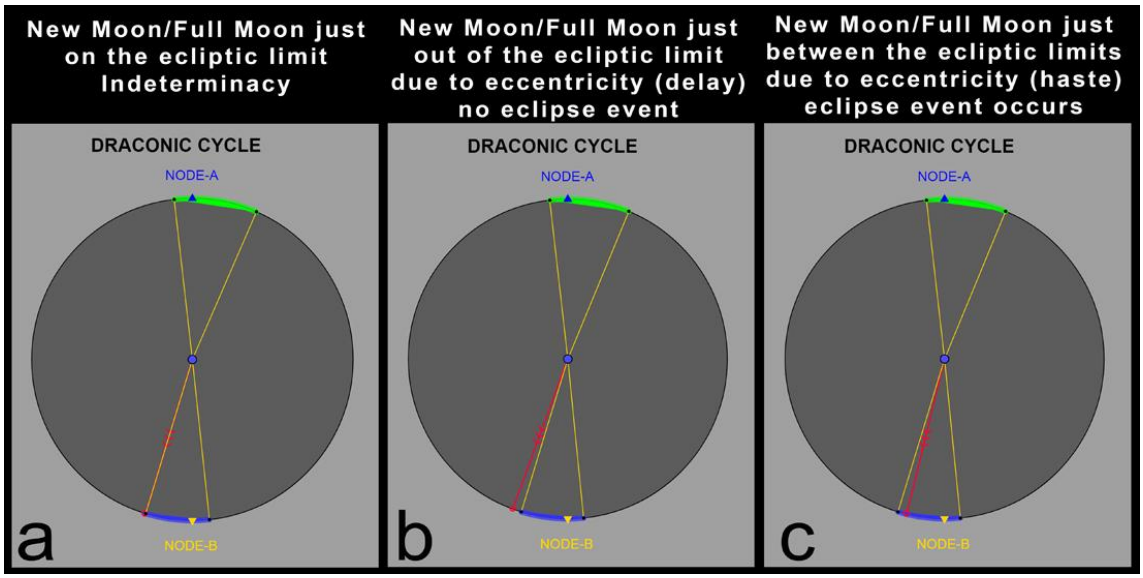

Figure 10. The error of Eccentricity affects the position of the Draconic pointer: **a –** the actual calculated position (via *DracoNod*) of the Draconic pointer during the New Moon of Cell-65 (ideal, without errors). The pointer aims just right on the ecliptic limit. This position presents a high indeterminacy; **b –** via a gearing instrument with errors, the Draconic pointer position is out of the ecliptic window (no eclipse event), due to the eccentricity error of -x° (phase of delay); **c –** the Draconic pointer position is inside the ecliptic window (eclipse event occurs), due to the eccentricity error of +x° (phase of haste). The gearing errors (gear or shaft/axis eccentricity, tooth un-uniformity) affect the position of the pointers and the final results (eclipse events). The eccentricity could also affect the classification of the events: e.g. an eclipse event (theoretically) occurred just on the Node, could be located out from the Node resulting to its different classification (see Appendix A to the text).

Let us examine a different condition: If there was no error of eccentricity, the Lunar pointer would aims at the Golden sphere-Sun and at the same time the Draconic pointer would aim just right of the ecliptic limit - indicating a solar eclipse occurrence. But if the Draconic pointer/gear presents an eccentricity of ±2°, then during the phase of delay (-2°) the Draconic pointer aims 2° before the ecliptic limit, i.e. out of the ecliptic 'window' - indicating no eclipse event occurrence (the inverse effect is also valid) (Fig. 10).

Even if no error of eccentricity existed in the Draconic gearing but an eccentricity of 0.2 mm existed on gear b1 (130 mm diameter and 225 teeth, Voulgaris et al. 2022), then the angle difference $\Delta\theta$ would be $\tan(\theta) = 0.2/65 \rightarrow \Delta\theta = 0.176°$. The angle difference would be transmitted via the engaged gears of the Draconic gearing (multiplier gearing) to the Draconic pointer as:

$\Delta\theta \cdot (b1/a1) \cdot (r1/s1) = 0.176 \cdot (225/48) \cdot (63/22) \approx \pm 2.36°$

During one rotation of the b1, the Draconic pointer is rotated about 13.42 times.

For the first 13.42/2 = 6.71 rotations, the Draconic pointer would be rotated with gradually increasing angular velocity up to $\Delta\theta = +2.36°$, whereas for the next 6.71 rotations it would be rotated with decreasing velocity up to $\Delta\theta = -2.36°$ (while it should be rotating at a constant velocity and with $\Delta\theta = 0°$).

Even if no error of eccentricity was existed in gear b1, but it did in gear b2, which is stabilized on gear b1, then the error of eccentricity would be transmitted to gear b1. An eccentricity of 0.1 mm on gear b2 corresponds to an angle difference $\approx \pm 4.86°$ on the Draconic pointer.

Therefore, the error of eccentricity affects the positioning of the gears on which the pointers are adapted, i.e. the extracted results/calculations of the Antikythera Mechanism (Edmunds 2011).

The ratio 'teeth/time' is also not constant if there is any dissimilarity on the gear teeth, i.e. the teeth of a gear have not the same dimensions or shape. This error is called pitch deviation.

For example, a (hypothetical) random accidental construction defect on a tooth of gear-b2, resulting in a shorter dimension by ≈15% corresponds to an epicenter angle of about 0.84° ≈1 subdivision on the Zodiac dial. Due to this error, the conjunction of the Lunar and the Golden sphere differs than to its original position, and changes the position of the Golden sphere-Sun on the Zodiac dial ring-Ecliptic.

These random errors also produce false results in a random distribution.

The omitted and the additional events were predicted by *DracoNod* they can be well justified as a result of the Draconic pointer eccentricity or the eccentricity of the (gearing/pointing) system of the Lunar Disc/Golden sphere-Sun (Fig. 10).

In the *world of the hand-made geared devices* (Voulgaris et al. 2019a) using conventional machine tools of the Middle Ages, the Renaissance and the early Industrial Revolution, the gear errors (around 0.1 mm-0.4 mm), as a result of the lower precision of the measuring procedures and the machine tools, are much more probable than today. In our era, the dimensional errors of the commercial mechanical constructions are significantly smaller, around 0.05 mm or less. Moreover, the use of high precision, special-cutting tools and of modern computerized machines (Computer Numerical Control-CNC) offers high repeatability in parts and shapes production, with dimensional errors around 0.02 mm. These precisions are achieved by the use of optomechanical measuring devices (macro lenses in high magnification and high resolution industrial machine vision cameras).

For a high precision quality of the gear teeth shaping, the cutting tools and the material that is cut, are immersed in cooled oil, in order to avoid overheating of the material during the process, which would result in thermal expansion of it.

Today, the simulation of the Antikythera Mechanism, which is carried out using computers simulations, has significantly progressed, yielding many answers and new discoveries. However, the mechanical errors of the Mechanism's gears are not taken into account (and it is difficult to be detected/measured, as some gears are missing and the preserved parts are deformed, shrunk

and in different material and volume, Voulgaris et al. 2019b). The results from the computer simulations presuppose that the AM was an ideal device, operating perfectly, without mechanical errors or reading errors or errors of indeterminacy. This way, any progress in the AM is achieved in a '*sterilized and perfect mechanical world*'.

However, in the '*real material world*', mechanical errors exist and they have a big impact on the final results presented by the Antikythera Mechanism. Taking into account the random/unknown errors of the Mechanism gears, the real results (pointers' position) could be different from the perfect/ideal results calculated by a computer and 3D simulations.

b) Re-calculating the actual ecliptic limits of the Draconic scale taking into account the gearing errors

The calibration of the ecliptic limits were located on the Draconic scale was calculated considering that there are no mechanical errors in the Antikythera Mechanism gearing. The calibrated ecliptic limits resulted in a common ecliptic window for the solar and the lunar eclipses:

For the Ecliptic Window-A: –22.5° and +6.5° from Node-A

For the Ecliptic Window-B: –16.9° and +5.4° from Node-B.

The relative high value of 22.5° for the ecliptic limit of Node-A and the relative low value of 16.9° for the ecliptic limit of Node-B seem quite asymmetrical and are difficult to be justified in astronomical terms. However, their mean value is 19°.7.

Taking into account the existence of the errors of eccentricity in some of the Mechanism gears (or scales and pointers), these asymmetrical values can be a result of an eccentric gear or gears or an eccentricity Draconic scale or errors in gears b2/b1 which define the synodic cycle. It seems that a complex combination of such errors is more likely. But each gear with eccentricity error affects the Mechanism's results in a different degree.

Thus, our calculated (non-symmetrical/eccentric) ecliptic limits of Nodes A and B are the result of the gear(s) eccentricities, tooth un-uniformity and Draconic pointer/scale eccentricity.

Therefore, the specific eclipse events are the outcome either of perfect gears and an eccentric Draconic scale, or a faultless Draconic scale and imperfect gears or a more complex combination of mechanical errors.

The approximate solution was found with the graphic design environment, the calculated error was ±0.5° and the ecliptic limits probably adopted from the ancient Manufacturer would be:

For the Ecliptic Window-A: **–19.9°** and **+5.7°** from Node-A

For the Ecliptic Window-B: **–19.4°** and **+6.2°** from Node-B.

The mean limit values for these Ecliptic Windows are 19.65° and 5.95°, very close to 20° and 6° (see Appendix A to the text).

Unfortunately, the new limits cannot be used for the Antikythera Mechanism calculations, as the specific results (eclipse events) were calculated by the specific instrument which has specific mechanical errors. By applying the calculated symmetrical limits on the Mechanism gearings without errors, the eclipse event sequence would differ from the present Saros event sequence (concerning the events were detected on/close to the ecliptic limits edge – the *omitted/additional* events see Figure 10 and Appendix A to the text, Section 10.

We don't know which of the gears have eccentricity errors, neither the degree of the eccentricity, nor the phase (direction axis) of the eccentricity, and we'll probably never find out, as some of the Mechanism gears are missing and the preserved ones have changed as regards

their composition (material) and volume, plus they are deformed, broken and shrunk (Voulgaris et al. 2019b).

c) The Antikythera Mechanism could also calculate the times of the eclipse events

The ancient Manufacturer engraved the times of the eclipse events on the cells with eclipse events (Anastasiou et al. 2016; Freeth et al. 2006, 2014; Iversen & Jones 2019; Jones 2020). The times mentioned are between in 12 hours daytime and 12 hours nighttime.

A question arises: What was the source of the information that the ancient Manufacturer used to define the eclipse events sequence and times of their occurrence?

- A Babylonian papyrus with written events and times of occurrence?
- A mathematical process?
- A catalogue with written observed events? (Freeth 2014; Carman & Evans 2014; Iversen & Jones 2019; Jones 2020).

- (*Finally, the engraved eclipse events on the Saros spiral are real observed events?*)

In the present work we showed that the eclipse events sequence could be calculated by the Antikythera Mechanism applying the Draconic gearing and the omitted events can be well justified taking into account the existing mechanical errors.

Below we present the procedure of the eclipse event time calculation by using solely the Antikythera Mechanism and no external information.

- (So, it will be resulted that *the engraved eclipse events on the Saros spiral are not real observed events, but were calculated by using the Mechanism*).

On the Antikythera Mechanism, during a full rotation of the Lunar pointer (i.e. one Sidereal cycle), the Lunar pointer scans the Zodiac month ring of the Mechanism and its subdivisions. Geminus, in his work *Introduction to the Phenomena,* in Chap. 18 refers that

1 Exeligmos = 669 Synodic cycles = 19756 days = 723 zodiac cycles +32° = 723+(32°/360°) = 723.08888 zodiac cycles (sidereal) (2).

19756^{d}/723.08888 sidereal cycles = 27.3216758^{d}/Sidereal cycle ≈ **655.72 hours/Sidereal cycle.**

Let us divide the Zodiac month ring in 365 equal subdivisions-days (unit of time measuring), instead of 360 un-equal degrees (unit of angle measuring) see Voulgaris et al. 2018a.

The Lunar pointer sweeps the 365.25 subdivisions (365+0.25 is achieved by the rotation of the zodiac month ring by one subdivision/4 years) in one Sidereal cycle:

655.72 hours/365.25 subdivisions = **1.795263 hours/subdivision** (≈ **1.8 hours/subdivision).**

Therefore, one (mean) synodic cycle of 29.5306427^{d} as resulted from (2) corresponds to

≈ 394.78 zodiac subdivisions = one full rotation (365.25)+29.53 subdivisions.

Geminus also writes: *Η ΣΕΛΗΝΗ ΑΝΩΜΑΛΩΣ ΦΑΙΝΕΤΑΙ ΔΙΑΠΟΡΕΥΟΜΕΝΗ ΤΟΝ ΖΩΔΙΑΚΟΝ ΚΥΚΛΟΝ , The Moon travels the zodiac circle at variable velocity*.

On the Antikythera Mechanism, during the re-aiming of the Lunar pointer to the Golden sphere (synodic cycle), the Lunar pointer scans a number of subdivisions. This number is not constant, because the synodic cycle duration varies as a result of the *pin&slot* variable angular velocity.

By applying the equations for the angular velocity produced by the *pin&slot* factor (without any external information or modern lunar theory), the synodic cycle duration varies between 29.31^{d} – 29.81^{d}, thus the lunar pointer could scan 391.9 – 398.55 subdivisions in a synodic cycle.

For each synodic cycle, the ancient manufacturer measured the total number of the (Zodiac) subdivisions and then multiplied by 1.8 in order to transform them into hours (on the Back Cover

Inscription Part-II, the words *ΕΓΛΕΙΠΤΙΚΟΙ ΧΡΟΝΟΙ*, probably *times of eclipses*, are mentioned, Bitsakis & Jones 2016). Afterwards, he transformed the number of hours into hours of daytime/nighttime.

This way, the calculation of the eclipse event times, is achieved by only using the Antikythera Mechanism without any use of external information which is not directly related to the Mechanism.

Moreover, if he copied the time information from a papyrus or by applying mathematical calculation models, this could create a mismatch between the times of the papyrus and the times appearing on his creation on the Zodiac dial ring. As the Zodiac subdivisions/hours correspond to a specific position of the Zodiac sky at which the eclipse occurs, a mismatch could place the eclipse at a different position than where it appears on the Mechanism's Zodiac subdivisions (see below, *Sky backround during an eclipse event*).

d) Errors in the eclipse events times calculations, as a result of the gears/axes constructional imperfections

The calculation of the eclipse times demands high accuracy: The eclipse time calculation is subject to a bigger relative error than the eclipse events calculation:

- The eclipse events calculation is based on the synodic month.

- The time of an eclipse event is based on the duration of the synodic month calculated in hours, i.e. $24x29.53^{d} = 708.7^{h}$, meaning that the eclipse time calculation demands accuracy that is 2.85 orders of magnitude higher than the synodic cycle calculation.

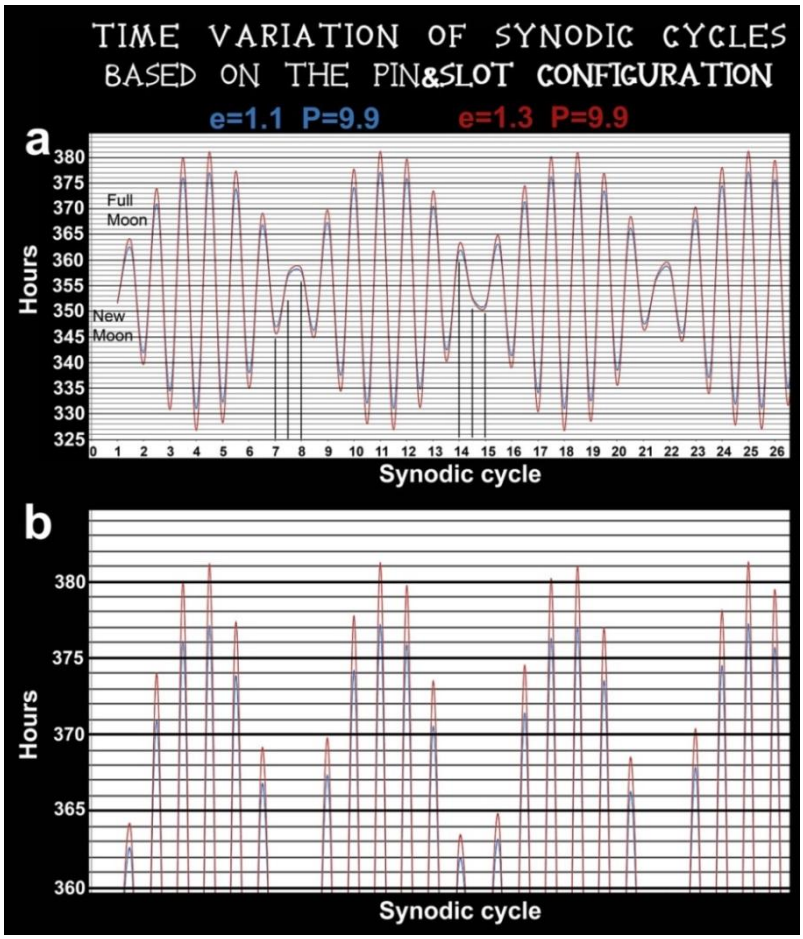

Figure 11. The variable duration each of of the half synodic month based on the *pin&slot* variable angular velocity of the Antikythera Mechanism: **a –** the graph present the duration of

each half synodic month (New Moon to Full Moon to New Moon), which was calculated based on the *pin&slot* configuration of the Antikythera Mechanism. X-axis: Synodic months-Saros cells (New Moon phase in Integer numbers, the Full Moon phase in integer +0.5. Y-axis: each half synodic month duration in hours. The mean synodic month is 708.7354 hours, and the mean half synodic month is 354.3677 hours. Blue graph: the results are based on current measurements of the pin position and the eccentricity of k-axis. Red graph: By increasing the value of k-axis eccentricity by =0.2 mm, the half synodic month duration increases significantly (max ≈ +8 hours). **b** – close-up of **a.**

Taking into account that in a geared machine there are constructional imperfections/mechanical errors, the time events calculation results would probably be affected by such errors.

On the Antikythera Mechanism, the variable duration each of synodic month is defined by the *pin&slot* operation. The dimensional characteristics of the *pin&slot*/eccentricity *e* of k-axis and the distance P of the pin from the gear axis (Freeth 2006; Voulgaris et al. 2018b), strongly affect the motion variability and the duration of each synodic month calculated by the Antikythera Mechanism gearing. The current values for the eccentricity of k-axis is e=1.1 mm and for the pin distance P=9.9 mm (measured on the parts in their present condition, as the bronze material has changed into Atacamite i.e. with different volume and dencity, Voulgaris et al. 2019b).

By slightly increasing the eccentricity *e* of k-axis by +0.2 mm (= 1.3 mm) the hours of the events could vary by about ±8 hours (Fig. 11). Keeping the value for k-axis eccentricity at 1.1 mm and increasing the pin distance at 10.1 mm, the synodic month duration changes by about one hour.

e) Sky backround (Zodiac constellations) during an eclipse event

During an eclipse event, e.g. a solar eclipse, the lunar pointer aims at the Golden sphere-Sun and the solar pointer aims at a zodiac subdivision. This subdivision belongs to a specific zodiac constellation. Let us assume that the solar pointer-ΗΛΙΟΥ ΑΚΤΙΝ aims at the first zodiac subdivision of Leo in which the index letter Π is engraved. The index letter Π, probably corresponds to the Parapegma event Π-ΛΕΩΝ ΑΡΧΕΤΑΙ ΕΠΙΤΕΛΛΕΙΝ (Leo begins to rise), which is partially preserved on the PPI-2 (Bitsakis & Jones 2016).

The brightest star of Leo is called ΒΑΣΙΛΙΣΚΟΣ (Regulus). Therefore, during the specific solar eclipse, the Sun, the Moon and Regulus are in conjunction. As Regulus begins to rise in conjunction to the Sun, this means that the specific solar eclipse will be occurred during sunrise, i.e. during the first hour (Η, ΩΡΑ Α, ΗΜ/solar eclipse hour 1st Daytime).

If the solar eclipse is total, then Regulus is visible to the naked eye during totality (Fig. 12), as also mentioned by *Diodorus of Sicily* in his *Library of History* (XX: 5–6, in eds. Bekker et al. 1903-1906), describing the total solar eclipse of Agathocles, which occurred on August 15, 310 BC: *On the next day there occurred such an eclipse of the Sun that utter darkness set in and the stars were seen everywhere* (see also Stephenson et al. 2020).

Figure 12. An overexposed wide angle photograph of the total solar eclipse of August 21, 2017, shot from Salem, Oregon,USA. Prominent are the bright inner corona (saturated), the extended outer corona with streamers, the polar plumes, the New Moon surface details and a number of stars. The brighter star is a-Leo-Regulus, which was visible to the naked eye during totality. The day of the eclipse, the Sun and Regulus rose at about the same time. Image and process by Aristeidis Voulgaris.

This way the Antikythera Mechanism provides information regarding the background sky at which an event will be occurred.

Conclusions

Based on the results of this work, the suggested by the authors Draconic gearing (Voulgaris et al. 2022 and in this work) appears less hypothetical and more likely to have really been a part of the Antikythera Mechanism, as it gives satisfactory results and answers to a number of important questions, that related to the specific eclipse events sequence and their times of occurrence. It also removes the question '*why did the ancient Manufacturer include in his creation only the three out of the four lunar cycles, rejecting the fourth, very important lunar cycle, well known and used during the Hellenistic era?*' It seems that the ancient Manufacturer was an experienced astronomer and constructor and knew for sure that the Draconic cycle is the key to real eclipse prediction. Moreover, the unplaced Fragment D-gear r1 can be well correlated to the Draconic gearing (Voulgaris et al. 2022).

We believe that the ancient Manufacturer, who lived before 178 BC (Voulgaris et al. 2023a), constructed the Mechanism in order to find out the forthcoming eclipse events and the hours of their occurrence. By introducing the four lunar cycles Sidereal, Synodic, Anomalistic and Draconic in his creation, he could predict the eclipse events sequence and the relative data based entirely on a mechanical procedure without any external information.

When he finished the assembly of his creation, the ancient Manufacturer set the Mechanism pointers on their initial positions according to the starting date of December 22/23, 178 BC (Voulgaris et al. 2023a) and at that time the 223 cells of the Saros spiral were blank cells - no engraved information.

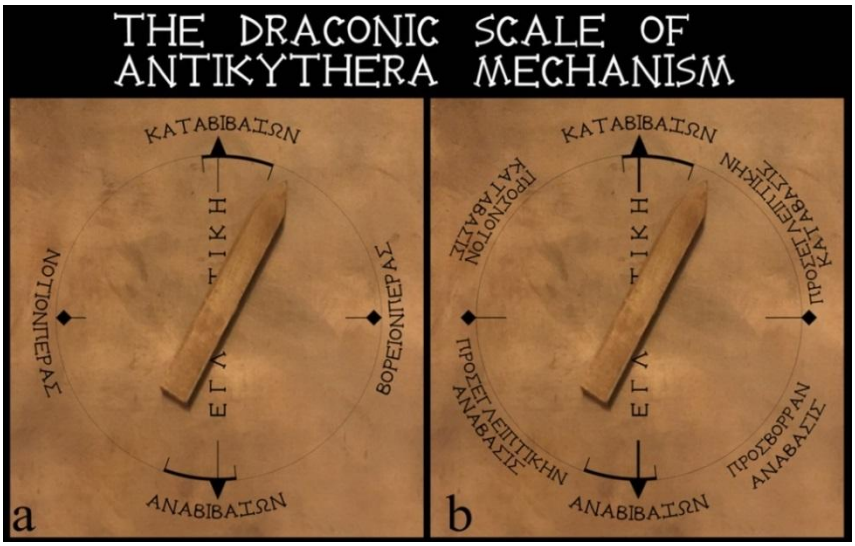

Figure 13. The two designs of the Antikythera Mechanism Draconic scale, suggested by the authors. The Draconic scale could be located at the right side of Fragment A1: **a –** The Greek words ΕΓΛΕΙΠΤΙΚΗ (Ecliptic), ΑΝΑΒΙΒΑΖΩΝ/ΚΑΤΑΒΙΒΑΖΩΝ (Ascending/Descending Node), ΒΟΡΕΙΟΝ ΠΕΡΑΣ (North maximum Declination) and ΝΟΤΙΟΝ ΠΕΡΑΣ (South maximum Declination); **b –** ΠΡΟΣ ΒΟΡΡΑΝ ΑΝΑΒΑΣΙΣ (The Moon ascends towards the North), ΠΡΟΣ ΕΓΛΕΙΠΤΙΚΗΝ ΚΑΤΑΒΑΣΙΣ (The Moon descends towards the Ecliptic), ΠΡΟΣ ΝΟΤΟΝ ΚΑΤΑΒΑΣΙΣ (The Moon descends towards the South), ΠΡΟΣ ΕΓΛΕΙΠΤΙΚΗΝ ΑΝΑΒΑΣΙΣ (The Moon ascends towards the Ecliptic). The black arcs depict the (symmetrical) ecliptic limits.

Then, he started to operate his construction: when the Lunar pointer aimed at the Golden Sphere-Sun/New Moon (or in opposite position Full Moon) and the Draconic pointer was located somewhere between the ecliptic window (Fig. 13, 15), a solar eclipse would occur (see Fig. 17 of Voulgaris et. al 2022). At the same time he measured the (scanned) zodiac subdivisions during the re-aiming of the Lunar pointer to the Golden Sphere (New moon-new synodic month).

Afterwards, the ancient Manufacturer engraved the specific event and the time of its occurrence on the cell at which the Saros pointer aimed (Fig. 14).

The ancient Manufacturer had the remarkable idea to construct a time-machine, an astronomical event predictor based solely on the mechanical procedure involving the engaged gears. This must have been a great achievement for that time!

His creation was a real predicting device of the future astronomical events. But the constructional imperfections/gearing errors created some deviations in the pointers' position by about 0°–3° (or 4°), affecting the final results.

In any measurement attempt, the use of a measuring instrument impacts more or less the outcome. Even the light emitted/reflected from an object, when is collected by an objective lens, the position of the rays are affected by the objective lens errors and the diffraction, which change the *Reality*, the *Truth* and the *Originality* of the object's information (known as *Module Transformation Function* Hecht 2016, p. 544, 569; Vanidhis 2022, p. 127-168). The smaller the impact of an instrument on the measurement, the better the proximity to the true value, and the closer to representing *Reality*.

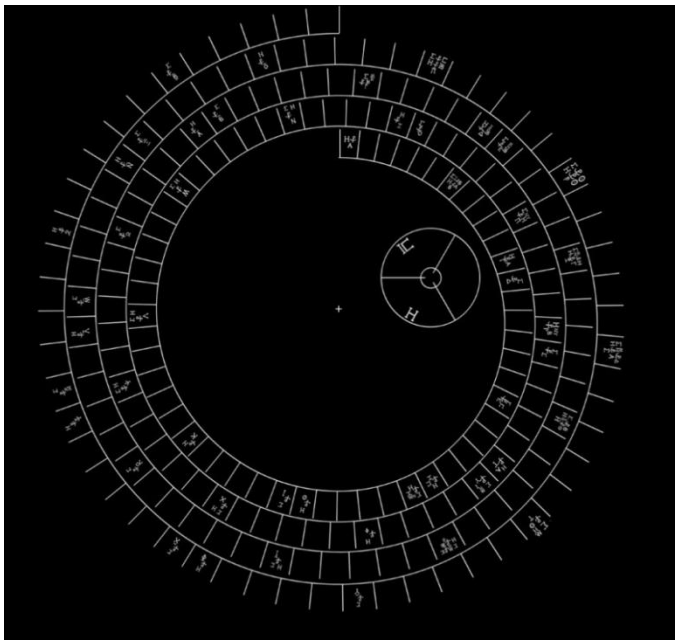

Figure 14. The reconstructed eclipse events of the Saros spiral by the *DracoNod* program and applying the Draconic gearing. The predicted events compromised according to the preserved events and the index numbering. The 64/(65) events in total are distributed in 50 cells (for the analysis, see Appendix A to the text).

Today, it can be measured dimensional errors that are impossible to be detected by the human eye. At the Hellenistic era, the only perceived dimensional/constructional errors were those that could be detected by naked eye, or by using some simple measuring tools (e.g. a compass), also having as a criterion the naked eye. As a result of the limited ability of error measuring for the mechanical parts construction, the mechanical calculations for the eclipse events prediction (could slightly) differed from current calculations that are based on the more complex calculations and the digital manipulation of the data (which are by about 4.5 orders of magnitude more accurate).

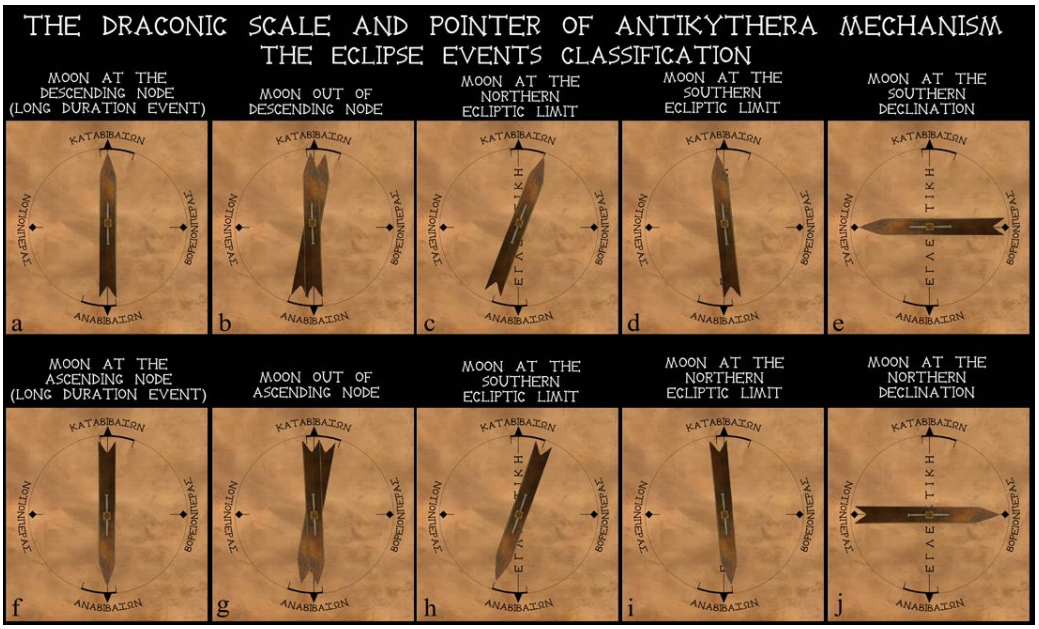

Figure 15. The different positions of the Draconic pointer during its rotation on the Draconic scale. The eclipse events classification presented by the ancient Manufacturer (engraved in

several places on the Back dial plate and today is partially preserved, Anastasiou et al. 2016; Freeth 2014, 2019; Iversen & Jones 2019; Jones 2020). According to the present work the classification resulted by the position of the Draconic pointer relatively to the ecliptic limits: Moon at Node, out of Node, on the ecliptic limit. When the Draconic pointer aims out of the ecliptic limits, no eclipse event occurs. When the Draconic pointer aims to the Northern/Southern limit (maximum Declination) the Moon is about 5.14° above/below Ecliptic.

Finally, a question arises: if we reconstruct 10 functional models of the Mechanism which have the same pointers' calibration, will each of the pointers, after applying the same number of Input rotations, be aiming exactly at the same position?
As the gears and their teeth, the axes, the shafts and the scales cannot be perfectly the same, finally these different constructional mismatches affect the final position of the pointers and the calculated results. As the ancient Greek philosopher Heraclitus quoted: Ποταμῷ γὰρ οὐκ ἔστιν ἐμβῆναι δὶς τῷ αὐτῷ, *No man ever steps in the same river twice* (as both the man and the river cannot be the same).

Acknowledgments

We are very grateful to prof. Xenophon Moussas (National and Kapodistrian University of Athens University) who provided us with the X-ray Raw Volume data of the Antikythera Mechanism fragments. Thanks are due to the National Archaeological Museum of Athens, Greece, for permitting us to photograph and study the Mechanism fragments. We also thank G. Pistikoudis of '*Astroevents in Greece*' company for his hospitality and support in Trilofos of Thessaloniki, North Greece, in order to measure the periodic errors of our equatorial mounts and D. Varvarousis for his help for the data recording during the penumbral eclipse of 2020.

Appendix A

Data presentation, the *DracoNod* program, Comments, and Notes

1. Introduction. DracoNod program information

We present the integrated eclipse events sequence of the Saros spiral, including the lost eclipse events. The lost eclipse events reconstruction was achieved by the use of the authors' program named *DracoNod*, which presents the phase correlation of the three (four) lunar cycles Synodic, Draconic and Anomalistic and Sidereal), in the graphic environment.

DracoNod program presents three cycles with their corresponding orbital radius and cycles subdivisions.

1st Circle: **Synodic cycle**, Period 1/223 of Saros. Two subdivisions: New Moon and Full Moon,

2nd Circle: **Draconic cycle**, Period 1/242 of Saros. Two subdivisions: Node-A and Node-B,

3rd Circle: **Anomalistic cycle**, Period 1/239 of Saros. Two subdivisions: Apogee and Perigee.

Synodic cycle index bar: for Number x = Cell (x+1) (New Moon phase - 29th or 30th day of synodic month), for Number (x+0.5) = Cell (x+1.5) (Full Moon phase - 15th day of synodic month). The epicenter angle of the ecliptic windows are depicted in yellow lines. The ecliptic windows depicted as arcs are presented in green and blue colors. The cycles' phase position is presented with the three independent orbital radii, black for Synodic cycle, red with three arrows for Draconic cycle and green for Anomalistic cycle.

When New Moon is located between the ecliptic limits (ecliptic window in green and in blue color) a solar eclipse occurs (symbol H-Helios-Sun on the cell x). When Full Moon is located between the ecliptic limits, a lunar eclipse occurs (symbol Σ-Selene-Moon on the cell x+0.5).

When Full Moon and New Moon of the same synodic month is located between the ecliptic limits, then the symbols Σ+H exist on the same cell.

The events presented in specific codification, e.g.

Figure A.x. Event 44. Cell 148/K2: Lunar eclipse event (Σ). Full Moon close to Node-A and at Apogee.

- Event 44: Is the 44th Eclipse event
- (or somewhere else as event with Latin number, e.g. Event IV): these events present a high indeterminacy, and are not joined to the main team of the eclipse events (I-V)
- Cell 148: this event is located at the Saros spiral cell no. 148 (new numbering according to Voulgaris et al. 2021).
- /K2: Is the index number introduced by the ancient Manufacturer of the AM (or resulted by the rest preserved index number).
- Lunar eclipse event (Σ): This event is a Lunar eclipse and is marked with the letter Σ.
- Full Moon close to Node-A and at Apogee: here are some comments (if it is needed).

For the (general consideration of) preserved eclipse events (well, partially, poorly etc. see Iversen & Jones 2019; Voulgaris et al. 2021) the word "(*preserved*)" is referred.

DracoNod program starts with New Moon at Node-A and at Apogee as resulted by the analysis of Geminus' definition for Exeligmos/(Saros) (Voulgaris et al., 2023a, see also https://arxiv.org/ftp/arxiv/papers/2203/2203.15045.pdf).

2. Antikythera Mechanism pointers' starting position

The pointers of the three lunar cycles located at their starting position (Voulgaris et al. 2023a).

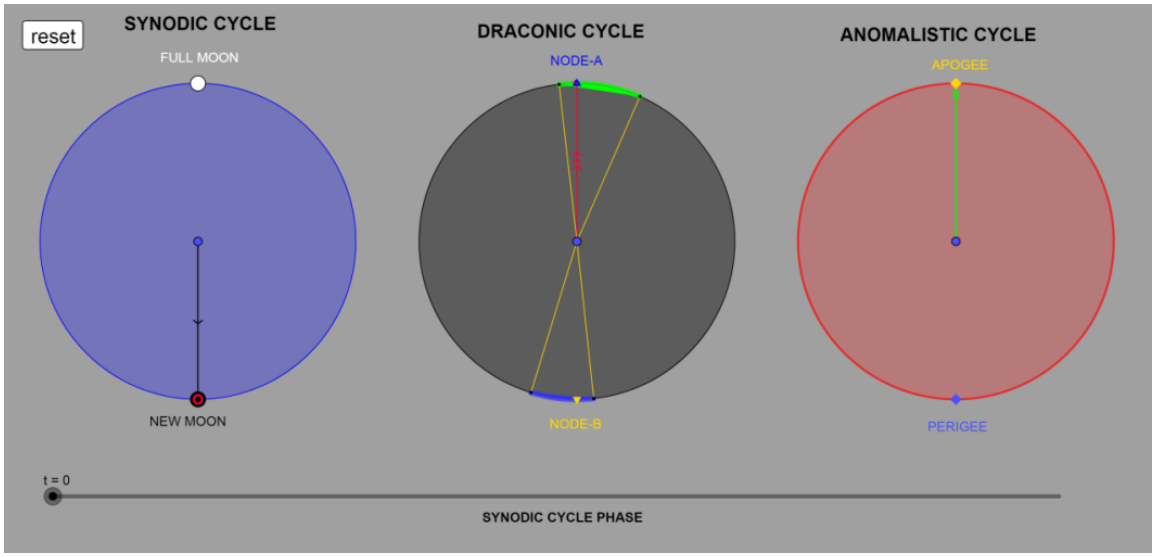

Figure A1. Cell 01/A1 (end of Cell-01): Solar eclipse event (H). New moon at Node-A and at Apogee. Saros/(Exeligmos) period begins.

3. Indeterminacy error or gearing errors

Below, we present two characteristic events, which were predicted from *DracoNod*:

- On cell 65 no event occurs: The position of New Moon is just on the ecliptic limit (a solar eclipse occurs or not?). The specific position of the Draconic pointer (red radius) presents a high indeterminacy. It is difficult for the user to decide if the Draconic pointer is located *on* or *out* of the ecliptic limit.

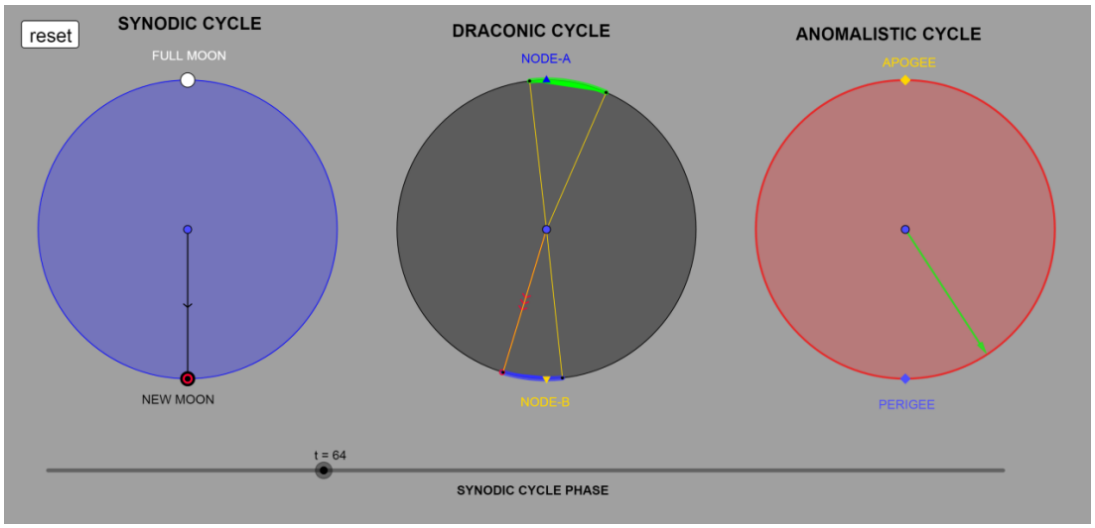

Figure A.2. *DracoNod* calculation for Cell 65: New Moon just on the ecliptic limit. The event presents a high indeterminacy.

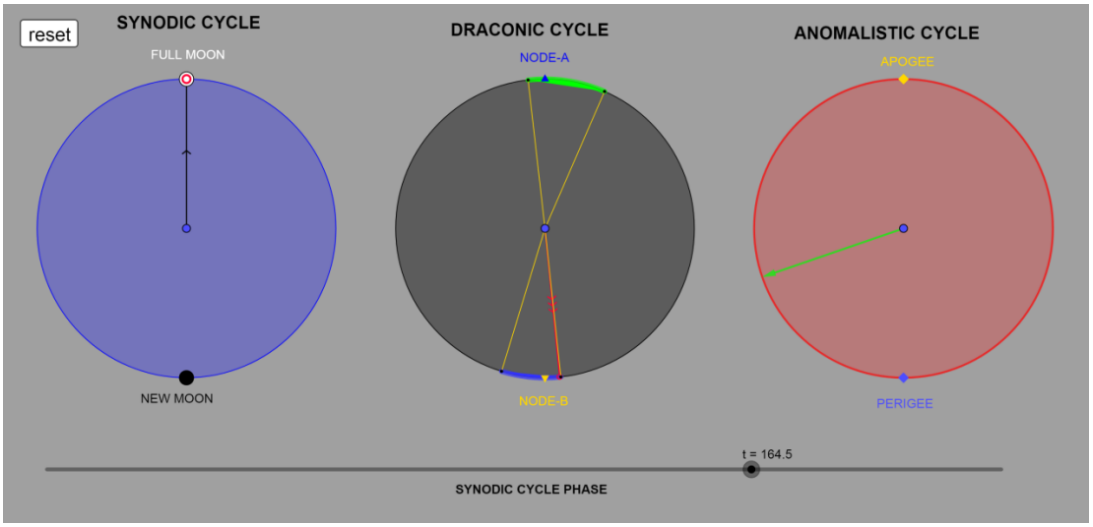

Figure A.3. *DracoNod* calculation for Cell 166: Lunar eclipse event (Σ). Full Moon too close to ecliptic limit, but inside the ecliptic window - event at the limit.

Additionally, the gear(s) error (eccentricity or teeth un-uniformity) affects the position of the Draconic pointer creating a deviation from the original position see Section 7, (as also the error of eccentricity of the pulleys affects the final position of the projected lunar shadow in the Earth's surface: see the cover image in Espenak & Meeus 2009). Events just on the ecliptic limit can be considered *inside* or *outside* the ecliptic window due to the gearing errors. On the preserved eclipse events sequence, three events should be existed. However, they are not engraved on the Saros spiral (Freeth 2014; Carman and Evans 2014; Anastasiou et al., 2016, Iversen and Jones 2019). The eccentricity also affects the classification of the events: e.g. an eclipse event (theoretically) occurred just on the Node, could be located out from the Node resulting to its different classification (Voulgaris et al.*).

4. Ecliptic limits and Eclipses

Some characteristic positions of the Moon relative to a Node are generally discussed:

- If the New Moon is located exactly at the Node, then this solar eclipse will be total or annular and the shadow path will be projected around the Earth's equator.
- If the New Moon is located to the north and faraway from a Node, the eclipse will be visible from the northern parts of the Earth.
- If the New Moon is located just right to the southern ecliptic limit, the solar eclipse will be visible from the South Pole and will be a partial eclipse.
- If a Lunar eclipse occurs just right on the Node, it is a total Lunar eclipse.
- If the Full Moon is located faraway from a Node, then this eclipse is partial.
- If it is located too close to an ecliptic limit, then it is a Penumbral eclipse.

When the New Moon/Full Moon is located exactly at a Node, the Gamma of the eclipse will be too close to 0 and the eclipse shadow will be very central.

There are two characteristic patterns when three eclipses occur in two successive synodic months:

- If a total/annular solar eclipse occurs and just right on the Node (https://eclipse.gsfc.nasa.gov/SEplot/SEplot2001/SE2020Jun21A.GIF), then one fortnight (half synodic month) before (https://eclipse.gsfc.nasa.gov/LEplot/LEplot2001/LE2020Jun05N.pdf) and one fortnight after this date

(https://eclipse.gsfc.nasa.gov/LEplot/LEplot2001/LE2020Jul05N.pdf) a Lunar penumbral eclipse will occur.

- If a total lunar eclipse occurs just right on the Node (https://eclipse.gsfc.nasa.gov/LEplot/LEplot2001/LE2018Jul27T.pdf), then one fortnight before (https://eclipse.gsfc.nasa.gov/SEplot/SEplot2001/SE2018Jul13P.GIF) and after (https://eclipse.gsfc.nasa.gov/SEplot/SEplot2001/SE2018Aug11P.GIF) this date, two partial Solar Eclipses will be visible alternately from the Earth's poles.

Two patterns of successive events are preserved on the Saros spiral:

Σ+H (in one cell) or H+Σ in two successive cells.

Not both of the eclipses can occur on/close to the Nodes. If one of the eclipses occurs on the Node (H: total/annular solar eclipse or Σ: total lunar), the second eclipse will occur out of the Node (Σ: partial lunar eclipse or H: solar eclipse visible in high latitudes).

5. The errors of the '*Instrument-User*' system

https://www.watelectrical.com/different-types-of-errors-in-measurement-and-measurement-error-calculation/;
https://www.webassign.net/question_assets/unccolphysmechl1/measurements/manual.html;
https://www.elprocus.com/what-are-errors-in-measurement-types-of-errors-with-calculation/.
https://www.wikihow.com/Read-a-Multimeter.

6. The Periodic Error Correction-PEC

The PEC (Periodic Error Correction) procedure: via an educated algorithm, the motor is not rotated at constant velocity, but at variable (inversed) velocity, in order to compensate the error of eccentricity. This procedure is used for the Equatorial mounts of telescopes and it is totally necessary for the astrophotography,

http://eq-mod.sourceforge.net/eqspeed.htm
https://astrojolo.com/gears/mount-periodic-error/.

7. Predicting of the eclipse events sequence using the *DracoNod* program

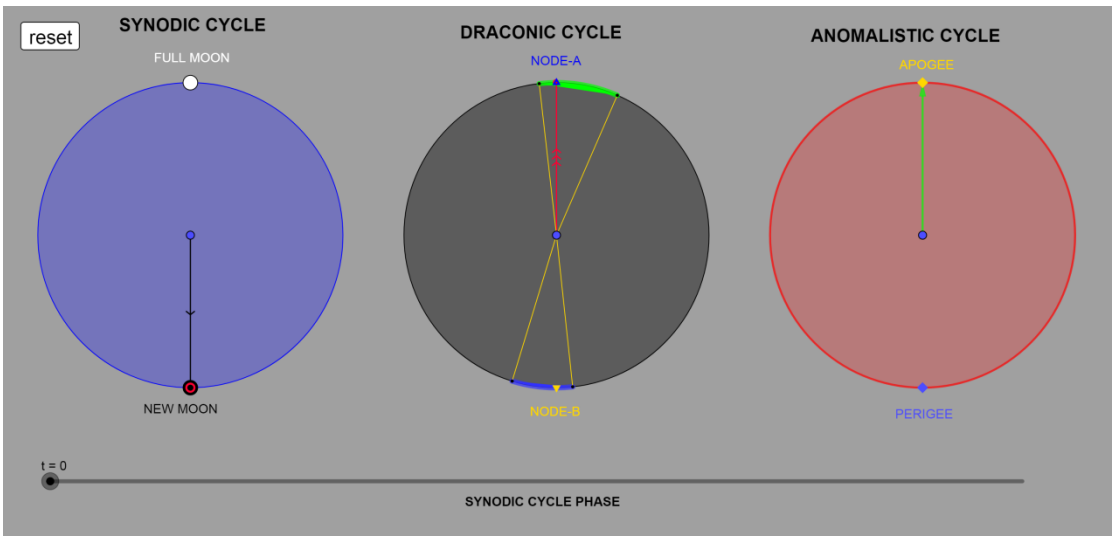

Figure A.4. Event 1. Cell 01/A1: Solar eclipse event (H). New moon at Node-A and at Apogee. Saros period begins.

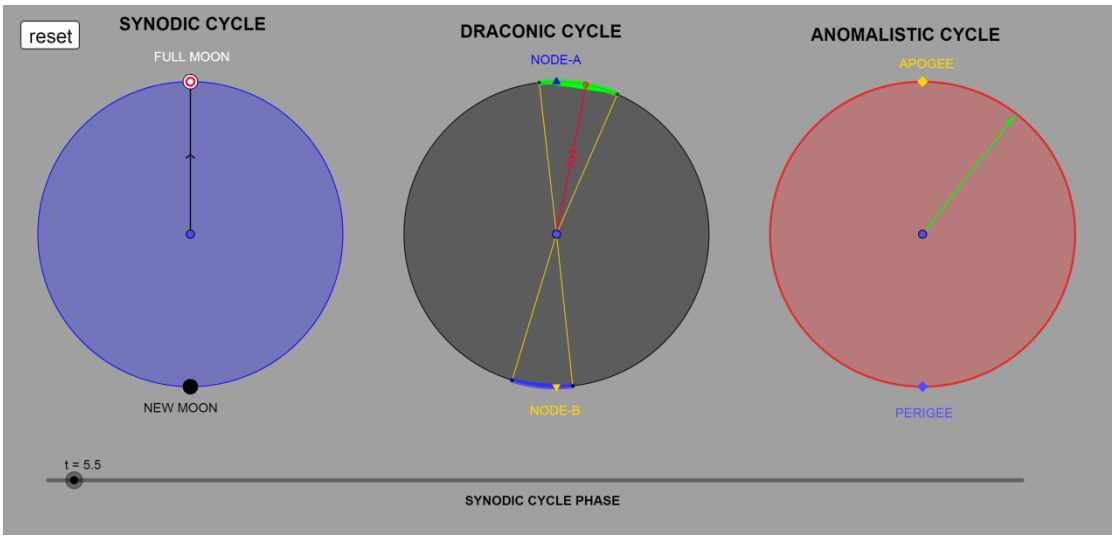

Figure A.5. Event 2. Cell 07/B1: Lunar eclipse event (Σ), (*preserved*).

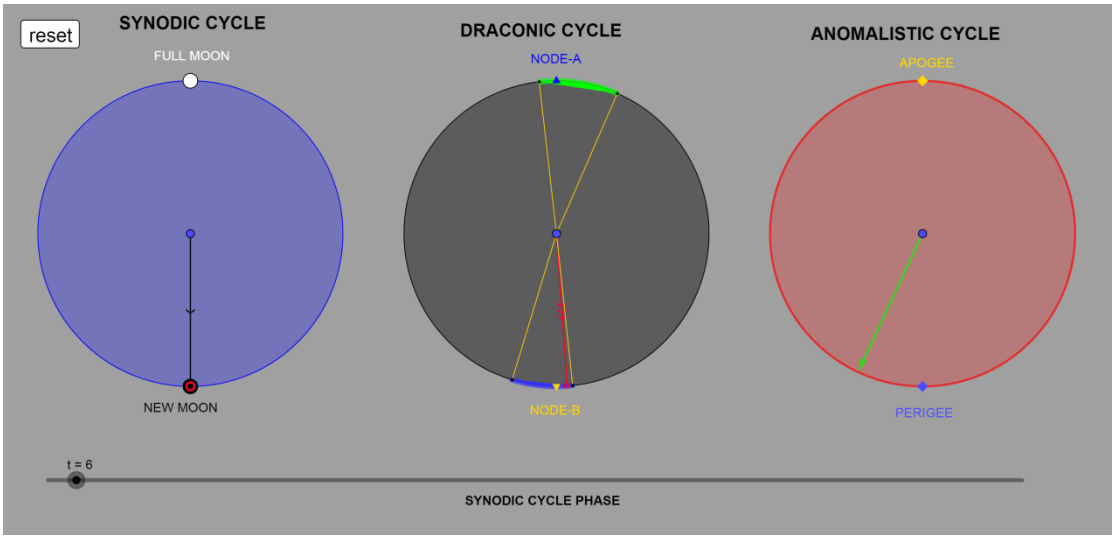

Figure A.6. Event 3. Cell 07/B1: Solar eclipse event (H) (*preserved*). New Moon close to the ecliptic limit.

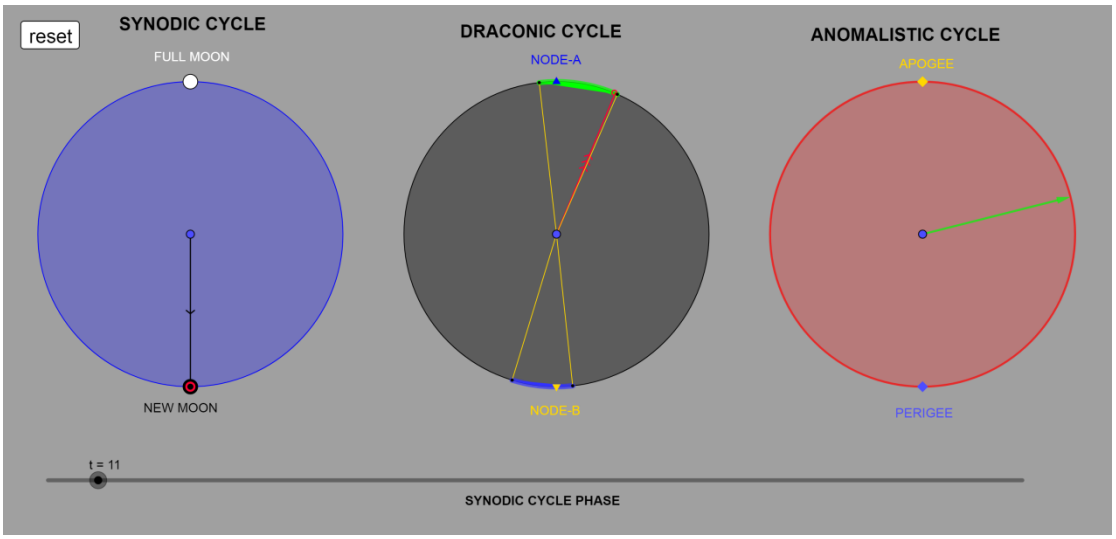

Figure A.7. Event 4. Cell 12/Γ1: Solar eclipse event (H) (*preserved*). New Moon close to the ecliptic limit.

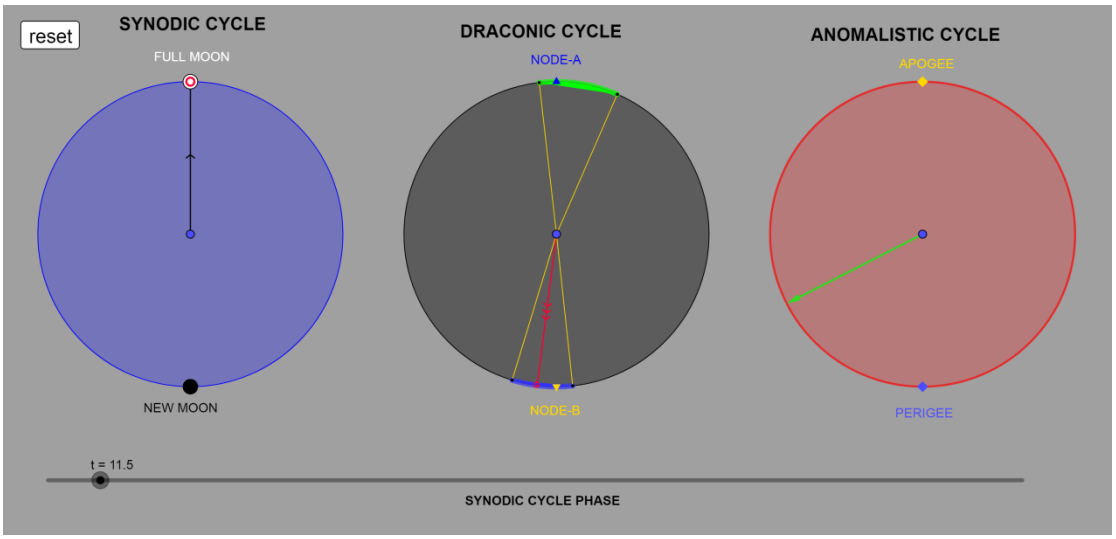

Figure A.8. Event 5. Cell 13/Δ1: Lunar eclipse event (Σ).

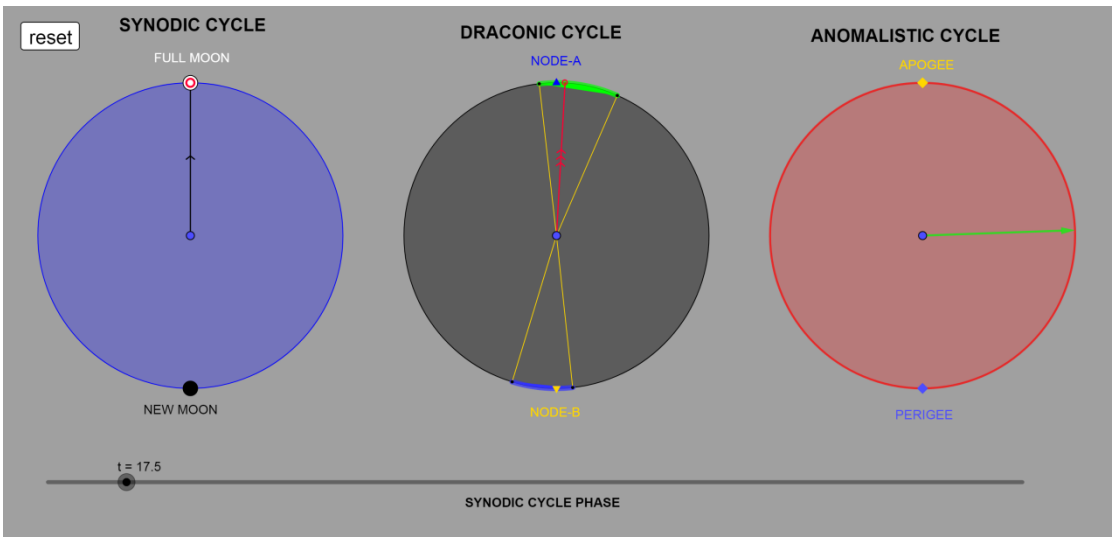

Figure A.9. Event 6. Cell 19/E1: Lunar eclipse event (Σ) (*preserved*). Full Moon close to Node-A.

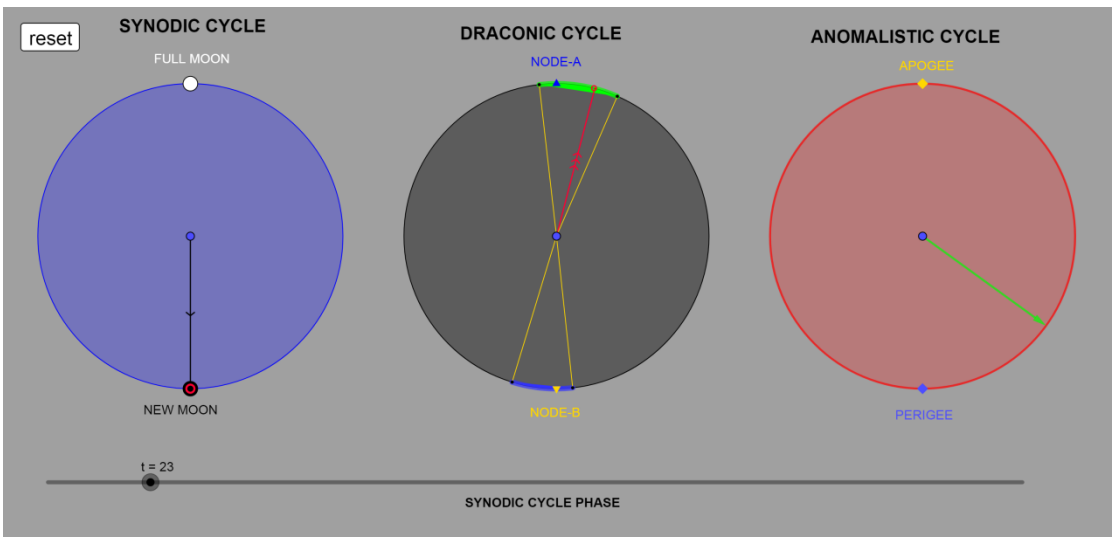

Figure A.10. Event 7. Cell 24/Z1: Solar eclipse event (H) (*preserved*).

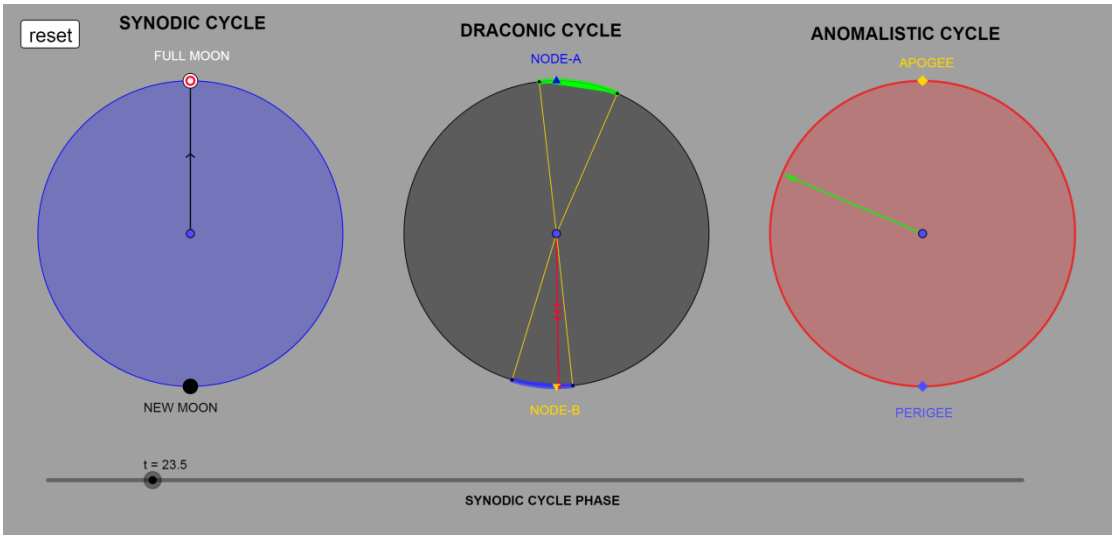

Figure A.11. Event 8. Cell 25/H1: Lunar eclipse event (Σ) (*preserved*). Full Moon at Node-B.

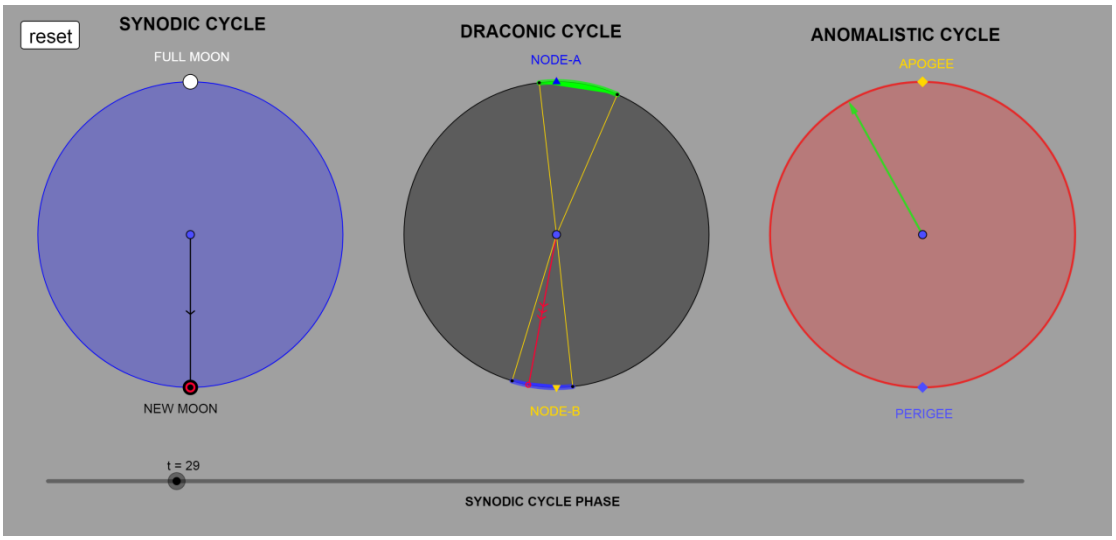

Figure A.12. Event 9. Cell 30/Θ1: Solar eclipse event (H).

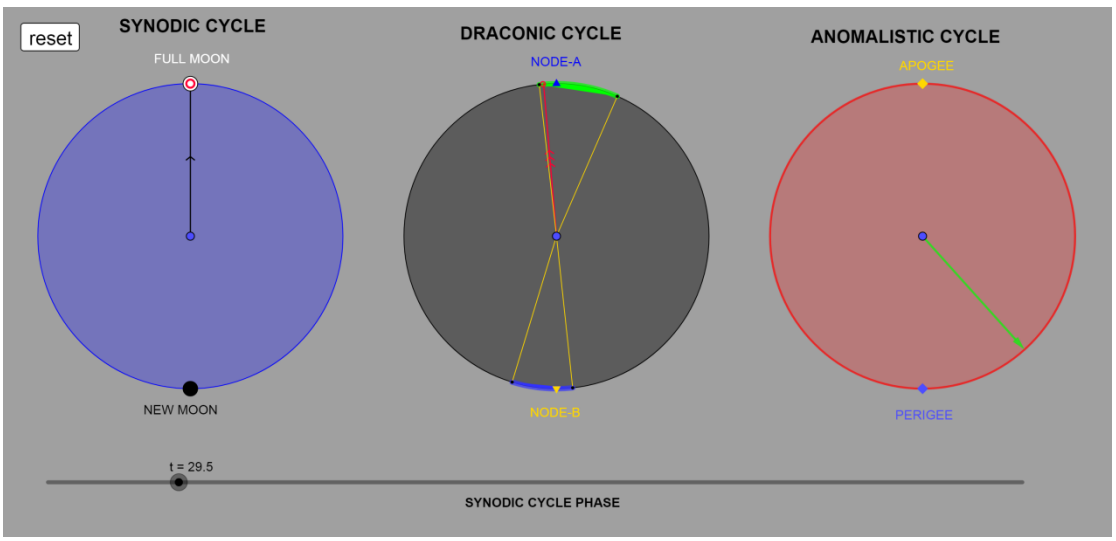

Figure A.13. Event 10. Cell 31/I1: Lunar eclipse event (Σ). Full Moon close to ecliptic limit.

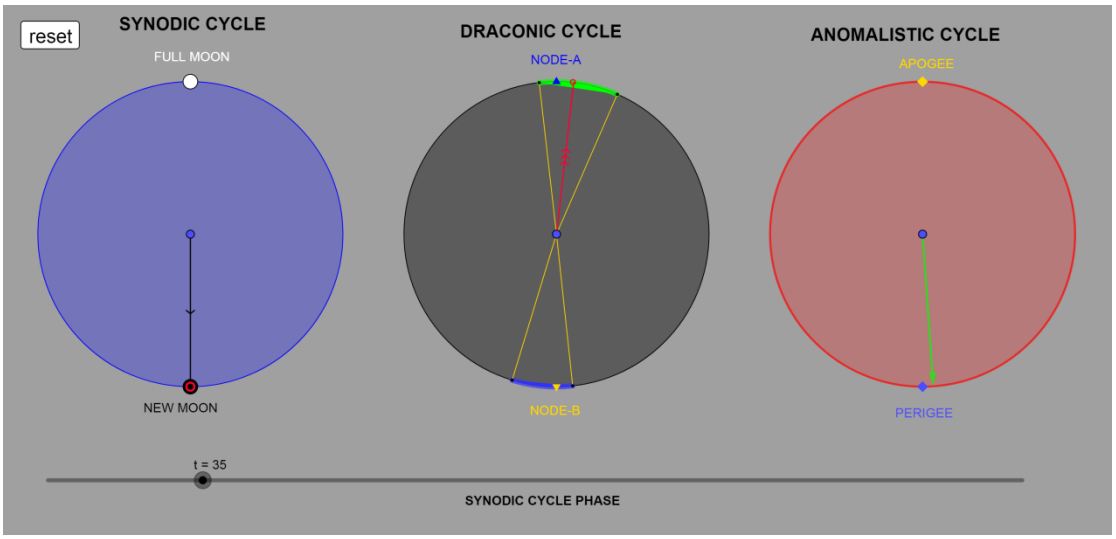

Figure A.14. Event 11. Cell 36/K1: Solar eclipse event (H). New Moon close to Node-A and at Perigee.

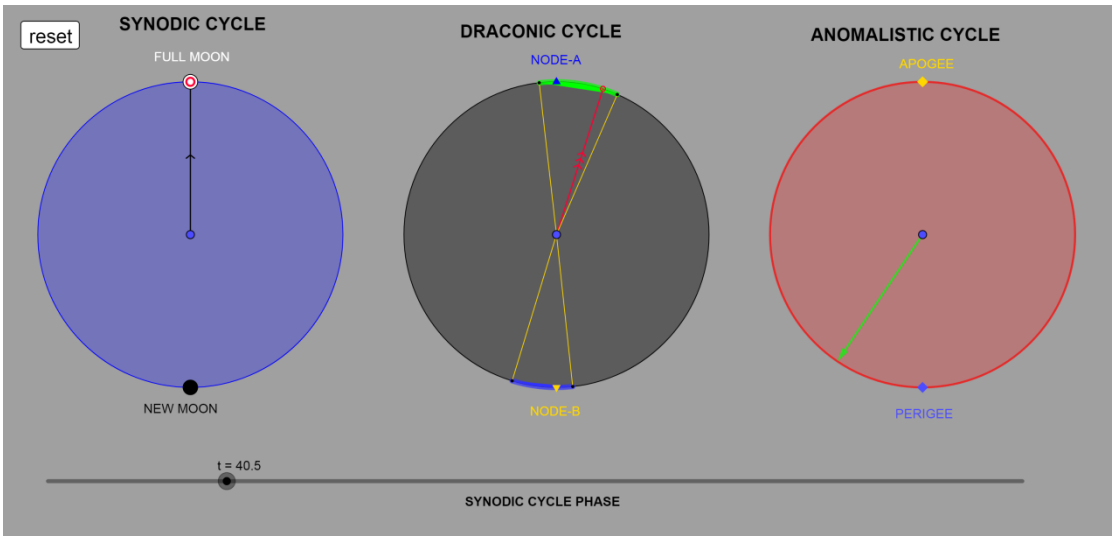

Figure A.15. Event 12. Cell 42/Λ1: Lunar eclipse event (Σ).

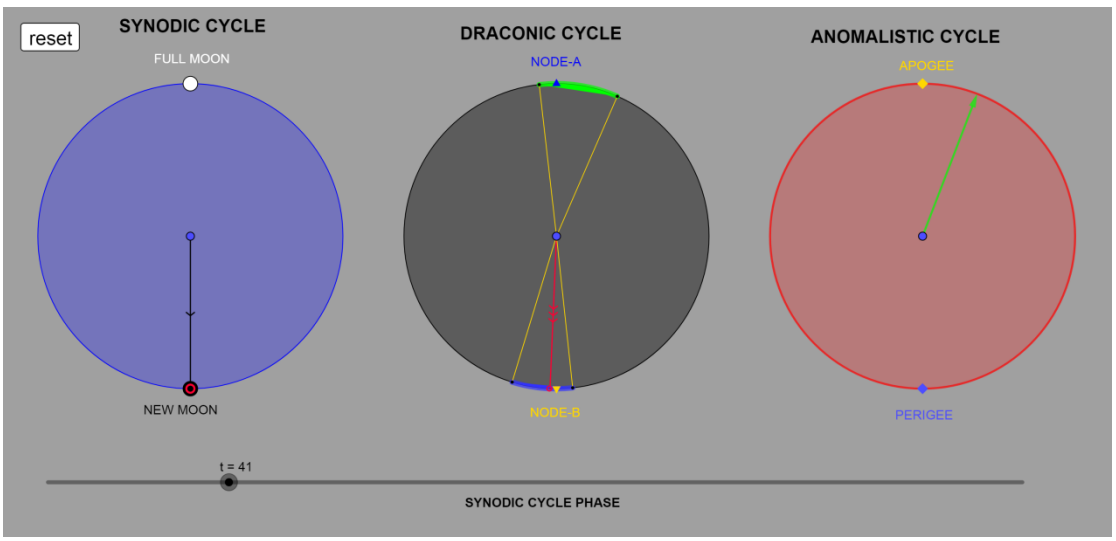

Figure A.16. Event 13. Cell 42/Λ1: Solar eclipse event (H). New Moon close to Node-B.

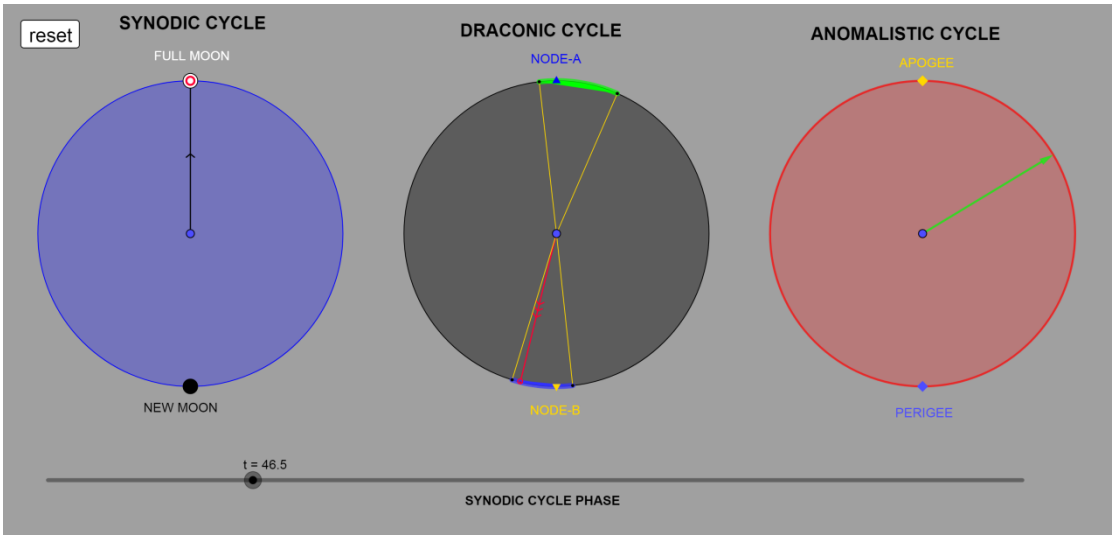

Figure A.17. Event 14. Cell 48/M1: Lunar eclipse event (Σ). Full Moon close to ecliptic limit.

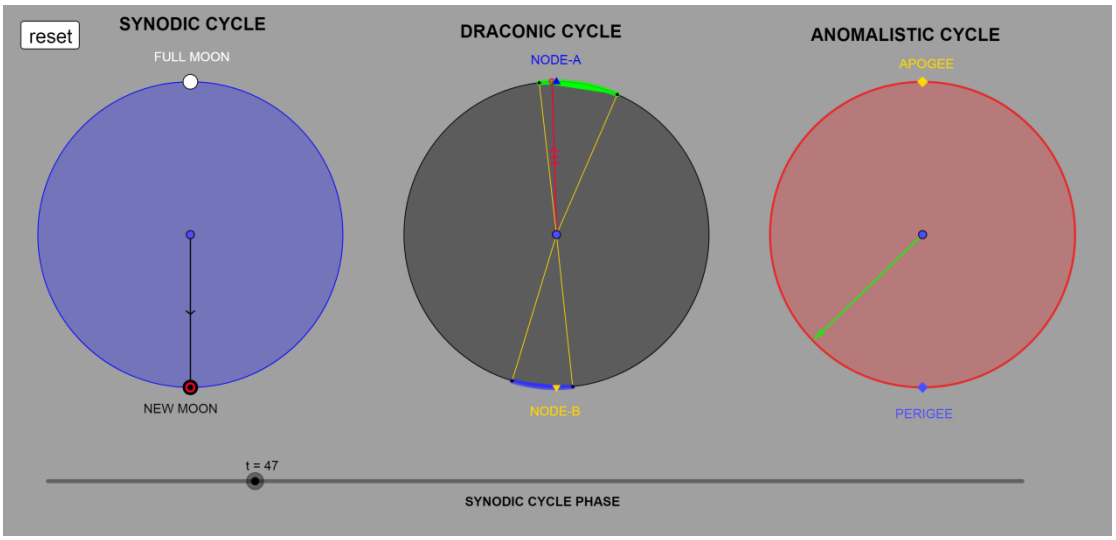

Figure A.18. Event 15. Cell 48/M1: Solar eclipse event (H). New Moon close to Node-A.

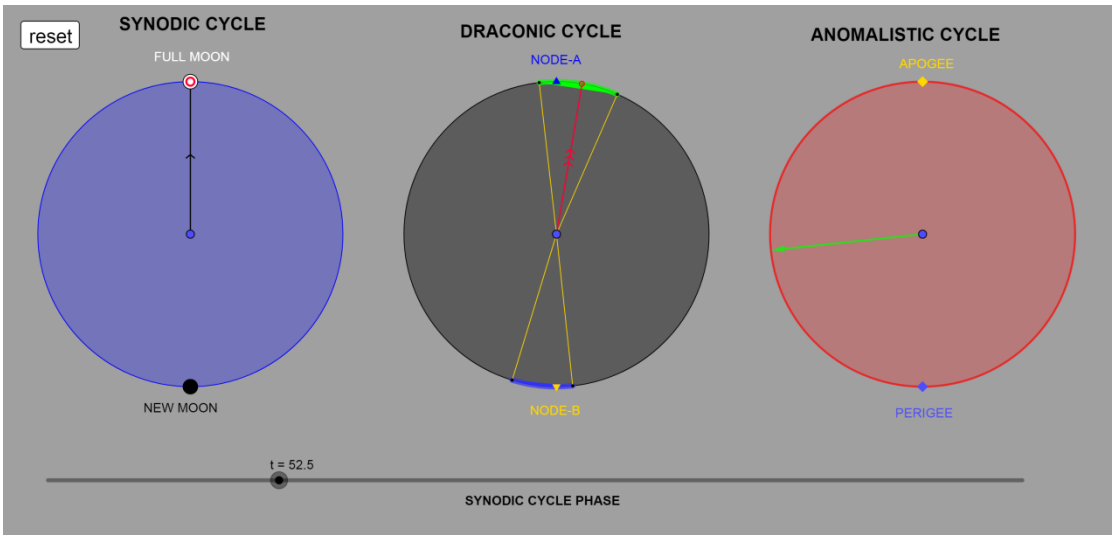

Figure A.19. Event 16. Cell 54/N1: Lunar eclipse event (Σ).

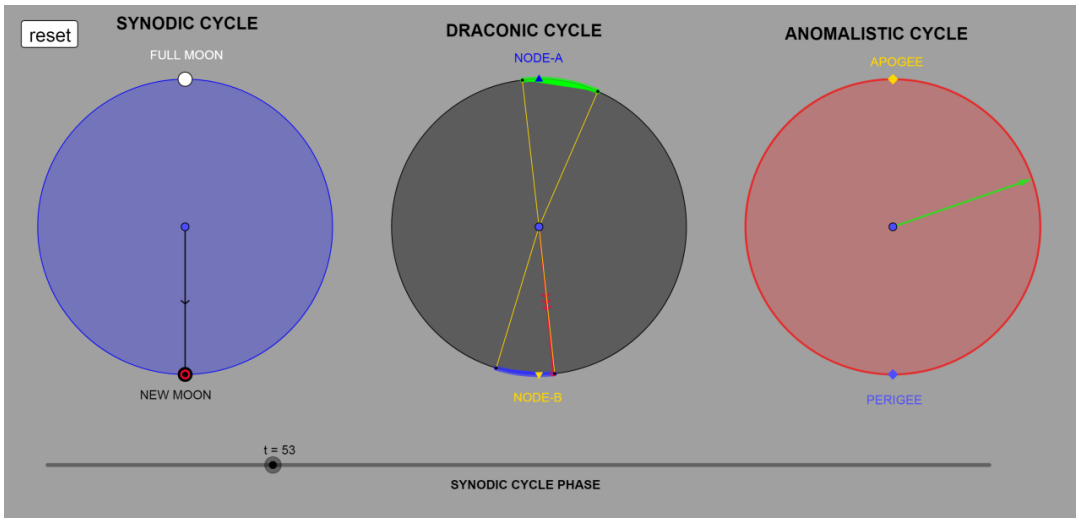

Figure A.20. Event 17. Cell 54/N1: Solar eclipse event (H). New Moon on the ecliptic limit, but inside the ecliptic window.

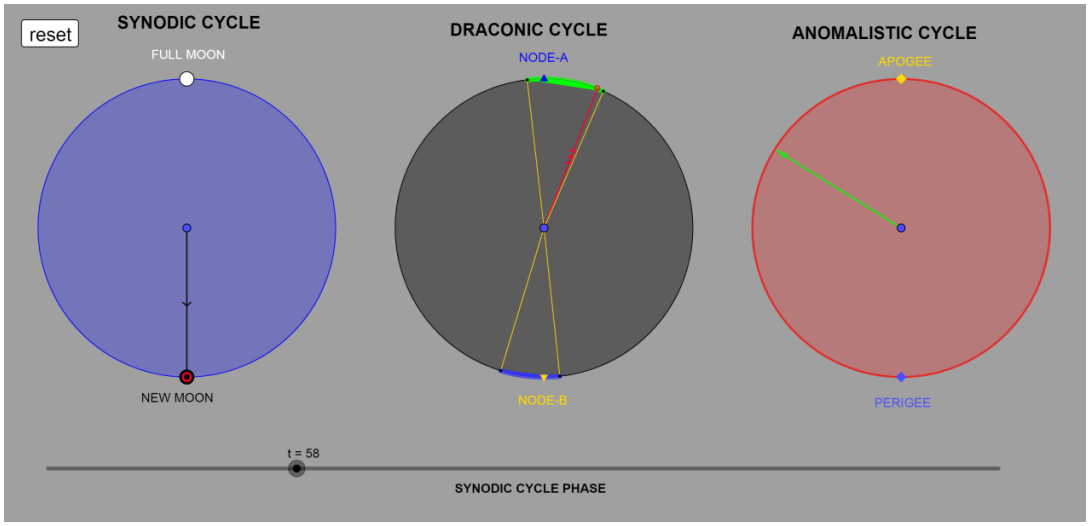

Figure A.21. Event 18. Cell 59/Ξ1: Solar eclipse event (H). New Moon too close to the ecliptic limit.

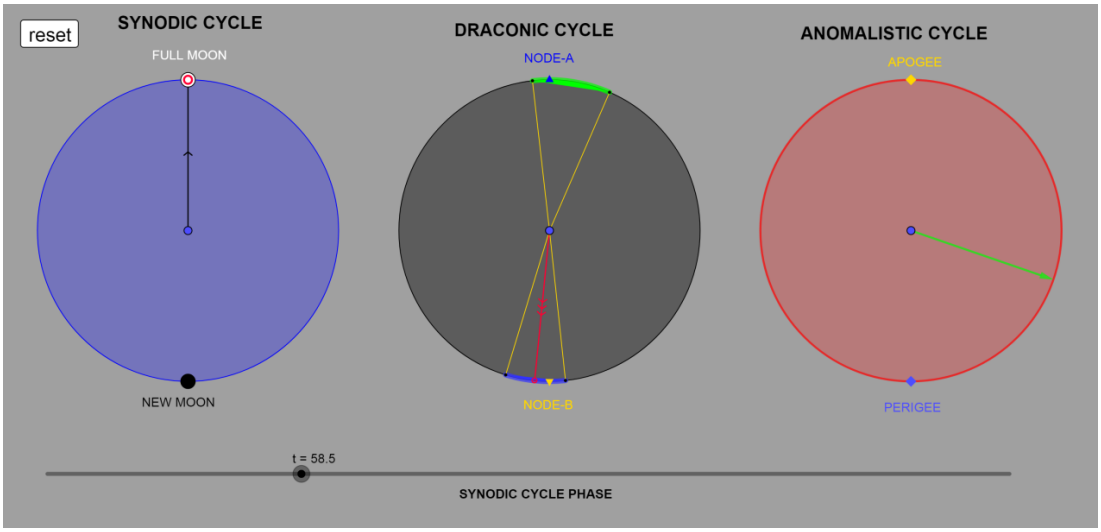

Figure A.22. Event 19. Cell 60/O1: Lunar eclipse event (Σ) (*preserved*). New Moon close to Node-B.

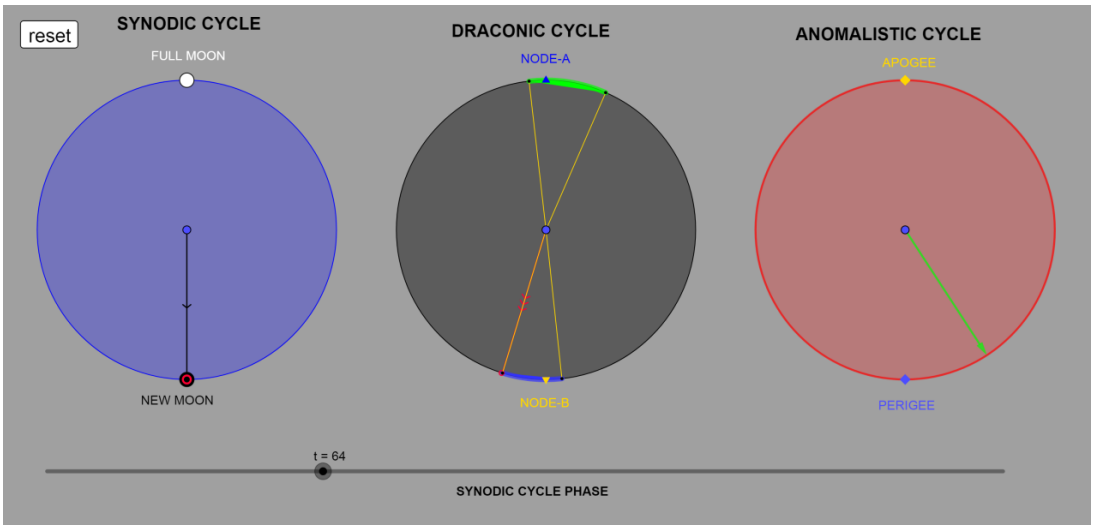

Figure A.23. Event I. Cell 65: Full Moon just right on the ecliptic limit. Based on the events' index numbering it should be no engraved event. Indeterminacy or eccentricity error.

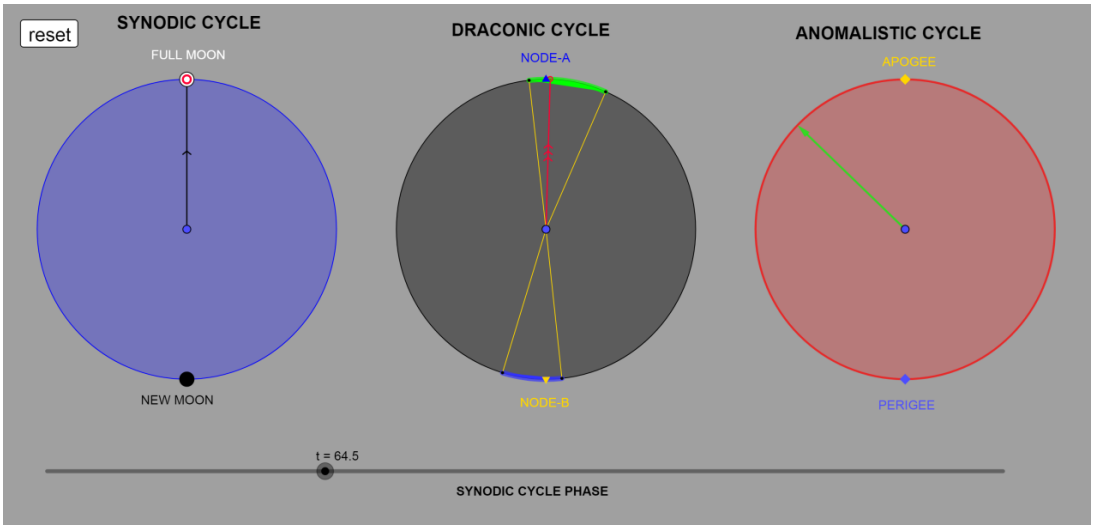

Figure A.24. Event 20. Cell 66/П1: Lunar eclipse event (Σ) (*preserved*). New Moon too close to Node-A.

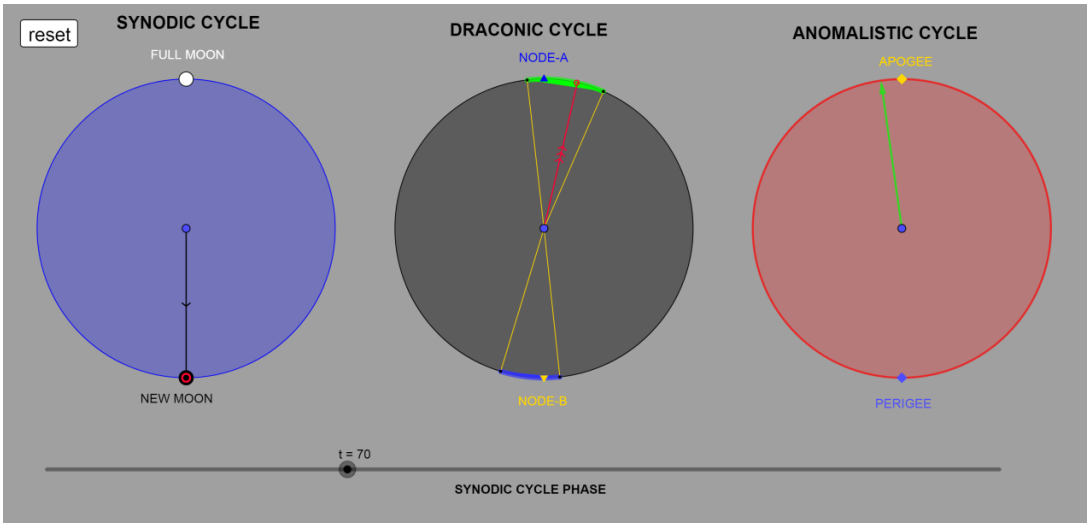

Figure A.25. Event 21. Cell 71/P1: Solar eclipse event (H) (*preserved*). Full Moon closes at Apogee.

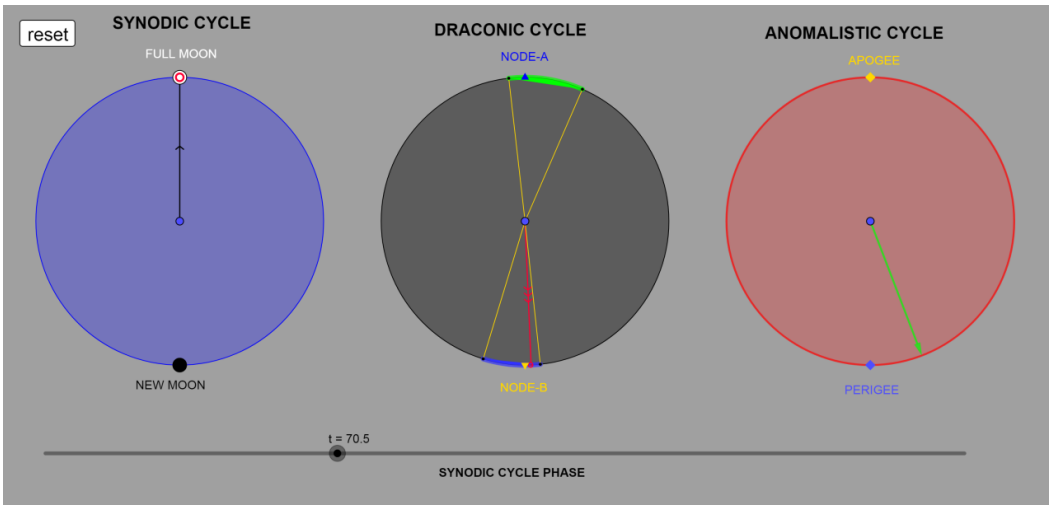

Figure A.26. Event 22. Cell 72/Σ1: Lunar eclipse event (Σ). Full Moon closes to Node-B and at Perigee.

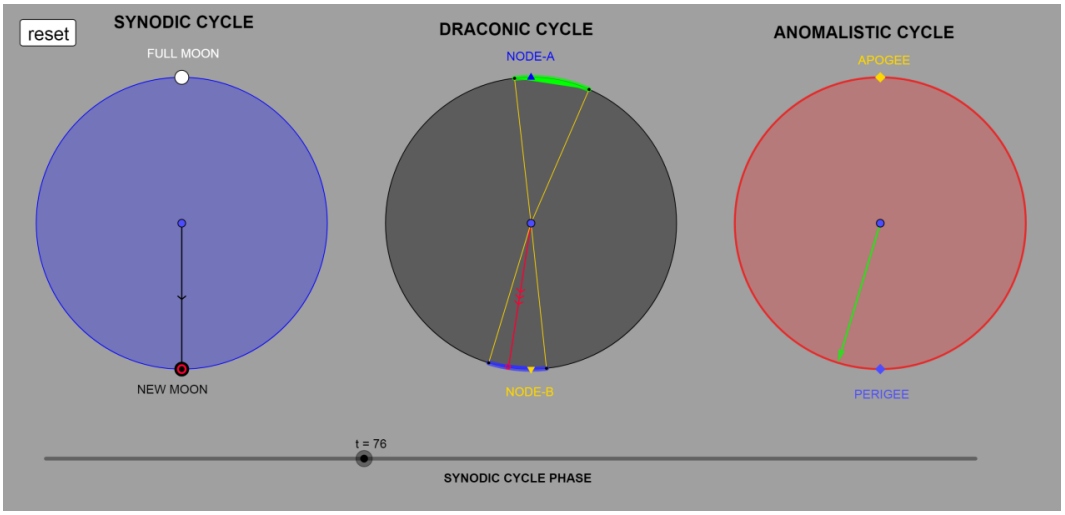

Figure A.27. Event 23. Cell 77/T1: Solar eclipse event (H) (*preserved*). Full Moon closes at Perigee.

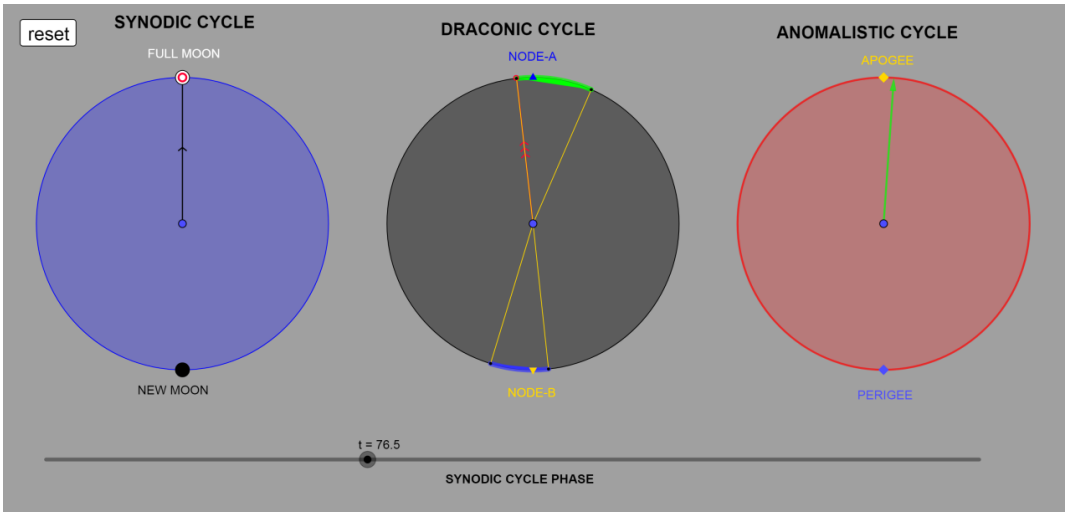

Figure A.28. Event 24. Cell 78/Y1: Lunar eclipse event (Σ) (*preserved*). Full Moon just on the ecliptic limit and at Apogee.

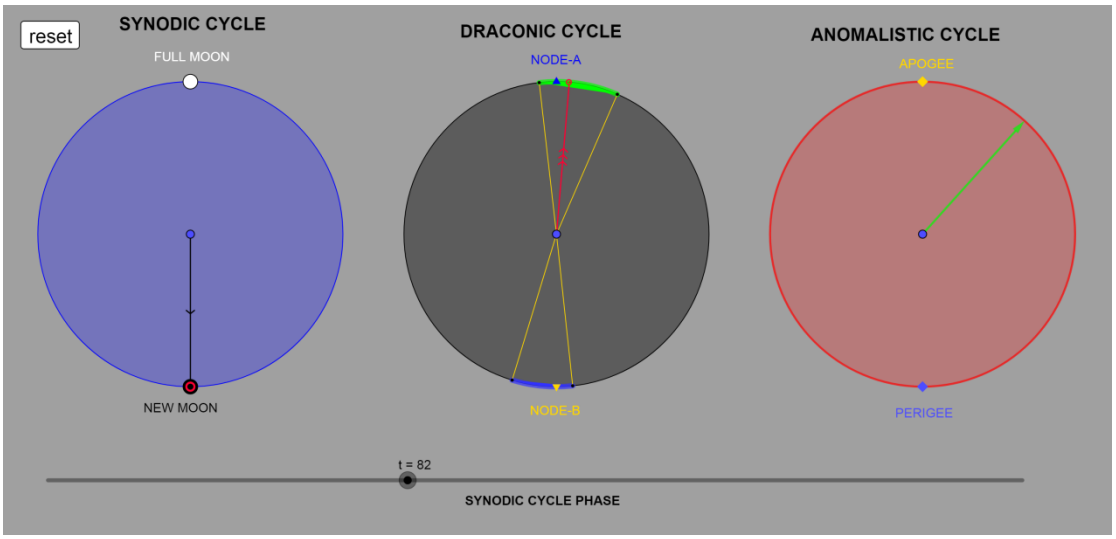

Figure A.29. Event 25. Cell 83/Φ1: Solar eclipse event (H). New Moon closes to Node-A.

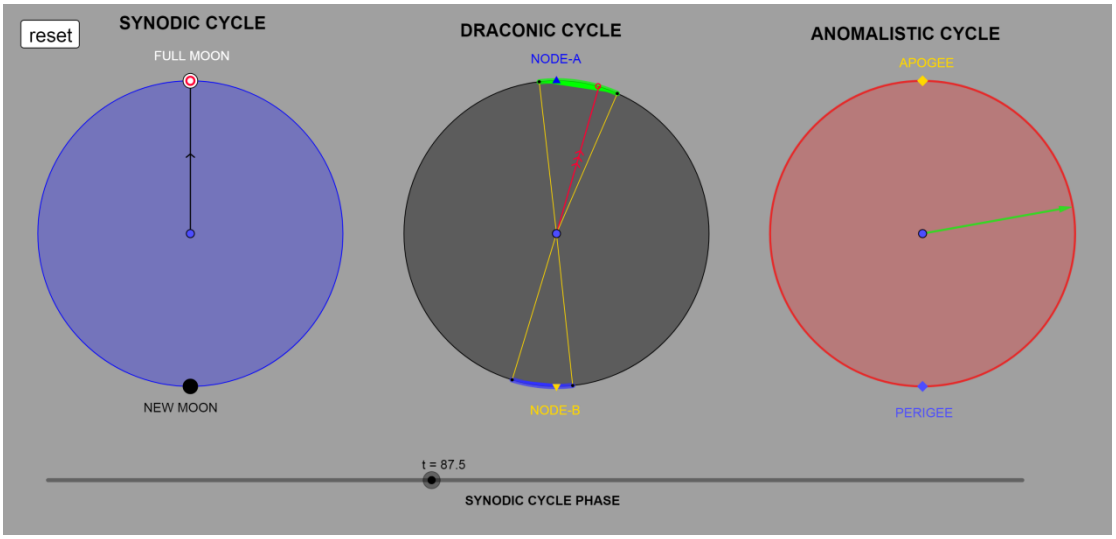

Figure A.30. Event 26. Cell 89/X1: Lunar eclipse event (Σ).

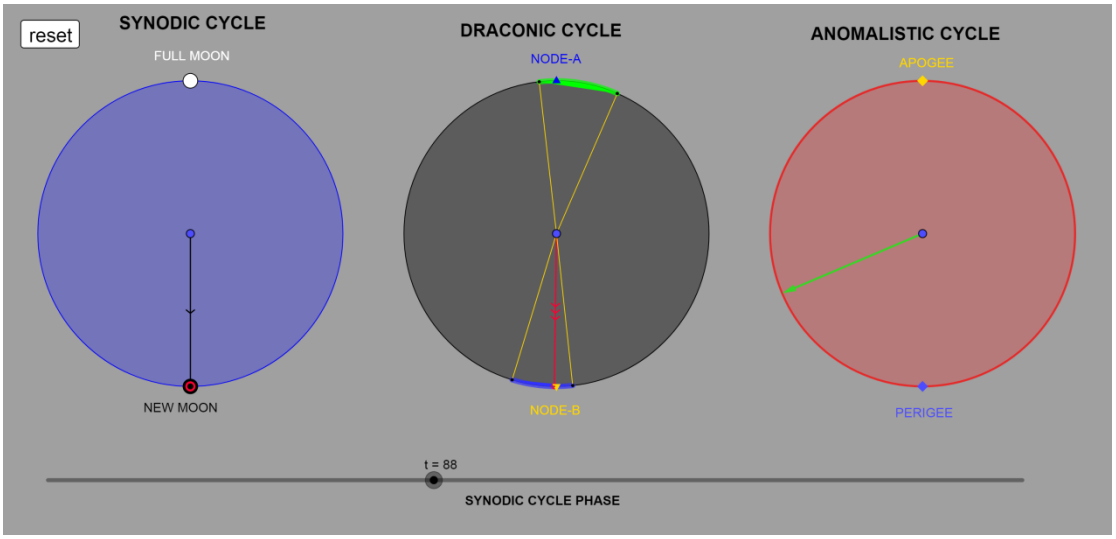

Figure A.31. Event 27. Cell 89/X1: Solar eclipse event (H). New Moon on Node-B.

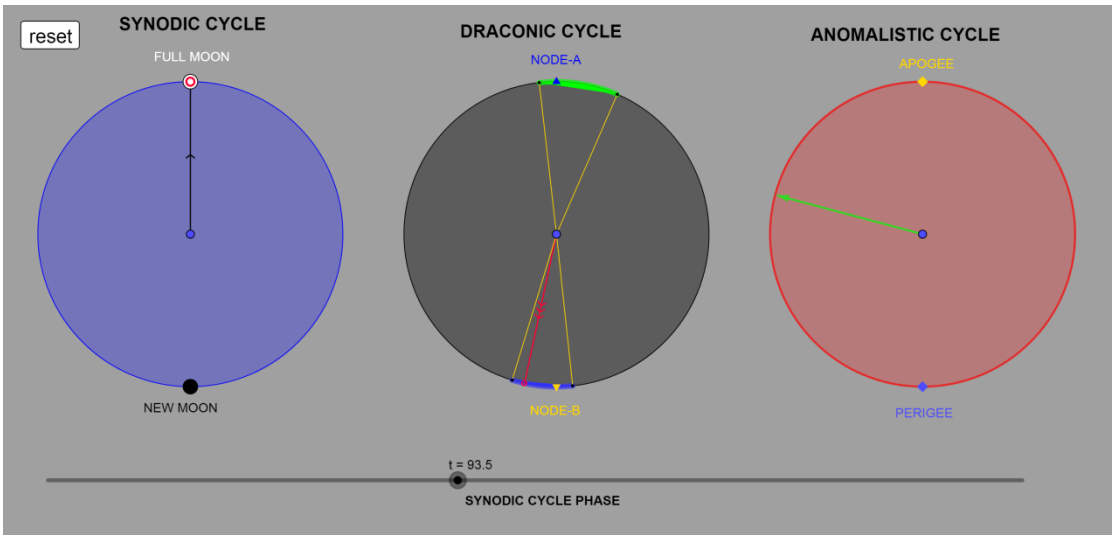

Figure A.32. Event 28. Cell 95/Ψ1: Lunar eclipse event (Σ).

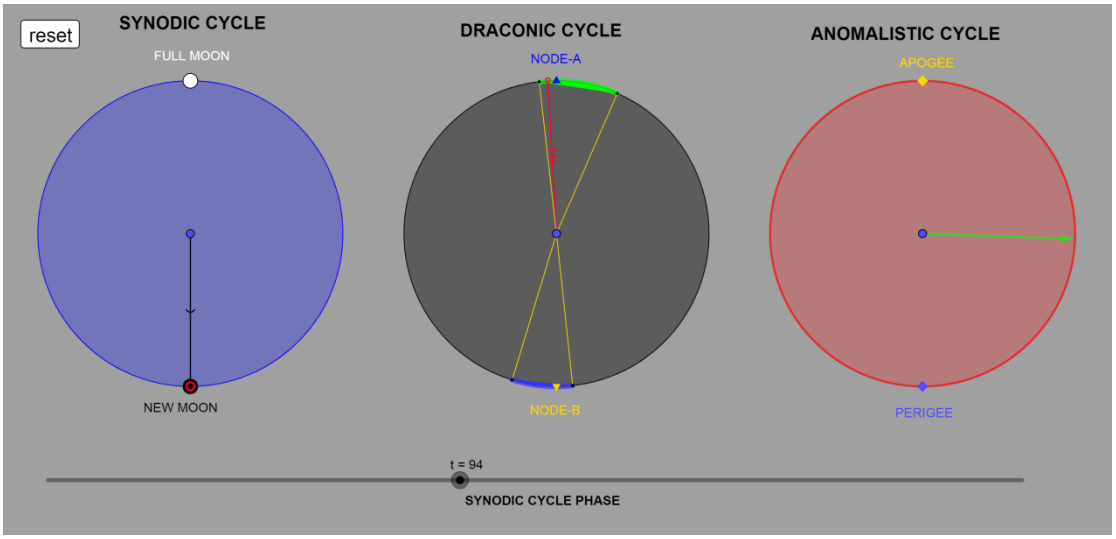

Figure A.33. Event 29. Cell 95/Ψ1: Solar eclipse event (H). New Moon close to ecliptic limit.

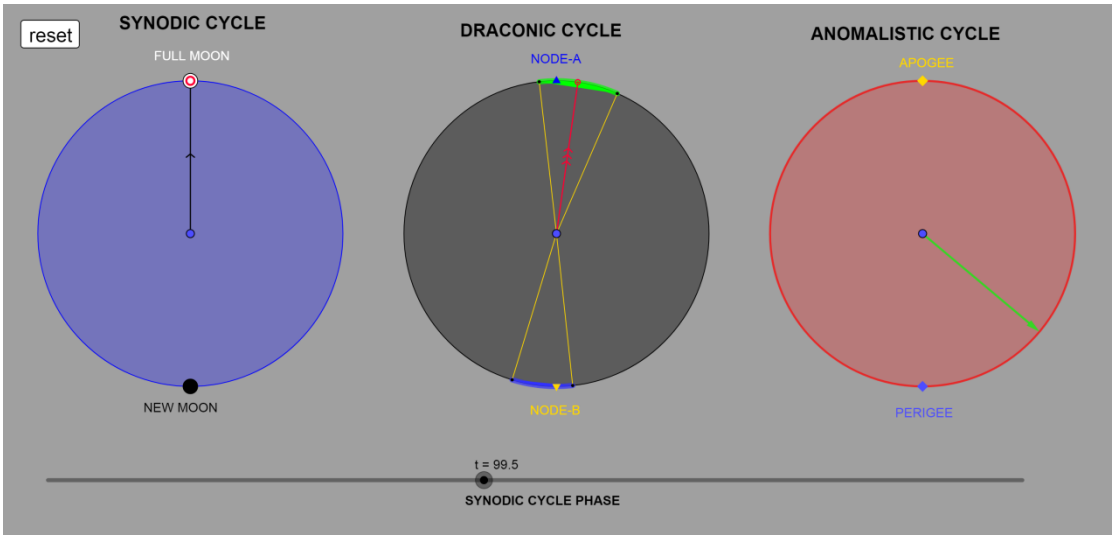

Figure A.34. Event 30. Cell 101/ↀ1: Lunar eclipse event (Σ).

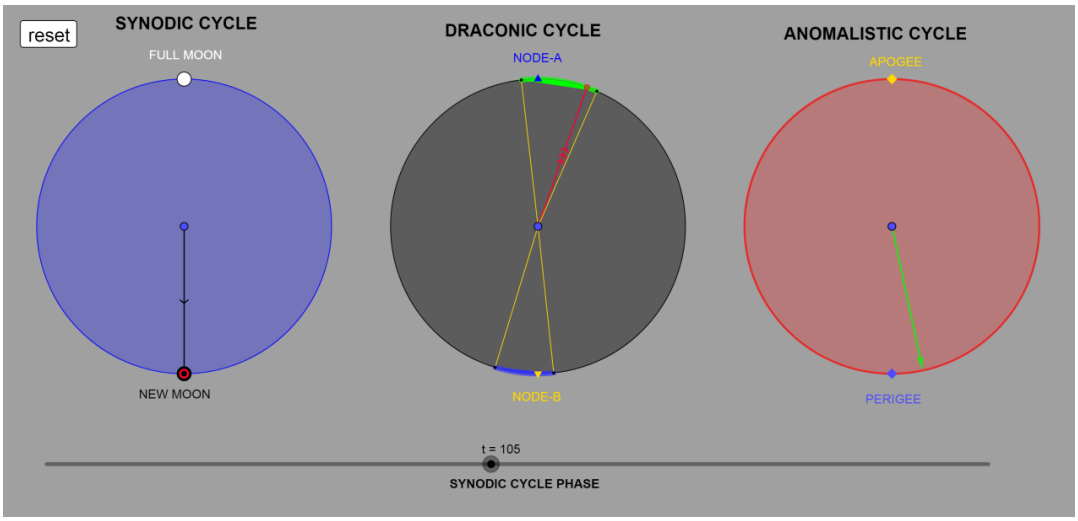

Figure A.35. Event 31. Cell 106/A2: Solar eclipse event (H). New Moon close to the ecliptic limit and at Perigee.

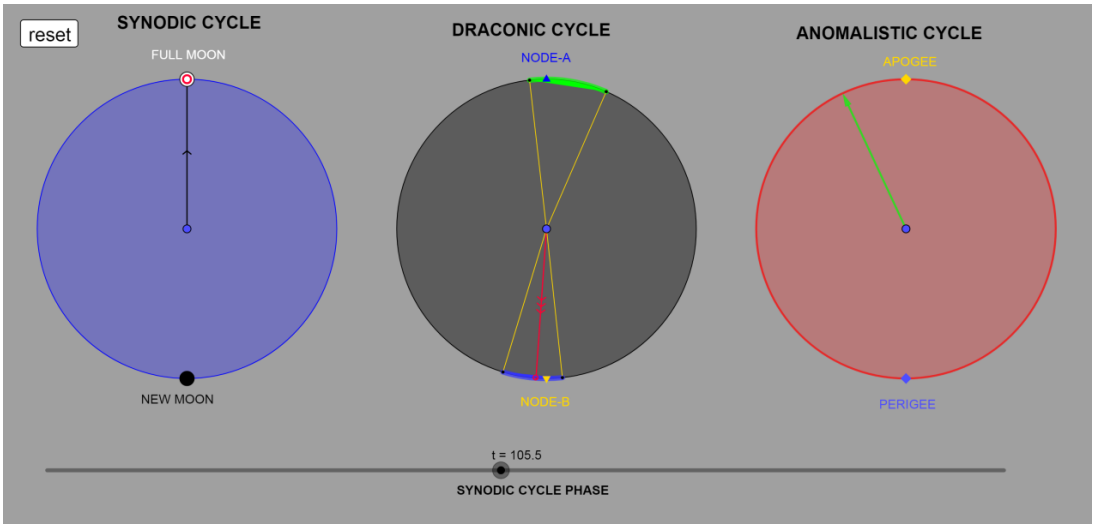

Figure A.36. Event 32. Cell 107/B2: Lunar eclipse event (Σ). Full Moon close to Node-B.

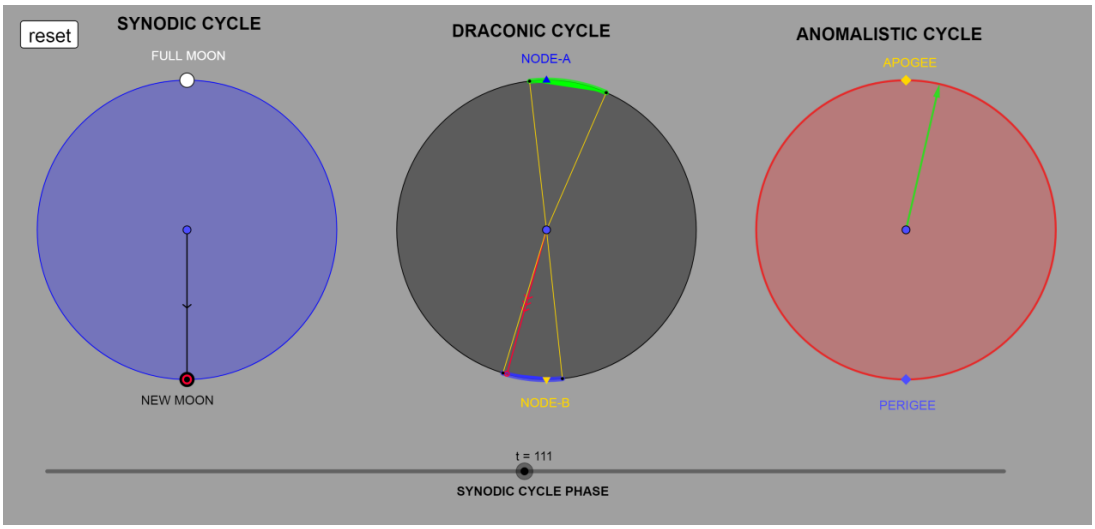

Figure A.37. Event II. Cell 112: Solar eclipse event (H). Calculated by *DracoNod* program but is not an engraved event, according to the present sequence of the index letters.
New Moon too close to the ecliptic limit. Indeterminacy or eccentricity error.

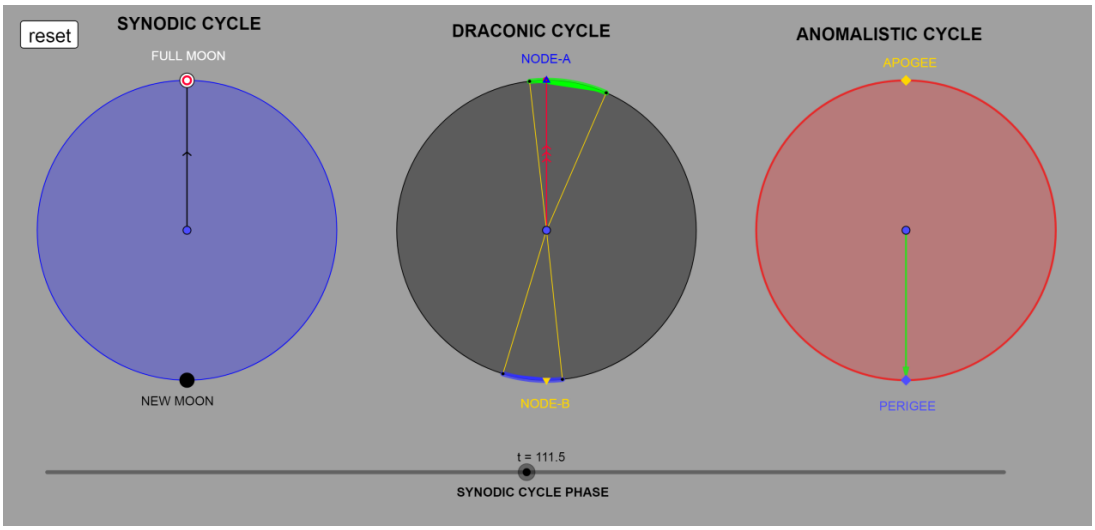

Figure A.38. Event 33. Cell 113/Γ2: Lunar eclipse event (Σ) (*preserved*). Full Moon at Node-A and at Perigee. A New Sar period begins.

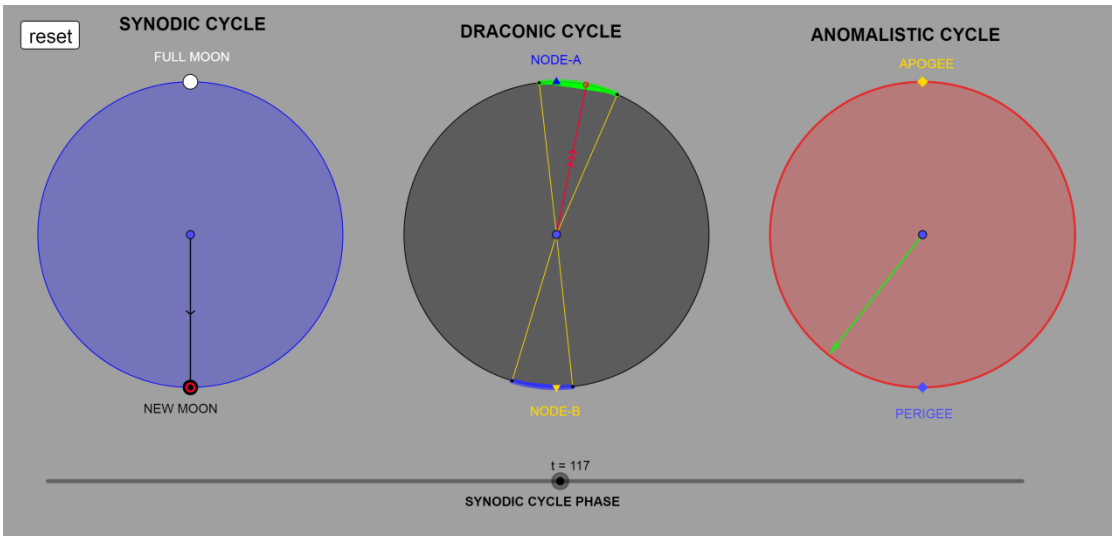

Figure A.39. Event 34. Cell 118/Δ2: Solar eclipse event (H) (*preserved*).

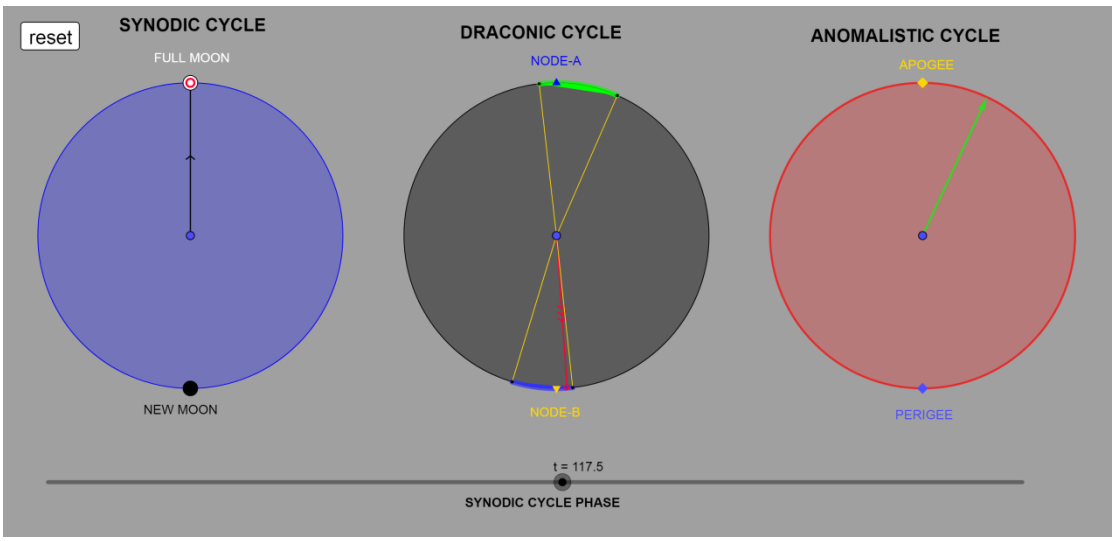

Figure A.40. Event 35. Cell 119/E2: Lunar eclipse event (Σ) (*preserved*). Full Moon too close to ecliptic limit.

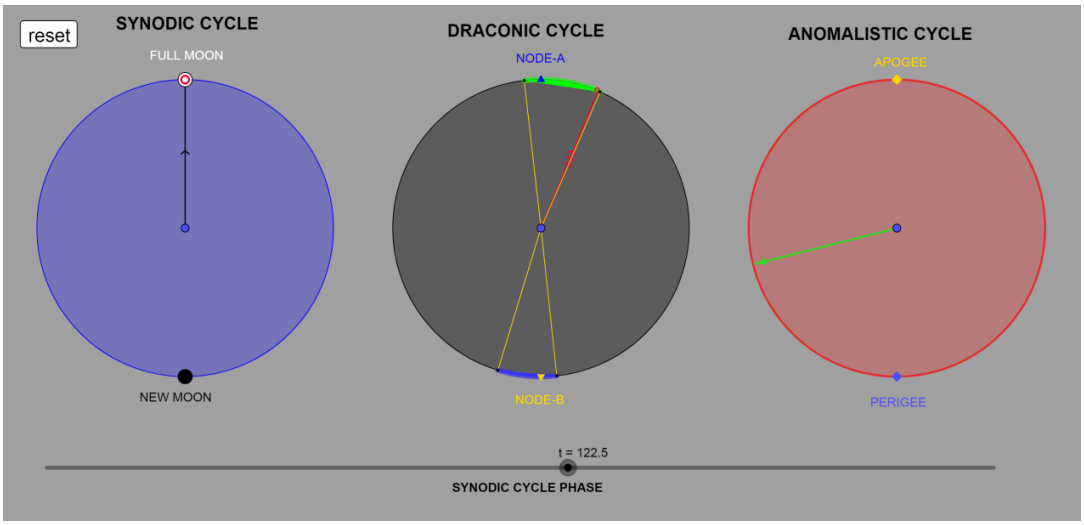

Figure A.41. Event 36. Cell 124/Z2: Lunar eclipse event (Σ) (*preserved*). Full Moon too close to ecliptic limit.

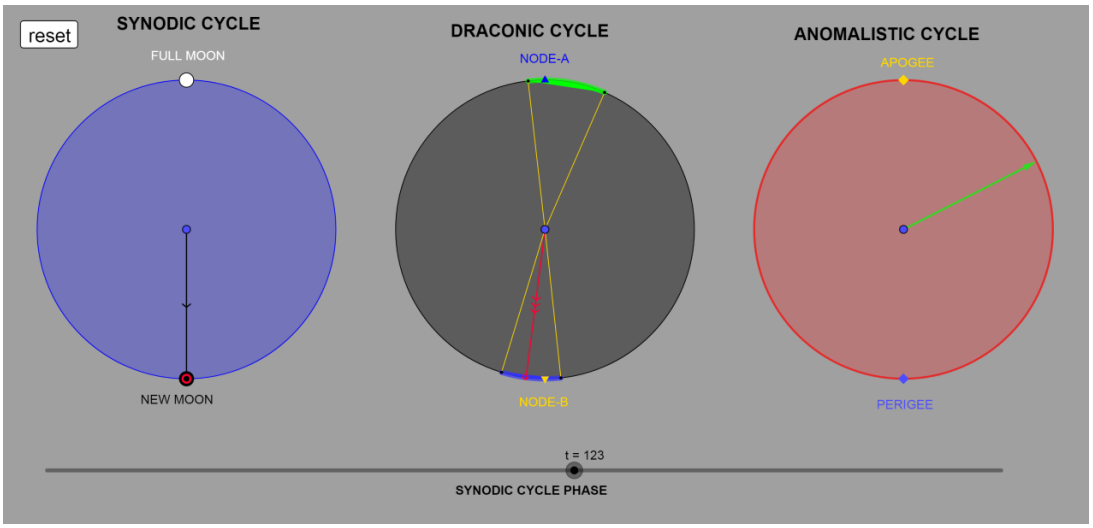

Figure A.42. Event 37. Cell 124/Z2: Solar eclipse event (H) (*preserved*).

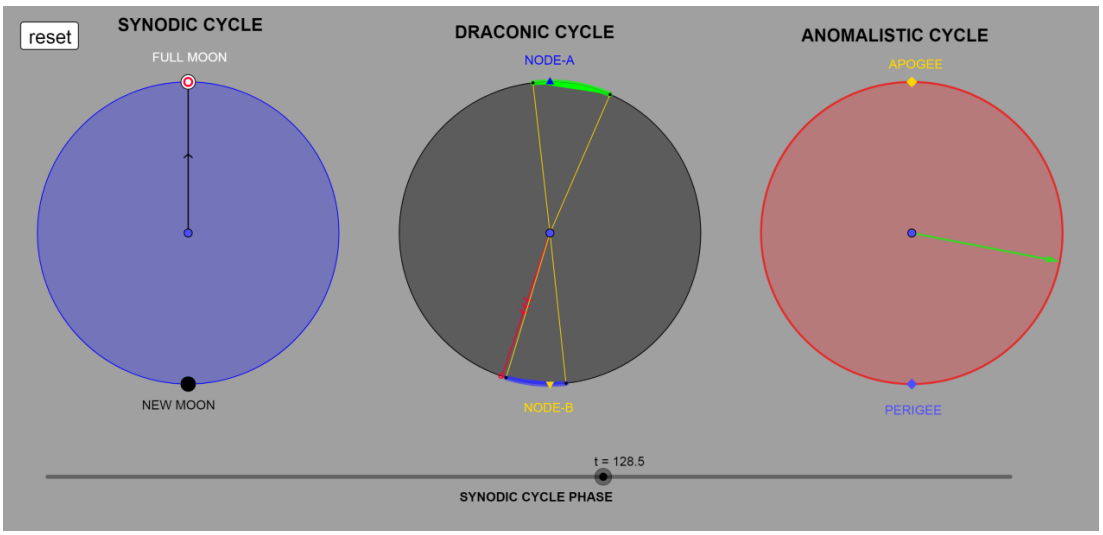

Figure A.43. Event 38. Cell 130/H2: engraved event Lunar eclipse-Σ (*preserved*), but according to *DracoNod* program no eclipse event: the Full Moon is just out of the ecliptic limit. Probably error of eccentricity or tooth un-uniformity.

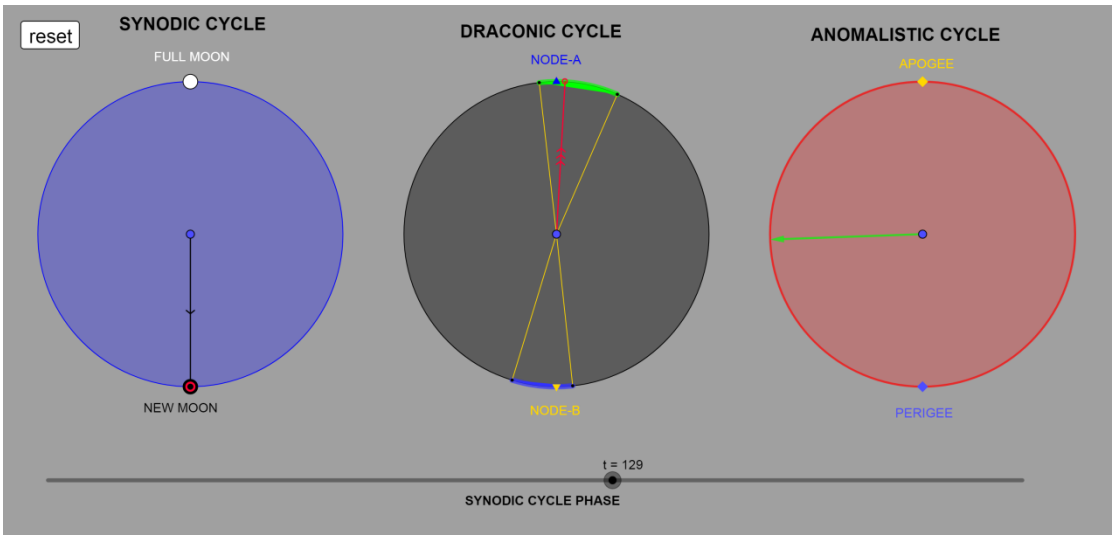

Figure A.44. Event 39. Cell 130/H2: Solar eclipse event (H) (*preserved*). New Moon closes at Node-A.

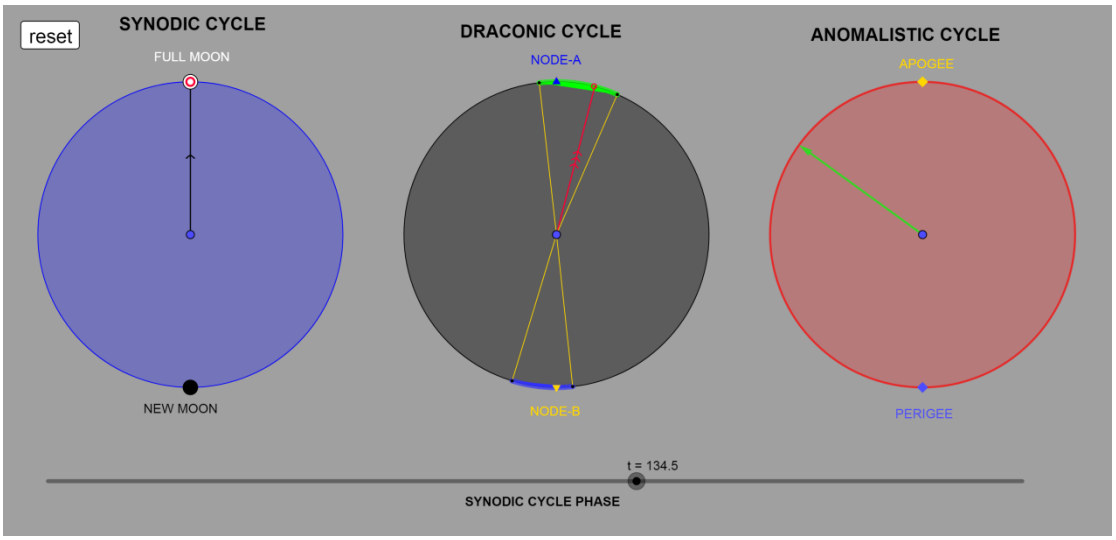

Figure A.45. Event 40. Cell 136/Θ2: Lunar eclipse event (Σ) (*preserved*).

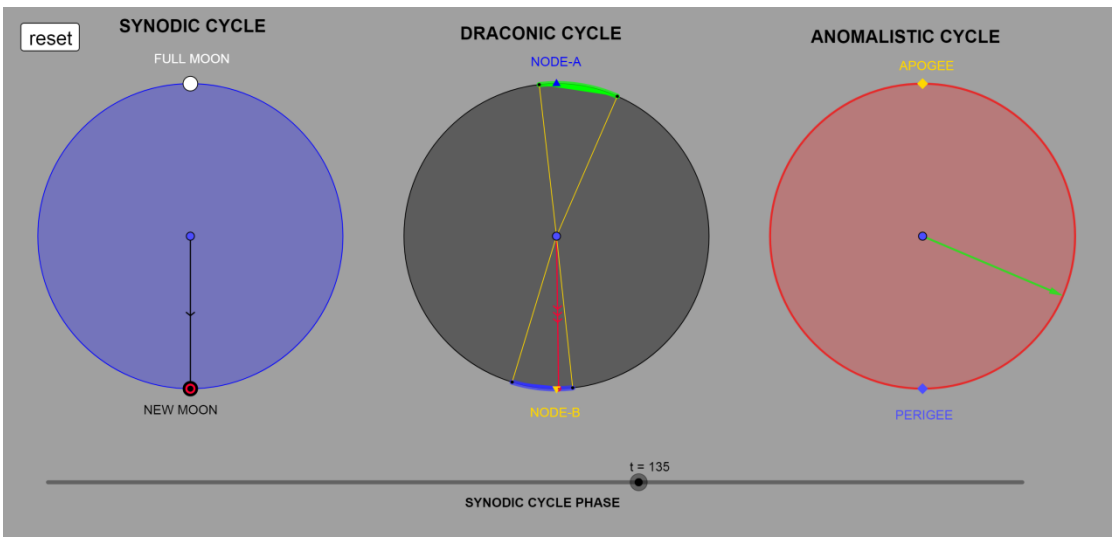

Figure A.46. Event 41. Cell 136/Θ2: Solar eclipse event (H) (*preserved*). New Moon at Node-B.

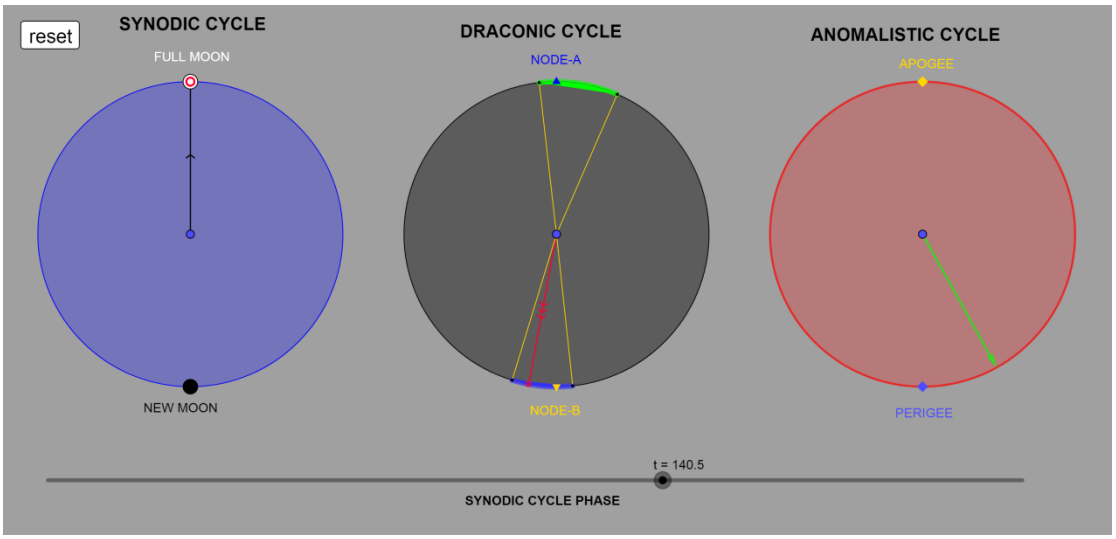

Figure A.47. Event 42. Cell 142/I2: Lunar eclipse event (Σ).

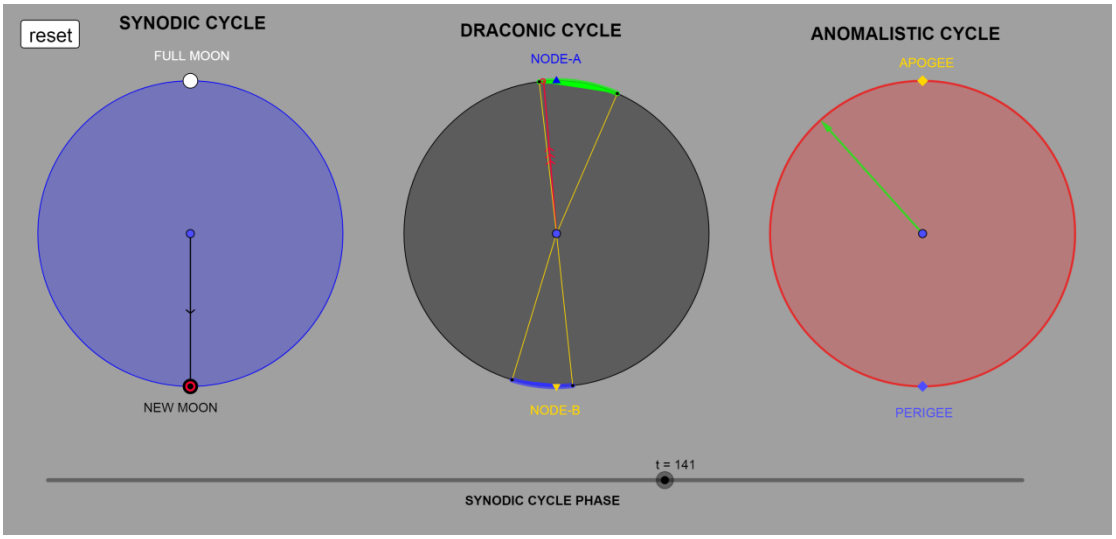

Figure A.48. Event 43. Cell 142/I2: Solar eclipse event (H). New Moon too close to ecliptic limit.

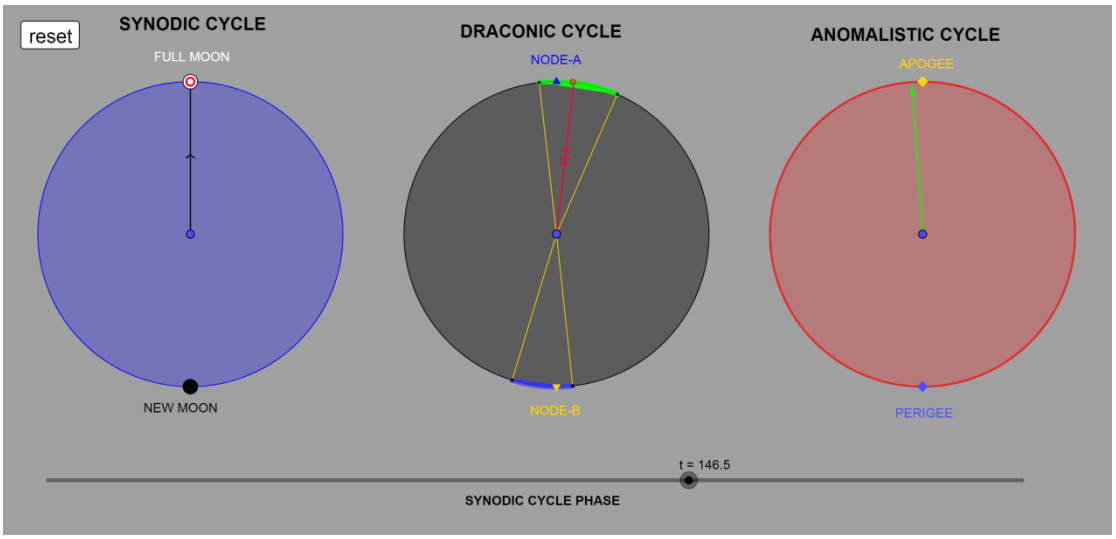

Figure A.49. Event 44. Cell 148/K2: Lunar eclipse event (Σ). Full Moon close to Node-A and at Apogee.

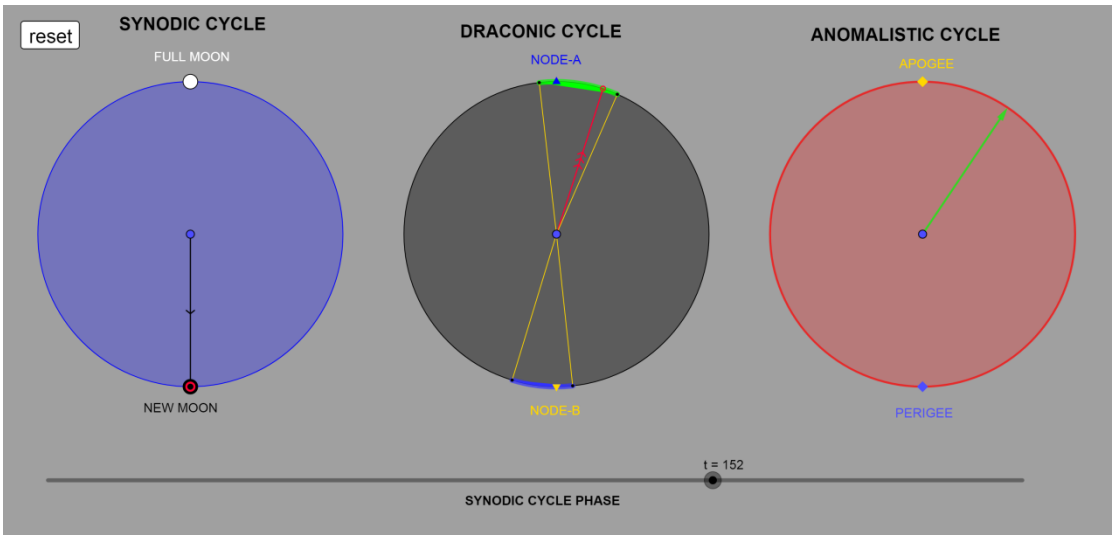

Figure A.50. Event 45. Cell 153/Λ2: Solar eclipse event (H). New Moon closes to ecliptic limit.

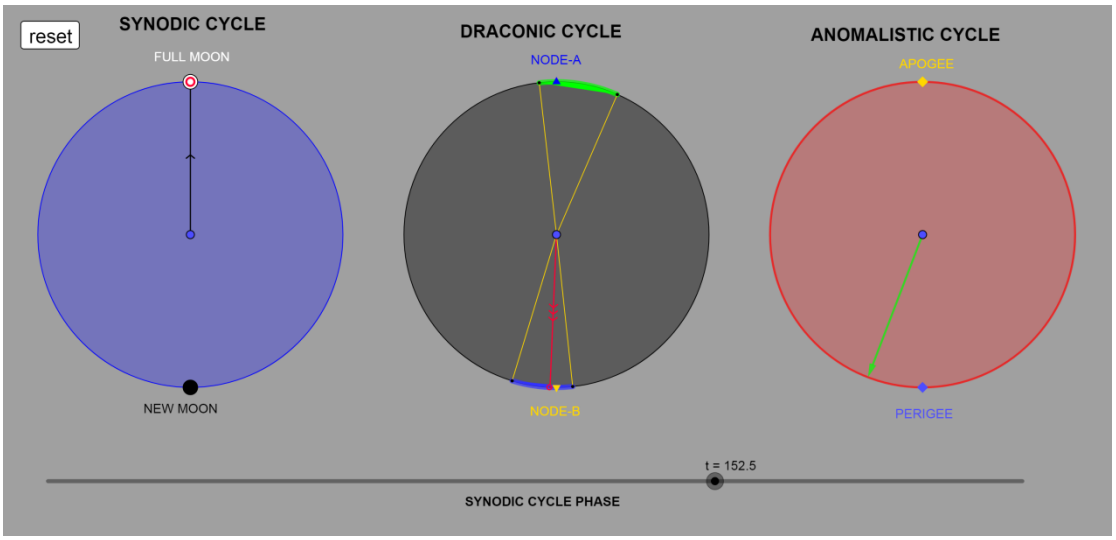

Figure A.51. Event 46. Cell 154/M2: Lunar eclipse event (Σ). Full Moon on Node-B.

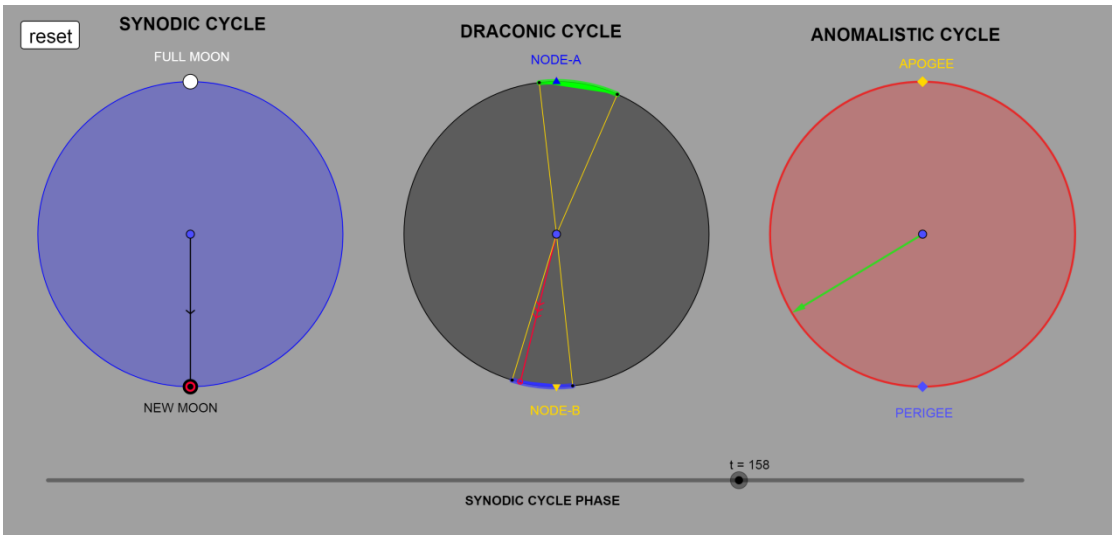

Figure A.52. Event 47. Cell 159/N2: Solar eclipse event (H). New Moon too close to ecliptic limit.

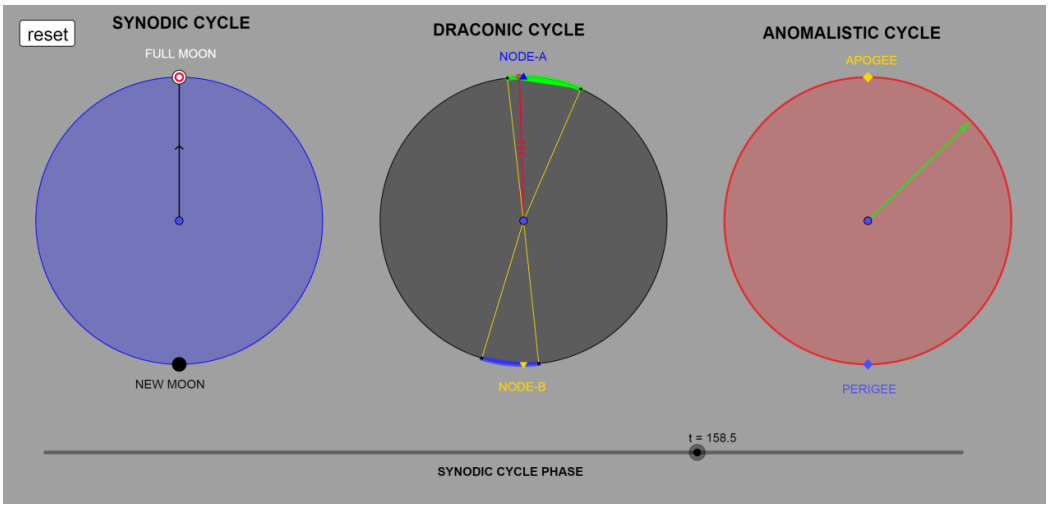

Figure A.53. Event 48. Cell 160/Ξ2: Lunar eclipse event (Σ). Full Moon at Node-A.

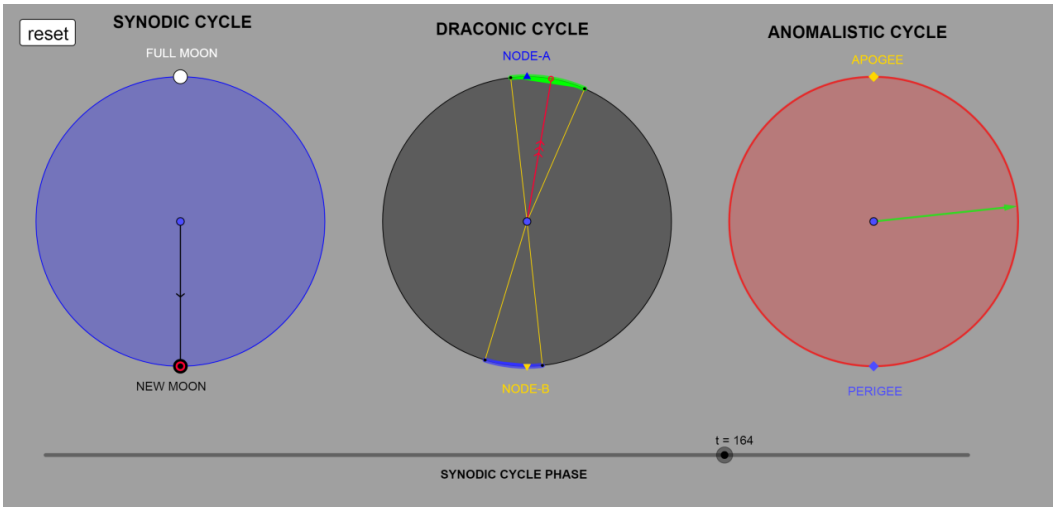

Figure A.54. Event 49. Cell 165/O2: Solar eclipse event (H).

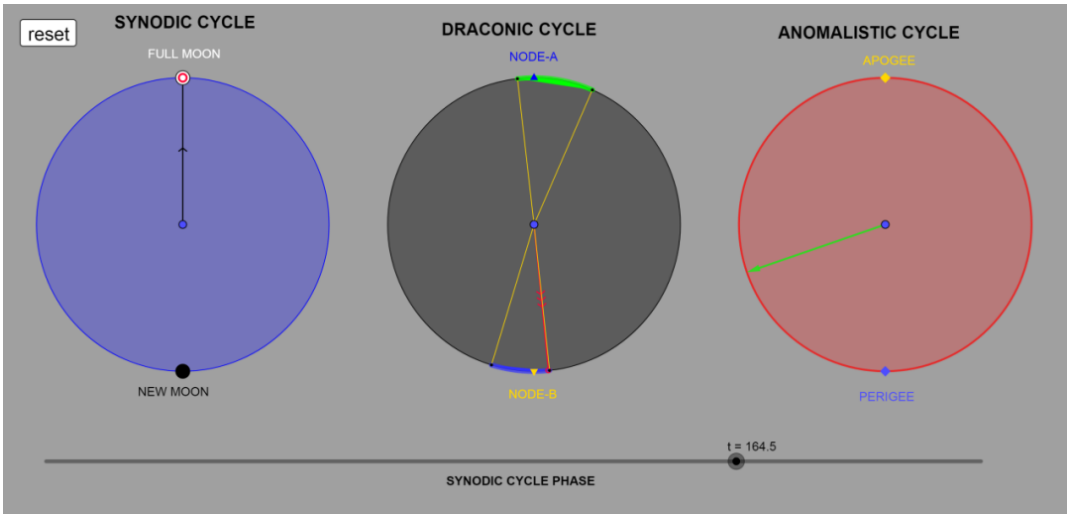

Figure A.55. Event III. Cell 166: *DracoNod* program predicts a Lunar eclipse. Full Moon just right on the ecliptic limit. Based on the events' index numbering, between cells 137 and 170 they should be 7 cells with events. Cell 166 is the 8th cell with event, and it is the only one event presenting high indeterminacy. Cell 166 is considered as cell without event.

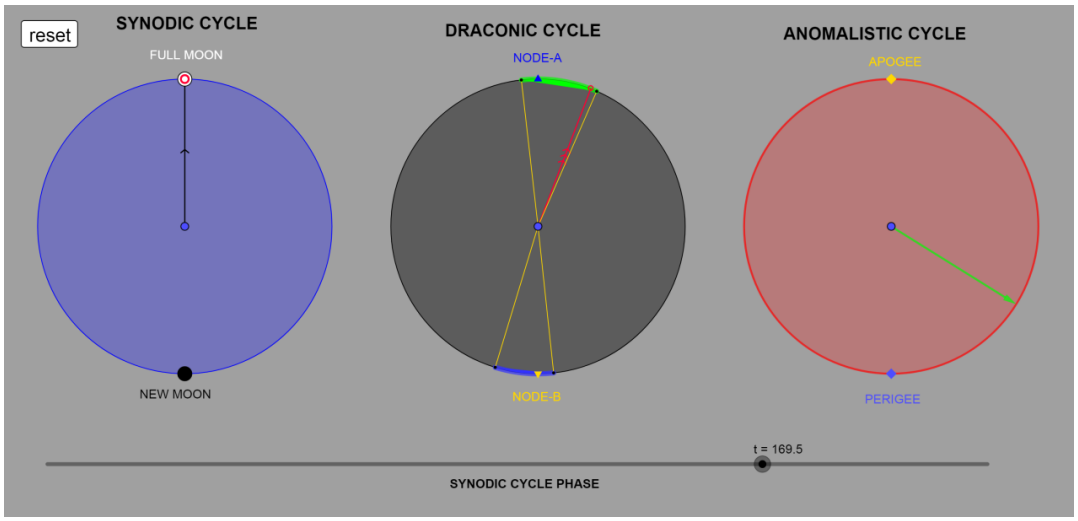

Figure A.56. Event 50. Cell 171/П2: Lunar eclipse event (Σ) (*preserved*). Full Moon close to ecliptic limit.

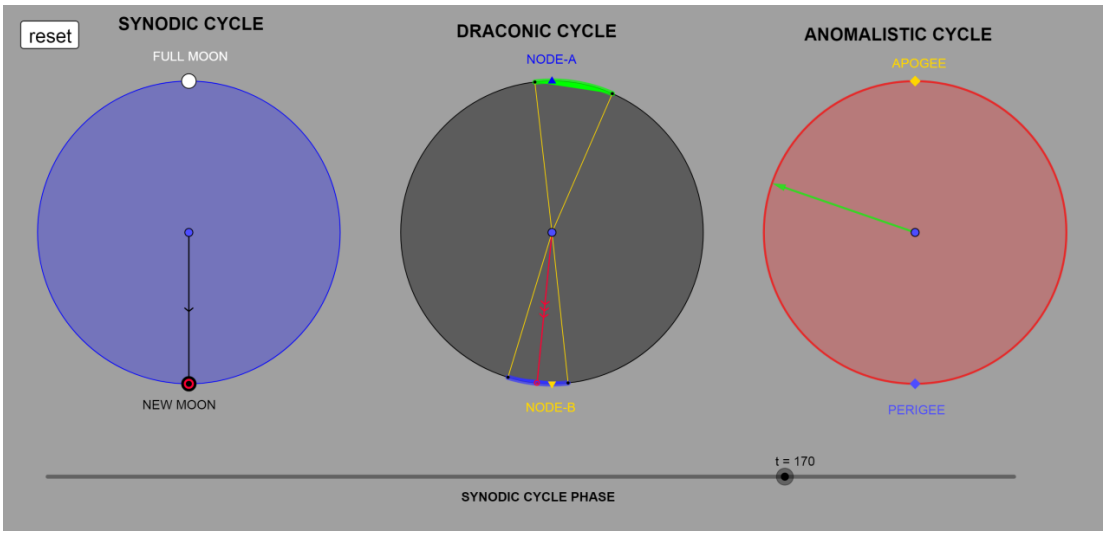

Figure A.57. Event 51. Cell 171/П2: Solar eclipse event (H) (*preserved*). New Moon close to Node-B.

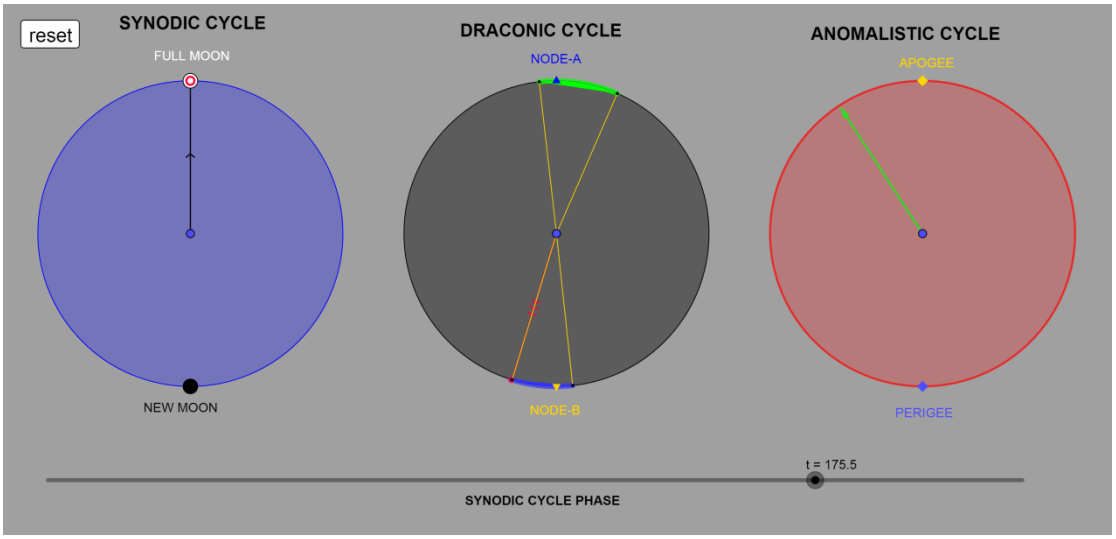

Figure A.58. Event 52. Cell 177/P2: Lunar eclipse event (Σ) (*preserved*). Full Moon just on ecliptic limit.

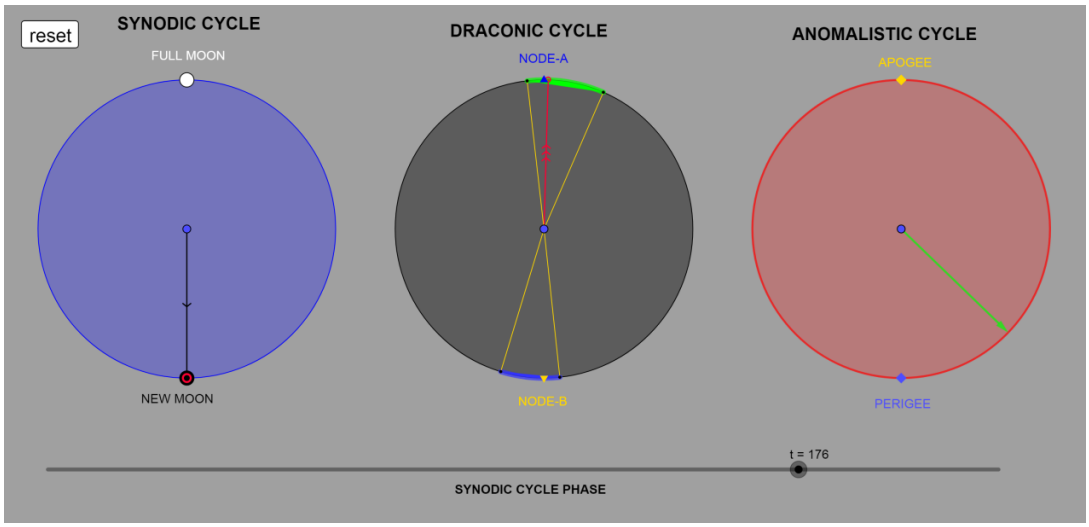

Figure A.59. Event 53. Cell 177/P2: Solar eclipse event (H) (*preserved*). New Moon at Node-A.

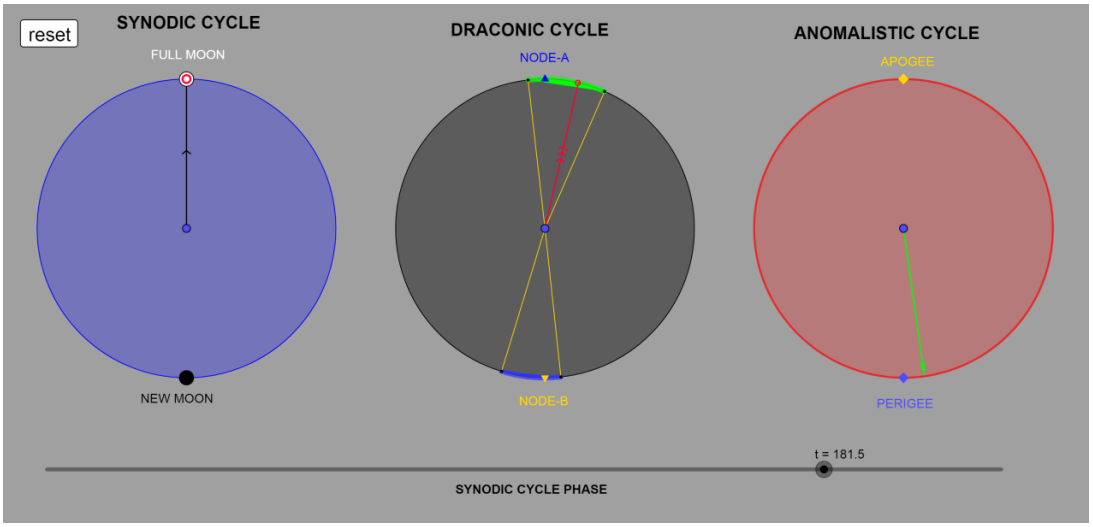

Figure A.60. Event 54. Cell 183/Σ2: Lunar eclipse event (Σ) (*preserved*). Full Moon closes at Perigee.

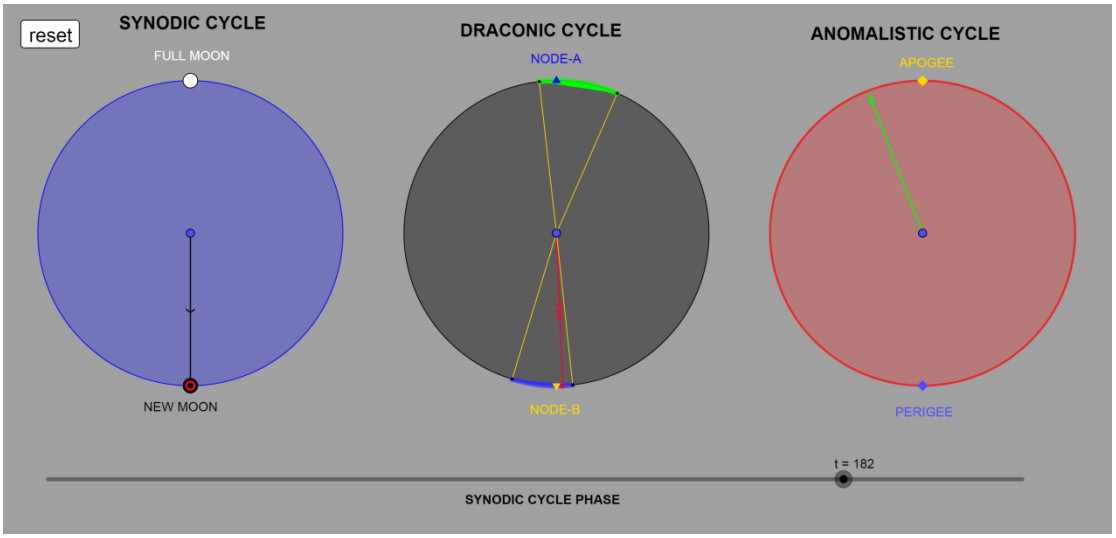

Figure A.61. Event 55. Cell 183/Σ2: Solar eclipse event (H) (*preserved*). New Moon closes at Node-B.

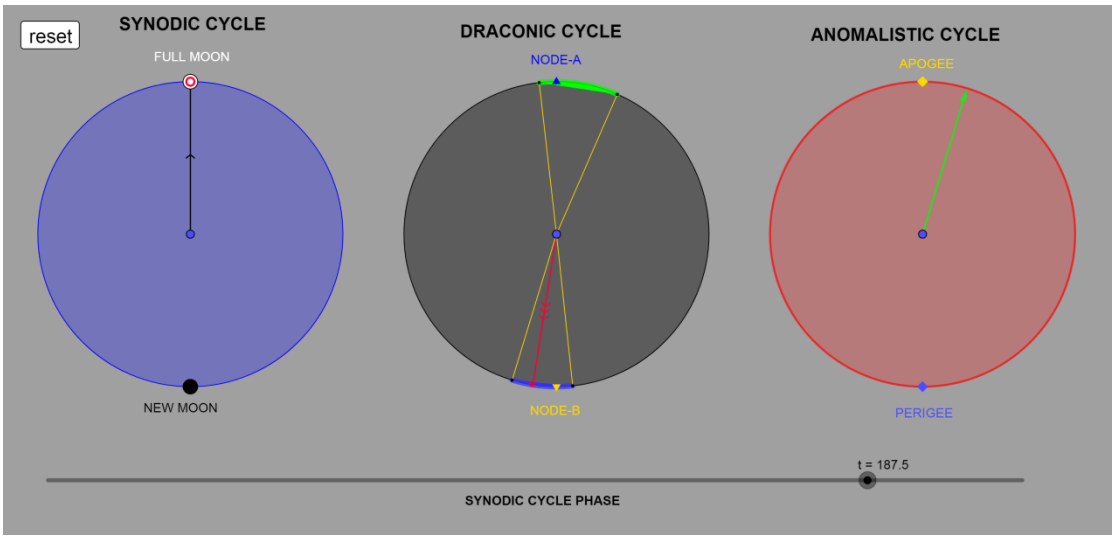

Figure A.62. Event 56. Cell 189/T2: Lunar eclipse event (Σ) (*preserved*). Full Moon closes at Apogee.

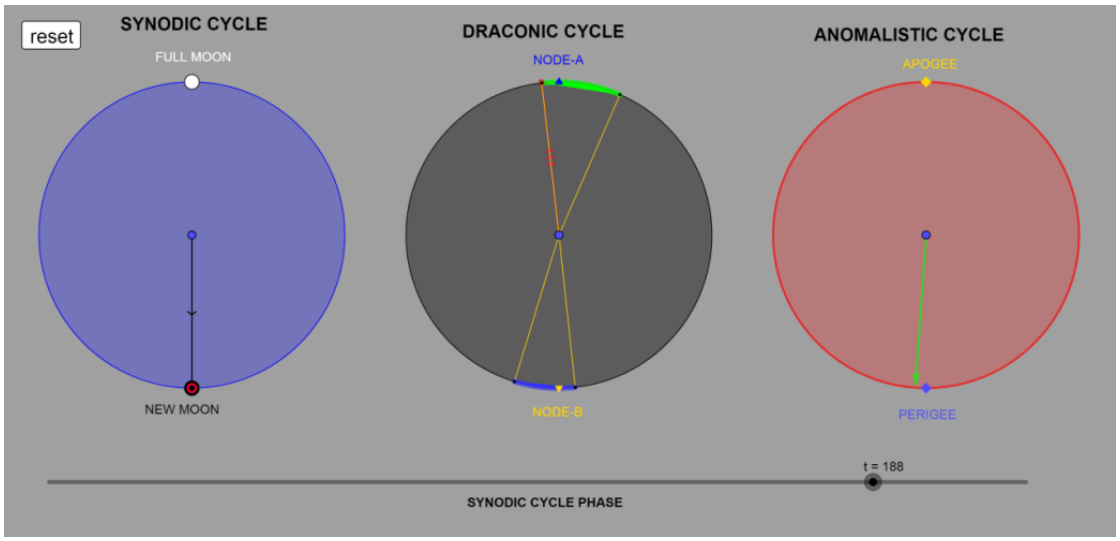

Figure A.63. Event IV. Cell 189: No engraved event. *DracoNod* program predicts a second event, a Solar eclipse. New Moon just right on the ecliptic limit. Indeterminacy or gearing errors.

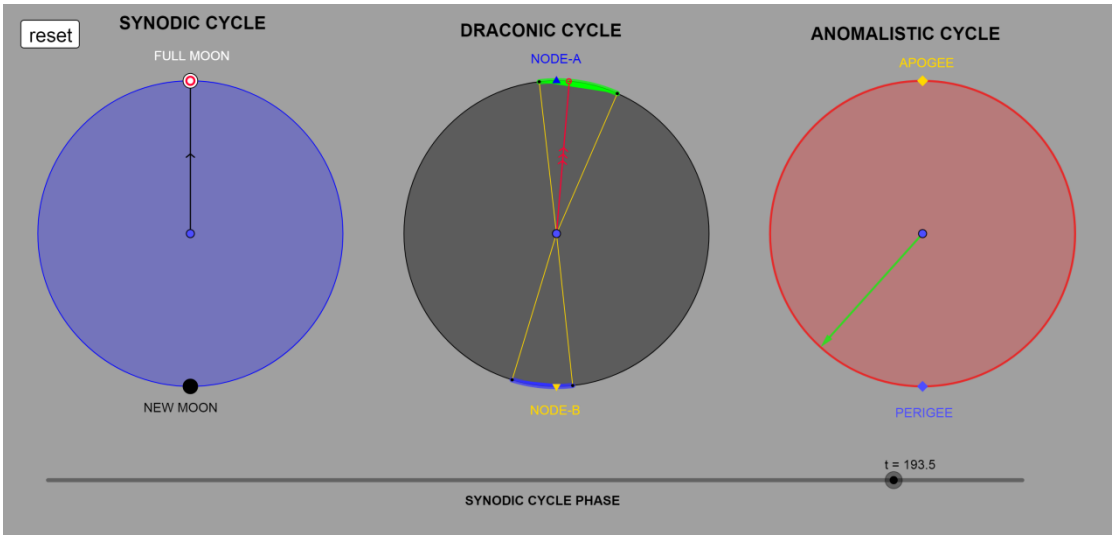

Figure A.64. Event 57. Cell 195/Y2: Lunar eclipse event (Σ). Full Moon close to Node-A.

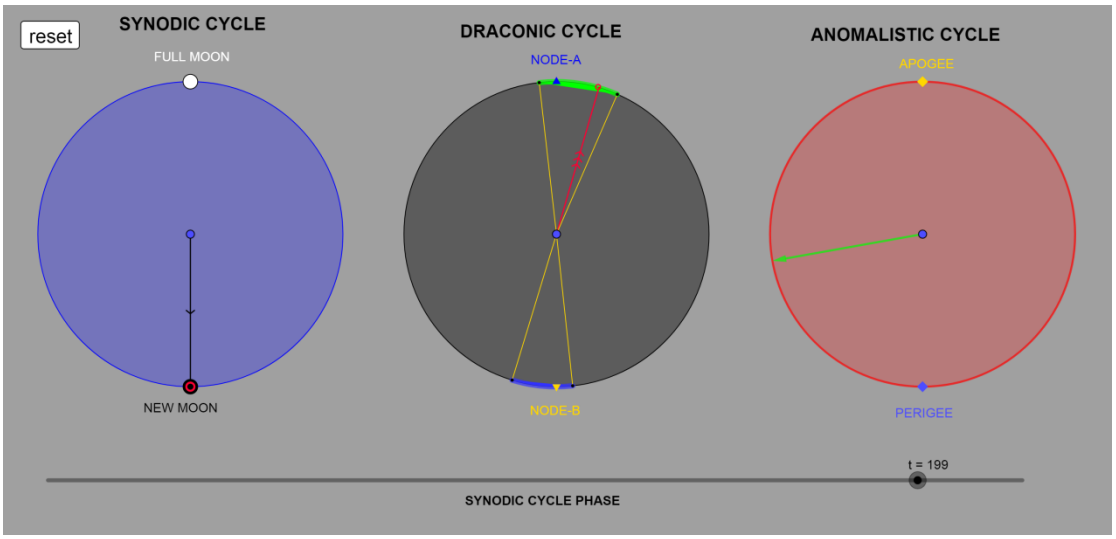

Figure A.65. Event 58. Cell 200/Φ2: Solar eclipse event (H).

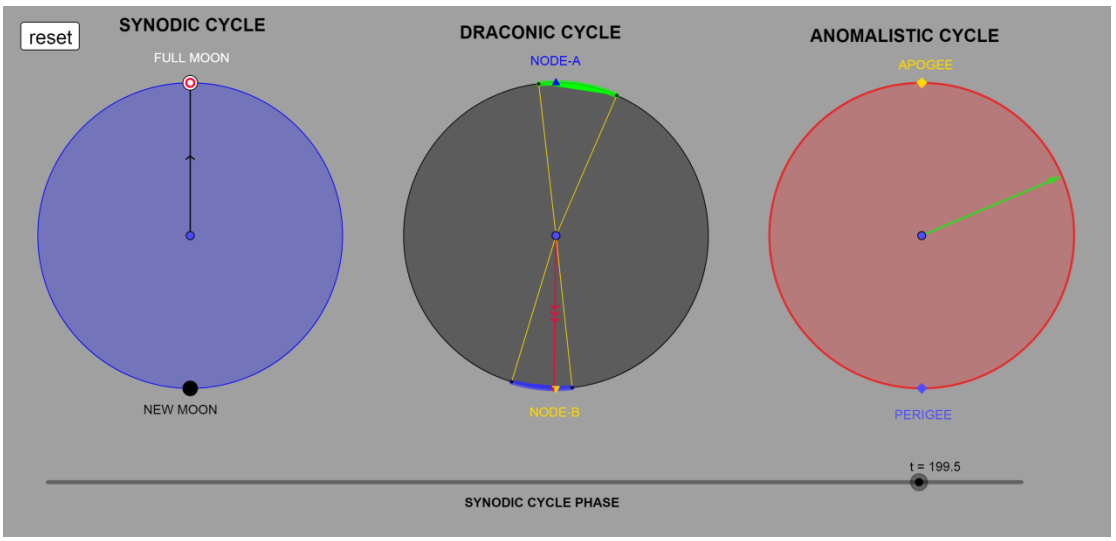

Figure A.66. Event 59. Cell 201/X2: Lunar eclipse event (Σ). Full Moon at Node-B.

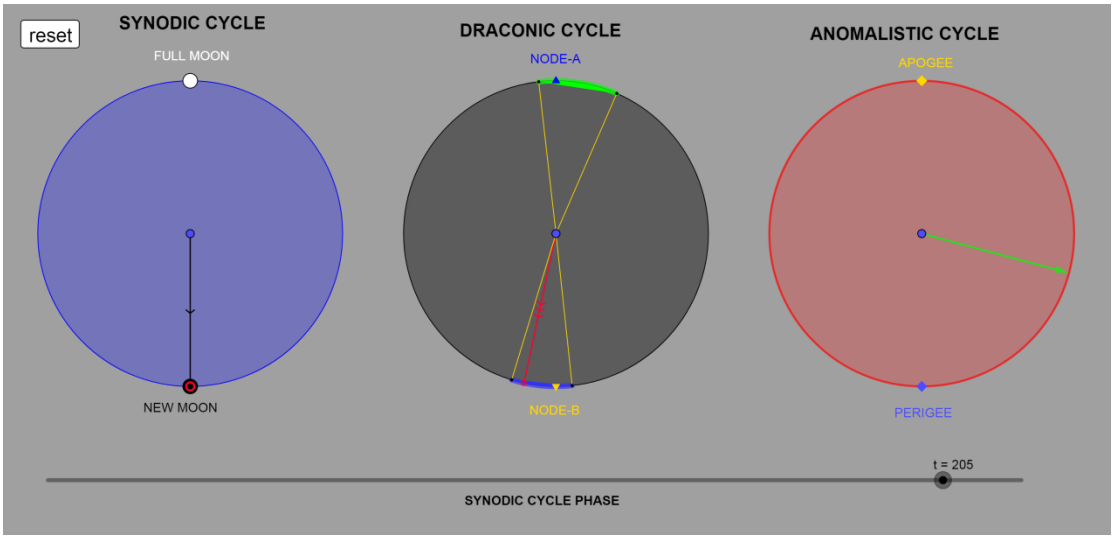

Figure A.67. Event 60. Cell 206/Ψ2: Solar eclipse event (H). New Moon closes to ecliptic limit.

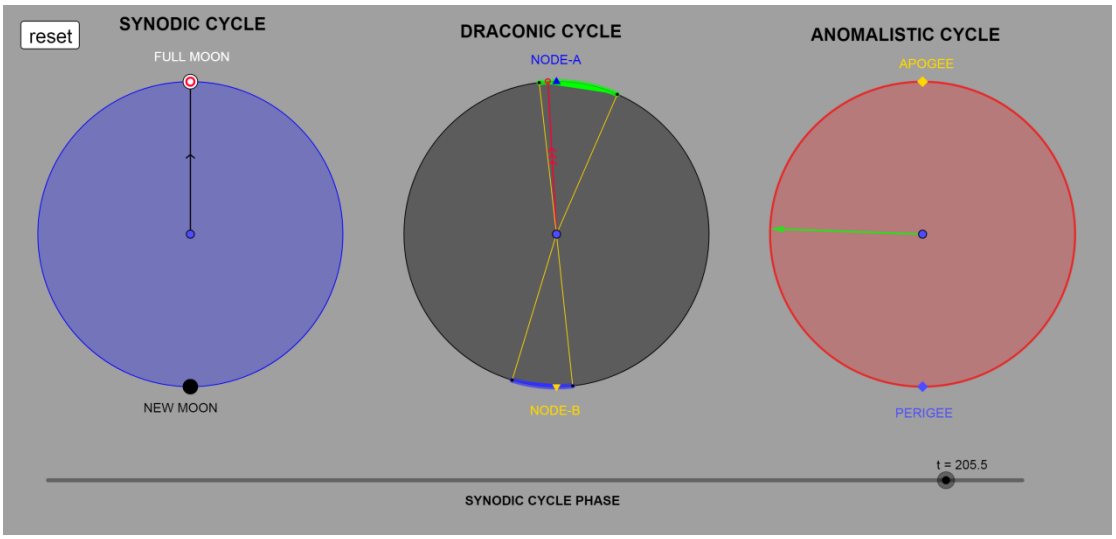

Figure A.68. Event 61. Cell 207/GƆ2: Lunar eclipse event (Σ).

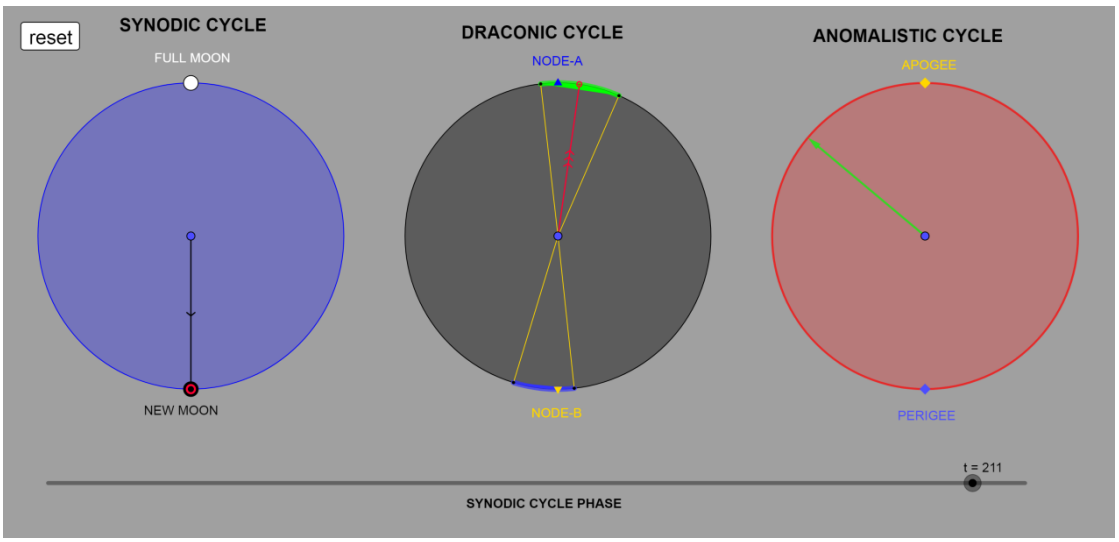

Figure A.69. Event 62. Cell 212/2̷ (A3): Solar eclipse event (H).

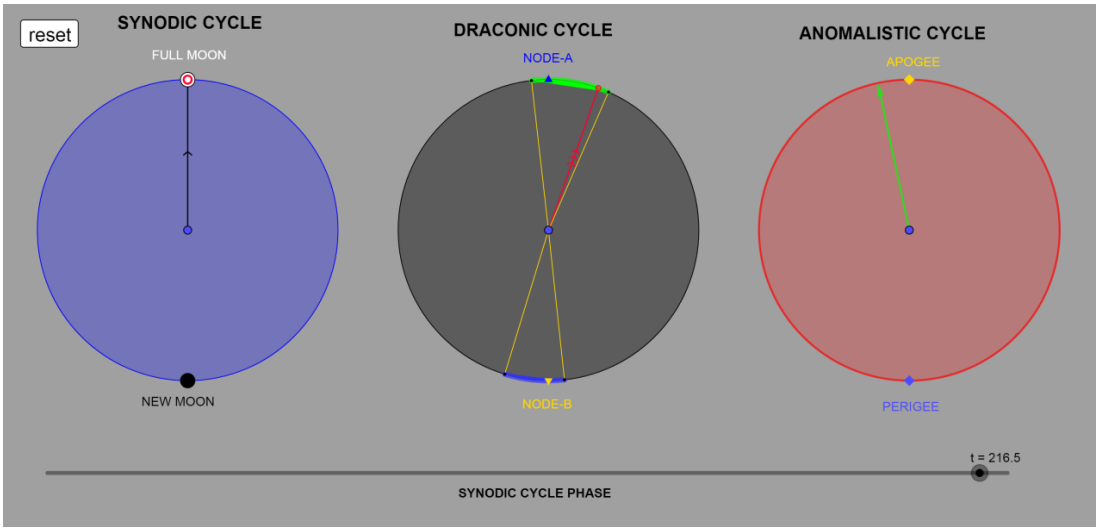

Figure A.70. Event 63. Cell 218/ß (B3): Lunar eclipse event (Σ). Full Moon close to ecliptic limit and at Apogee.

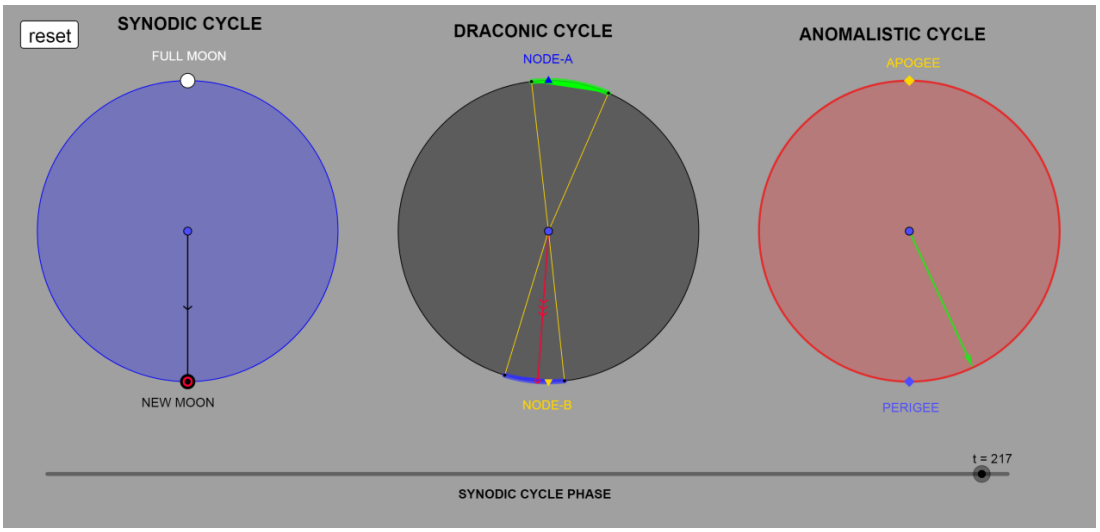

Figure A.71. Event 64. Cell 218/ß (B3): Solar eclipse event (H). New Moon close to Node-B.

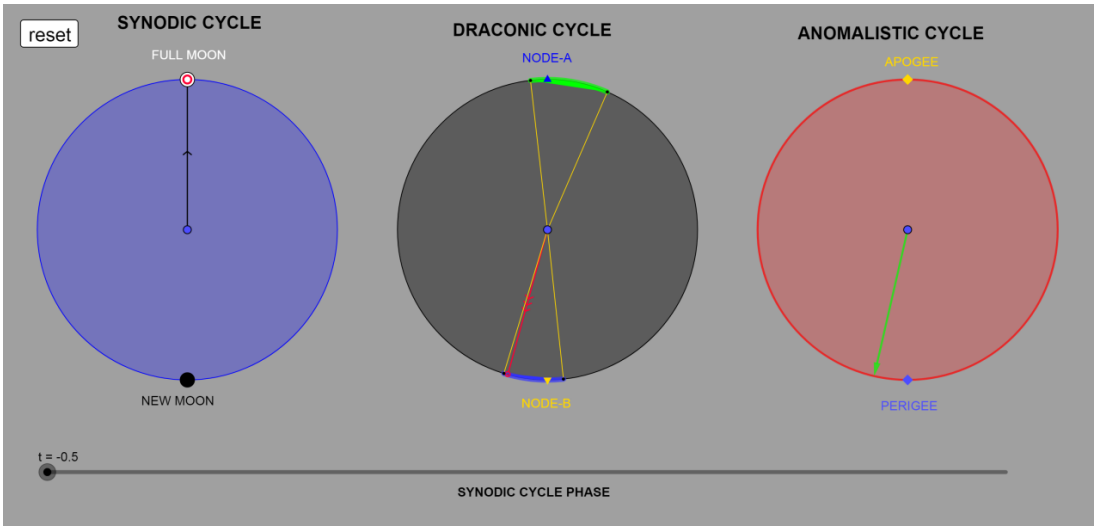

Figure A.72. Event V. Cell 01/A1/(Cell 224): *DracoNod* predicts a Lunar eclipse event (Σ). Full Moon close to the ecliptic limit. On Cell 112 (one Sar after Cell 01), is not engraved the solar eclipse event. It is doubtful if a lunar eclipse was engraved on Cell 01 (it could be a result of eccentricity error).

8. Eclipse event Statistics and Comments

Eclipse events, occurred just right on or too close to the ecliptic limit, present a high indeterminacy. Moreover, as result of the possible gear(s) eccentricities and the teeth un-uniformity, the final position of the Draconic pointer, or the Lunar pointer, or the Golden sphere pointer, may (slightly) differ than the ideal position, which was calculated via *DracoNod* program. Minor gear(s) imperfections affect and change the position of the Draconic pointer: sometimes the Draconic pointer is located out of the ecliptic window (therefore no eclipse event occurs), although it should be on the ecliptic window (an omitted eclipse event is created). Other times the Draconic pointer is located inside the ecliptic window (therefore an eclipse event occurs), although it should be out of the ecliptic limit (an additional eclipse event is created).

Table A1. Eclipse events summary calculated by DracoNod program.

***DracoNod* eclipse events prediction**	
Solar eclipse events on Cell:	**Lunar eclipse events on Cell:**
1, 7, 12, 24, 30, 36, 42, 48, 54, 59, 71, 77, 83, 89, 95, 106, 118, 124, 130, 136, 142, 153, 159, 165, 171, 177, 183, 200, 206, 212, 218 **(31 events)**	7, 13, 19, 25, 31, 42, 48, 54, 60, 66, 72, 78, 89, 95, 101, 107, 113, 119, 124, 130, 136, 142, 148, 154, 160, 171, 177, 183, 189, 195, 201, 207, 218 **(33 events)**
Lunar and Solar eclipse events in Cell:	
1(?), 7, 42, 48, 54, 89, 95, 101, 124, 130, 136, 142, 171, 177, 183, 189, 218	
Additional/omitted eclipse events	
Omitted event: Cell-65 non engraved event-predicted H, Pointer at the limit (indeterminacy or gearing error)	Additional event, Cell-130 Σ, engraved-not predicted, Pointer just out of limit (indeterminacy? or gearing error)
Omitted event: Cell-112 non engraved-predicted H, Pointer close to the limit (gearing error)	Omitted event: Cell-166 predicted Σ at limit (indeterminacy or gearing error), based on the preserved index numbering this event is not exists
Omitted Cell-189 non engraved-predicted H, Pointer at the limit (indeterminacy or gearing error)	Omitted event (?) Cell-01/(Cell-224) predicted Σ. It could be exist or not exist

DracoNod predicted all the preserved solar eclipses plus three additional eclipses which are non-engraved events and present high indeterminacy.

DracoNod predicted all the preserved lunar eclipses except one which presents high indeterminacy. Was also predicted one non-engraved eclipse which also presents high indeterminacy. The predicted lunar eclipse on cell 01 is doubtful if finally was real engraved.

Below, the omitted/additional Events I-V and Event 38 predicted by the *DracoNod* program are presented.

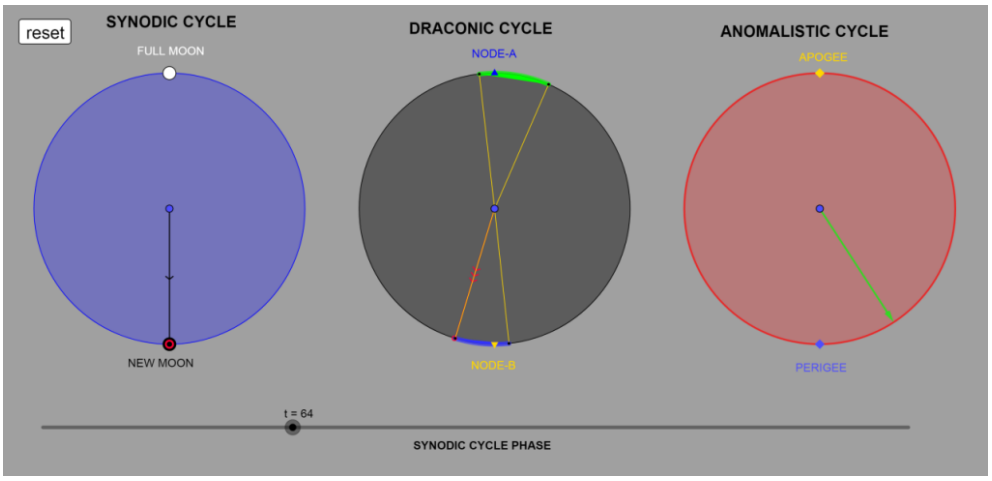

Figure A.73. Event I. Cell 65: New Moon just right on the ecliptic limit. Based on the events' index numbering it should be no engraved event. Indeterminacy or eccentricity error.

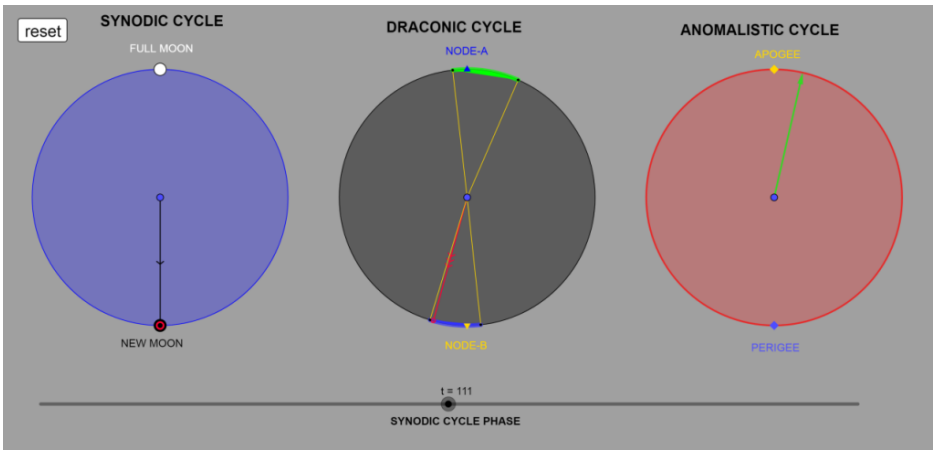

Figure A.74. Event II. Cell 112: Solar eclipse event (H). Calculated by the *DracoNod* program but is not an engraved event, according to the present sequence of the index letters. New Moon too close to the ecliptic limit. Indeterminacy or eccentricity error.

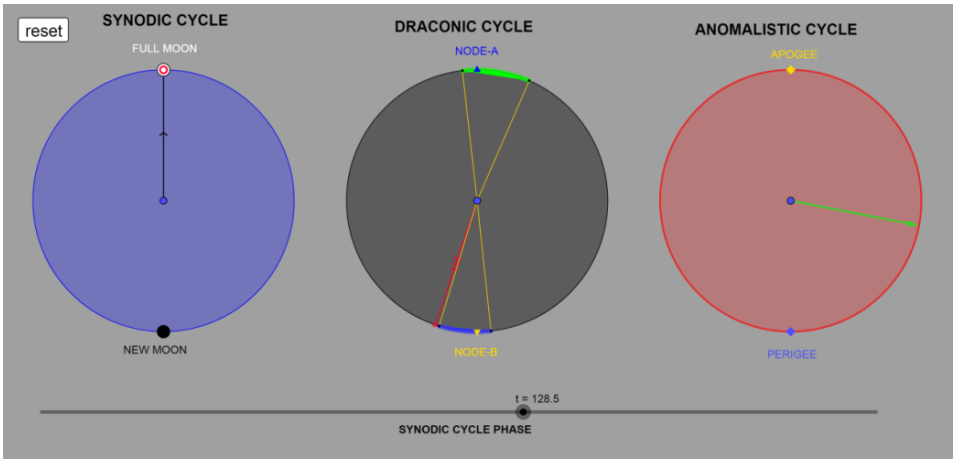

Figure A.75. Event 38. Cell 130/H2: engraved event Lunar eclipse-Σ, but according to *DracoNod* program no eclipse event: the Full Moon is just out of the ecliptic limit. Probably error of eccentricity.

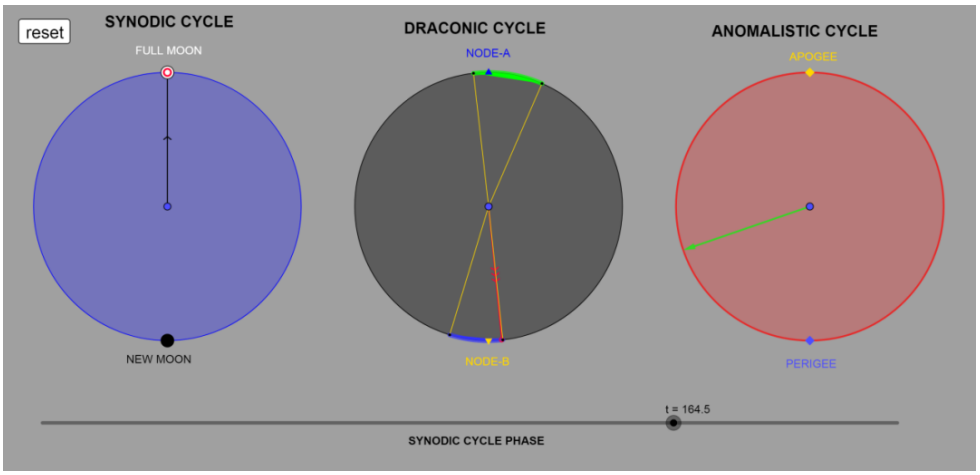

Figure A.76. Event III. Cell 166: *DracoNod* program predicts a Lunar eclipse. Full Moon just right on the ecliptic limit. Based on the events' index numbering, between cells 137 and 170 they should be 7 cells with events. Cell 166 is the 8th cell with event, and it is the only one event presenting high indeterminacy. Cell 166 is considered as cell without event.

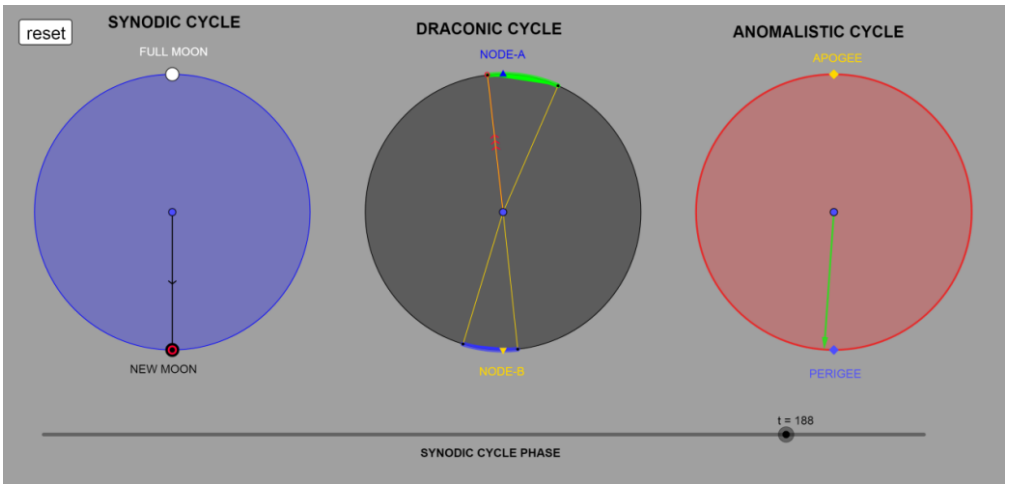

Figure A.77. Event IV. Cell 189: No engraved event. *DracoNod* program predicts a second event, a Solar eclipse. New Moon just right on the ecliptic limit. Indeterminacy or gearing errors.

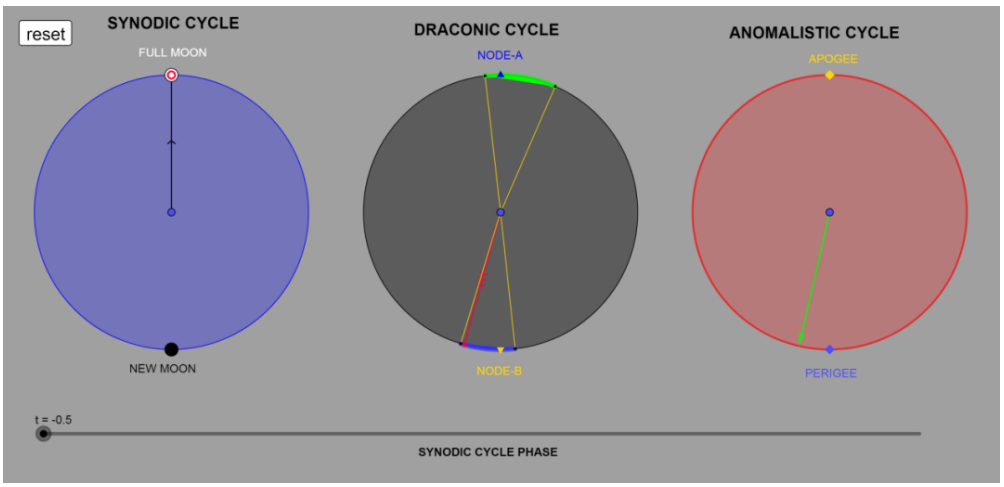

Figure A.78. Event V. Cell 01/Cell 224/A1: *DracoNod* predicts a Lunar eclipse event (Σ). Full Moon close to the ecliptic limit. On cell 112 (one Sar after Cell 01), is not engraved the solar eclipse event. Therefore, on Cell 01 could not be engraved the lunar eclipse event.

9. The Sar period (half Saros) of the Antikythera Mechanism

Dividing by two the equality of 223 Synodic months = 242 Draconic months = 239 Anomalistic months, the equality of the 111.5 Synodic months = 121 Draconic months = 119.5 Anomalistic months arises. Starting with the New Moon at Node-A and at Apogee, after 111.5 Synodic months, the Full Moon is located at the same Node-A and at Perigee. After a half Saros period, named Sar, the sequence of the eclipse events is repeated in inversed eclipse kind and distance (Neugebauer 1975; Voulgaris et al., 2021). Below, five pairs of eclipse events in time span of one Sar are presented [(Cell 01 A1/Solar – Cell 113 Γ2/Lunar), (Cell 07 B1/Lunar – Cell 118 Δ2/Solar), (Cell 19 E1/Lunar – Cell 130 H2/Solar), (Cell 101 Ω1/Lunar – Cell 212 ⅋/Solar, ⅋=A3), (Cell 107 B2/Lunar – Cell 218 ß /Solar, (ß=B3)]. The Moon is located at the same position relative to the same Node and symmetrically in inversed distance from the Earth.

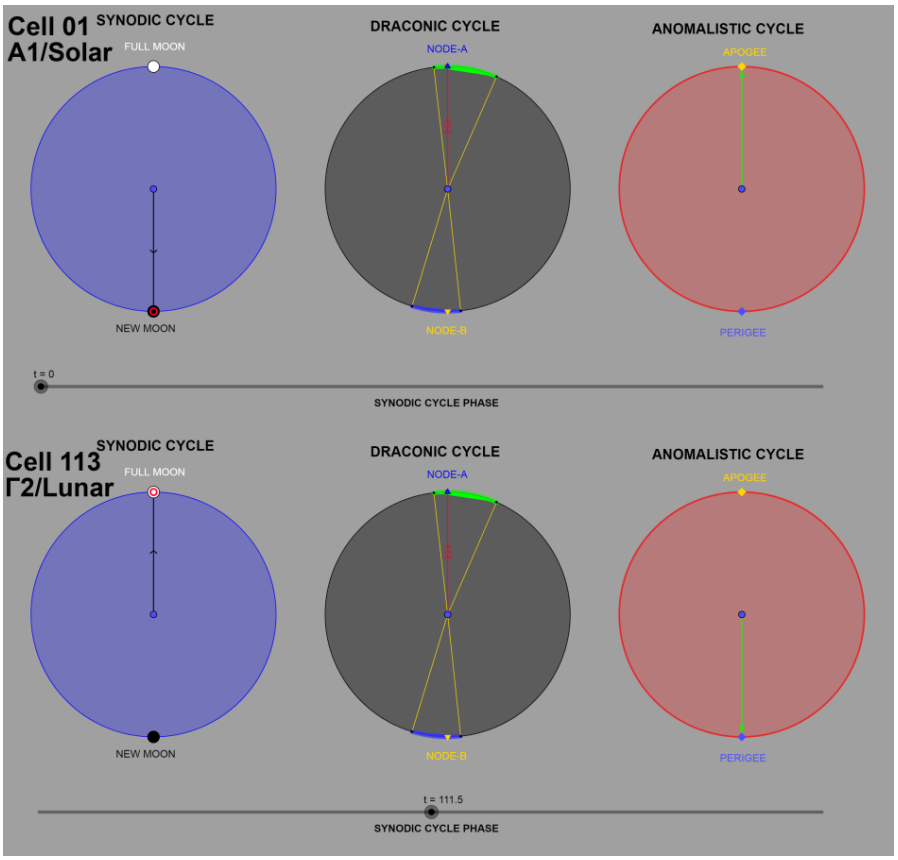

Figure A.79. Cell 01 A1/Solar – Cell 113 Γ2/Lunar.

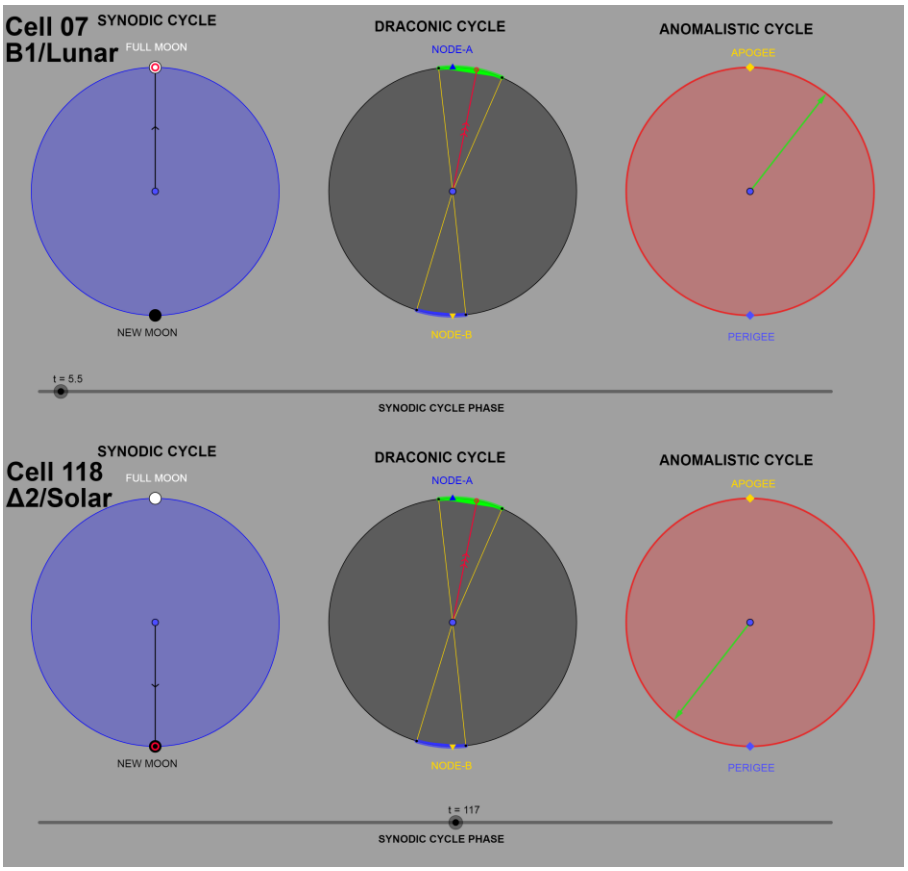

Figure A.80. Cell 07 B1/Lunar – Cell 118 Δ2/Solar.

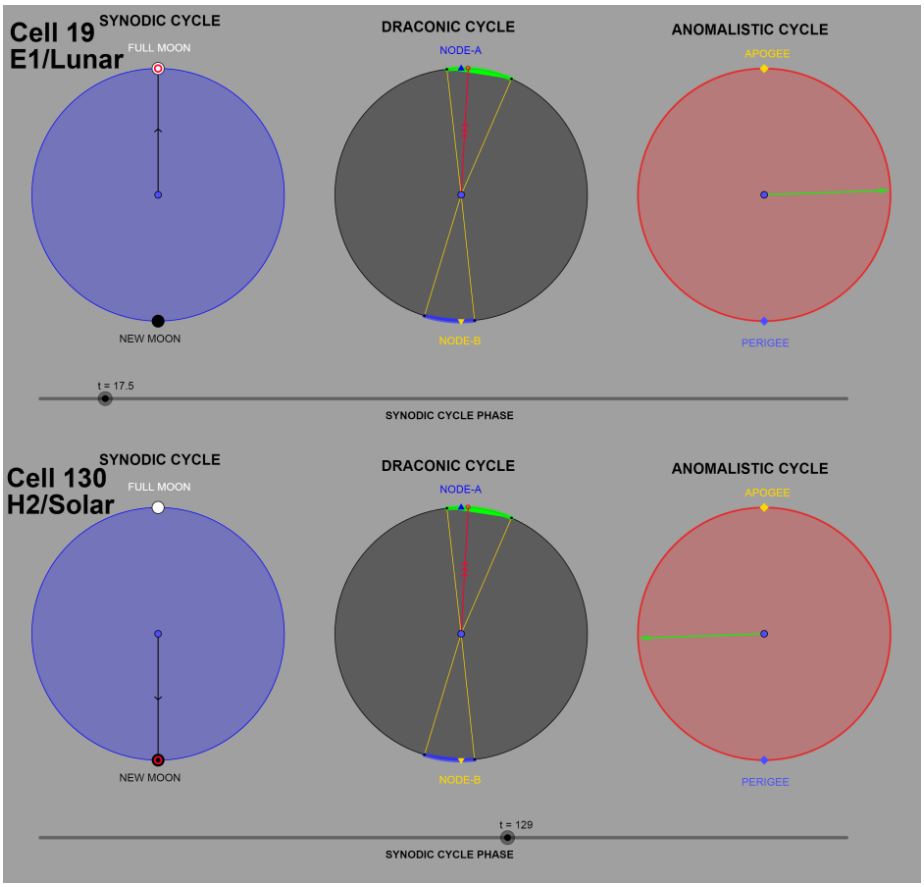

Figure A.81. Cell 19 E1/Lunar – Cell 130 H2/Solar.

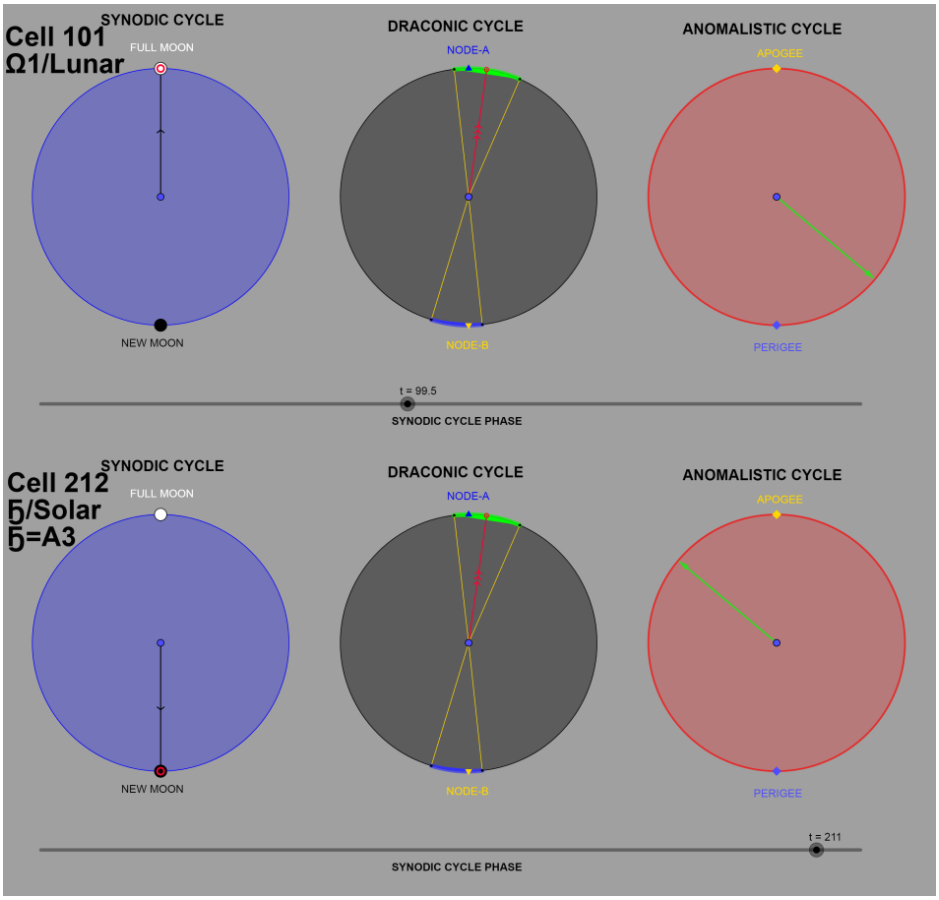

Figure A.82. Cell 101 Ω1/Lunar – Cell 212 Ƕ/Solar (Ƕ=A3).

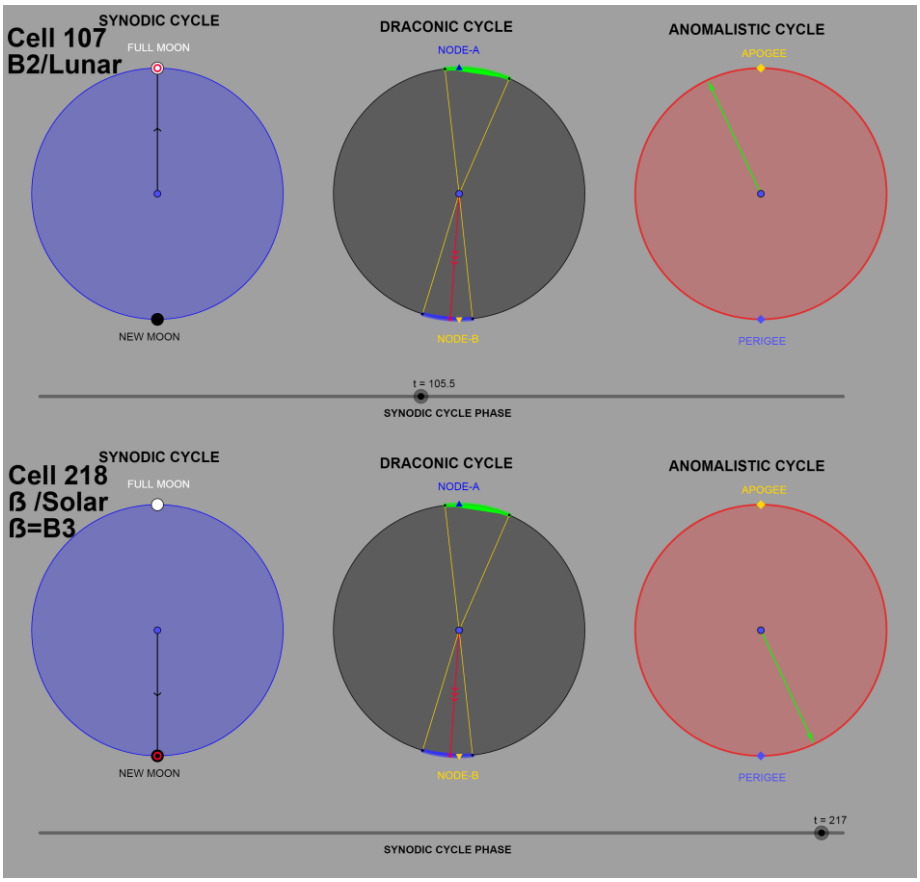

Figure A.83. Cell 107 B2/Lunar – Cell 218 ß /Solar (ß=B3).

10. Calculating the true (symmetrical) ecliptic limits of the Draconic scale

In order to find the actual symmetrical ecliptic limits (Green 1985; Smart 1949, p. 378), we attempted to detect the position of the 4 points (2 points ×2 ecliptic limits) placed on a circular perimeter-Draconic scale, so that the epicenter angles defined by the points, to present central symmetry. At the same time, the line connects the two Nodes (Line of Nodes) should be a diameter of the circle and the Nodes should be points on the perimeter of the Draconic scale.

The approximate solution was found in the graphic design environment with error ±0.5°: The symmetrical ecliptic limits, probably adopted from the ancient Manufacturer, might be:

- For the Ecliptic Window-A: –19.9° and +5.7° from Node-A (measured CCW).
- For the Ecliptic Window-B: –19.4° and +6.2° from Node-B (measured CCW).

The mean values for both of the Ecliptic Windows are 19.65° and 5.95°, approaching the values 20° and 6°.

This solution (which is not the only one that occurs) places the center of the Draconic scale/axis pointer about 4 mm lower to the initial center and exact on the Line of Nodes. The new center creates an eccentricity of the Draconic pointer relative to the Draconic scale.

Therefore, there are two options exist:

i) Symmetrical ecliptic limits and Draconic pointer with eccentricity,

ii) Asymmetrical ecliptic limits and Draconic pointer without eccentricity.

On both of the above options the prediction of the eclipse events sequence is (approximately) the same, but the second seems to be more realistic.

As the value of the eccentricity is relative high (4 mm), this result is the final resultant of some of parts' errors, mostly eccentricity (gears, shafts, scale, pointer, and also gear tooth).

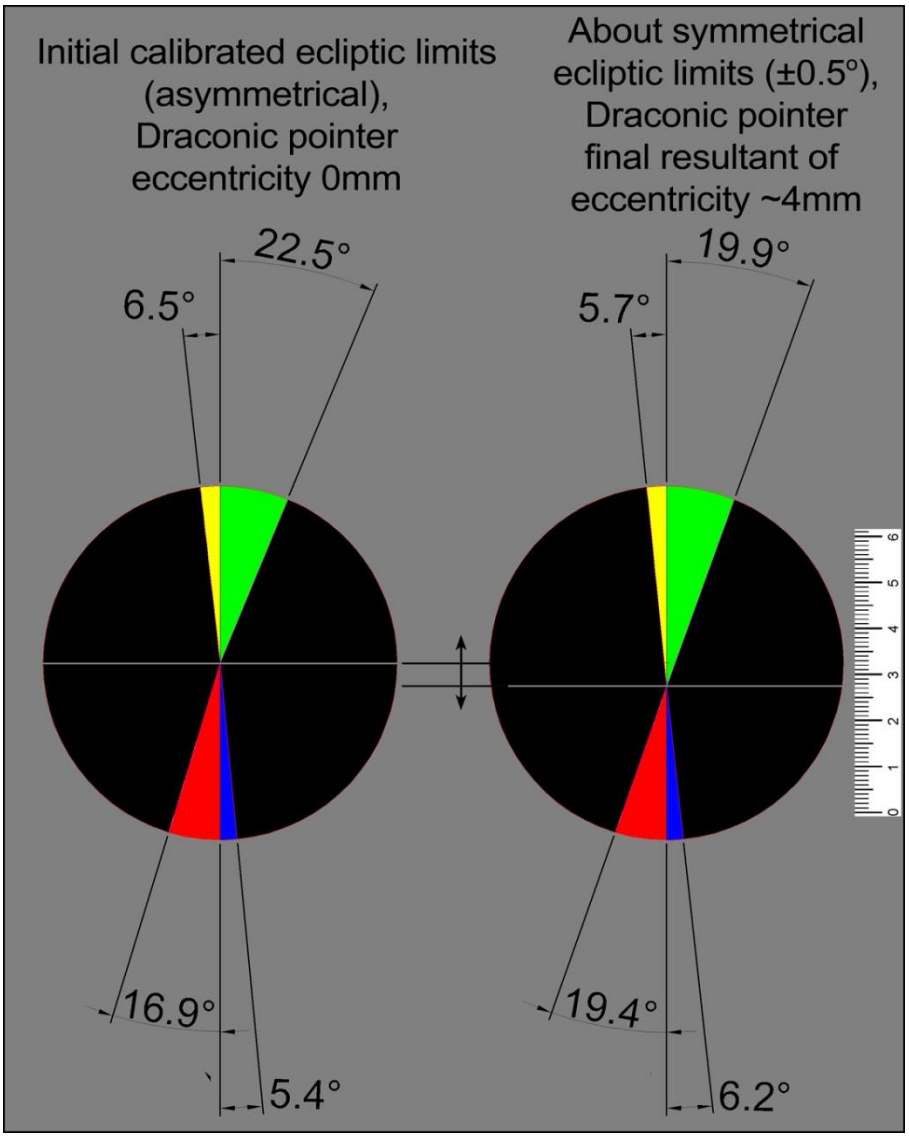

Figure A.84. A geometrical calculation in order to detect symmetrical ecliptic limits. The symmetrical ecliptic limits created by changing the center (Draconic pointer) of the circle (Draconic scale).

11. Changing *DracoNod* parameters

DracoNod program was designed for parameterization of several factors.

We can replace the general equality of the lunar cycles for one Saros for more precise values, using the values presented in NASA eclipse page, *Periodicity of solar eclipses, § 1.10 Secular Variations in the Saros and Inex,*

https://eclipse.gsfc.nasa.gov/SEsaros/SEperiodicity.html#section106, by Fred Espenak, NASA's GSFC.

For era 1 AD, it is valid that 223 Synodic months = 241.998703 Draconic months = 238.991950 Anomalistic months.

After running *DracoNod* program, the shifting of Node and the Apogee/Perigee positions per each Saros/Exeligmos time is visible.

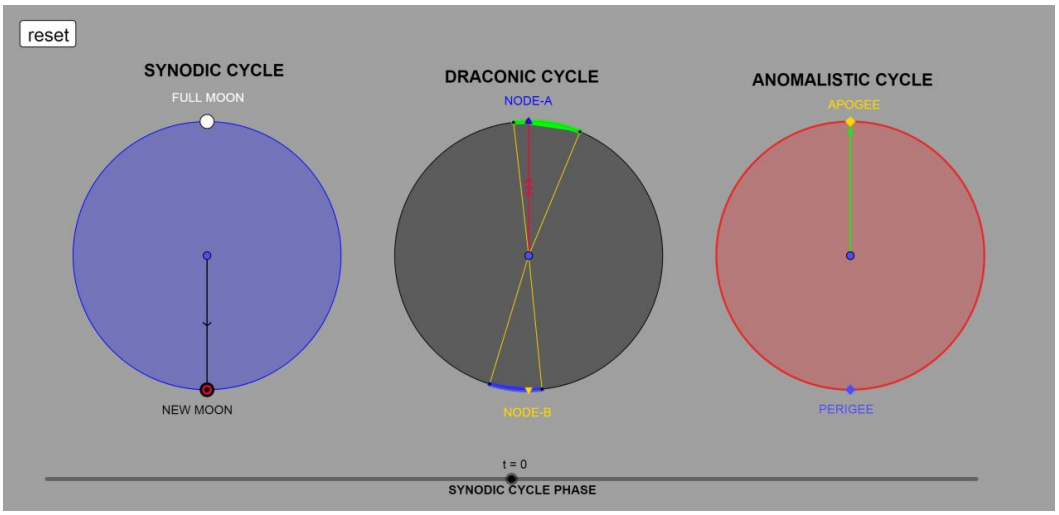

Figure A.85. Exeligmos/Saros 0. New moon at Node-A and at Apogee.

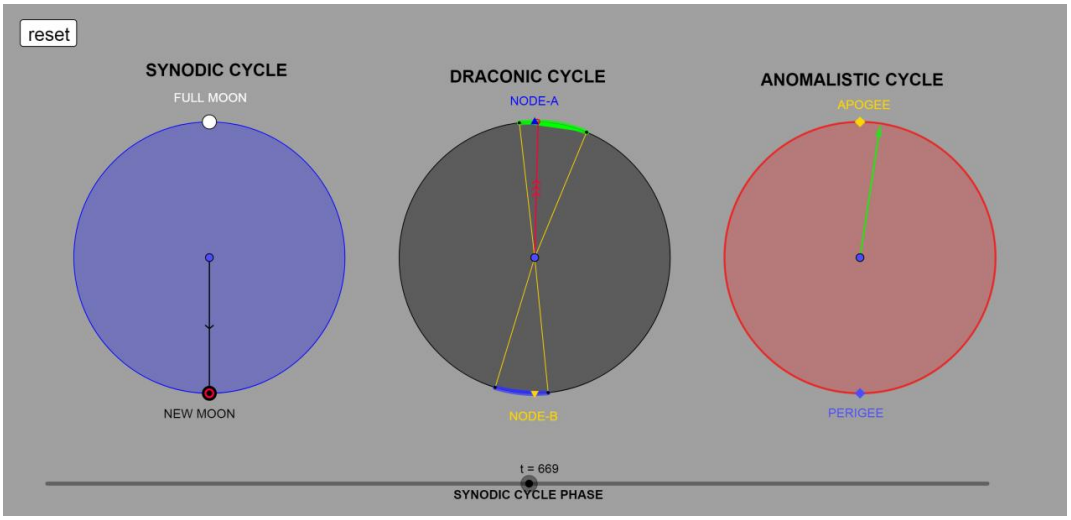

Figure A.86. After one Exeligmos/3 Saros.

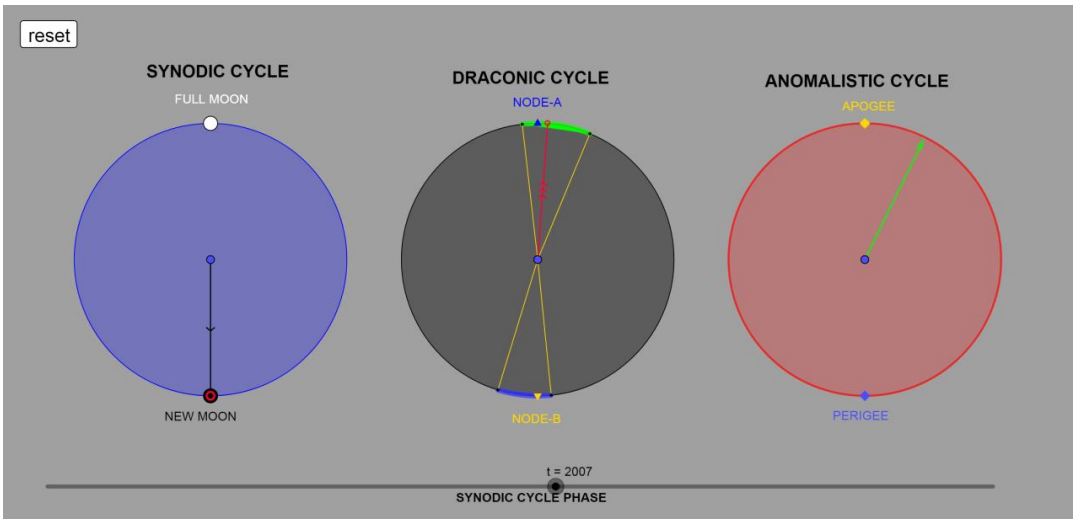

Figure A.87. After 3 Exeligmos/9 Saros.

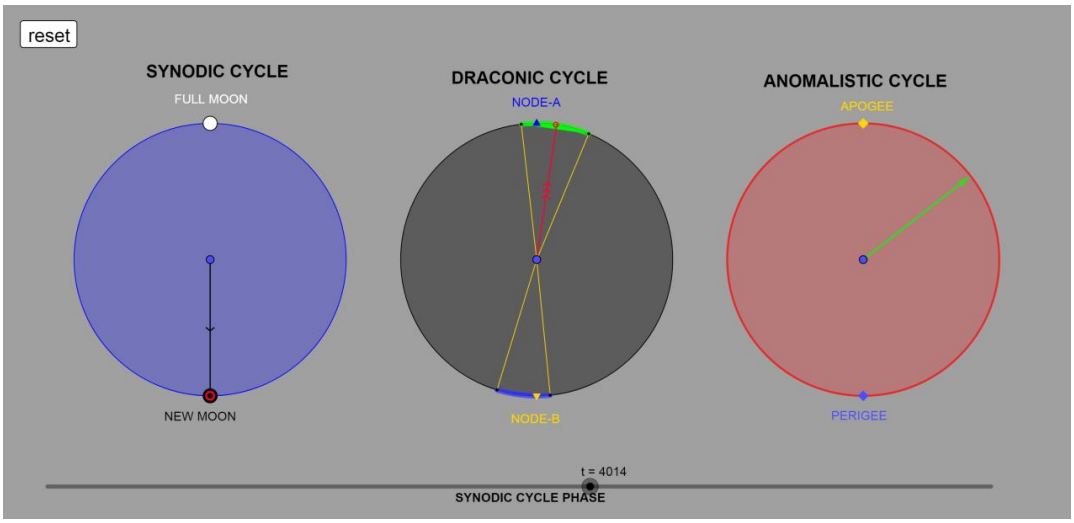

Figure A.88. After 6 Exeligmos/18 Saros.

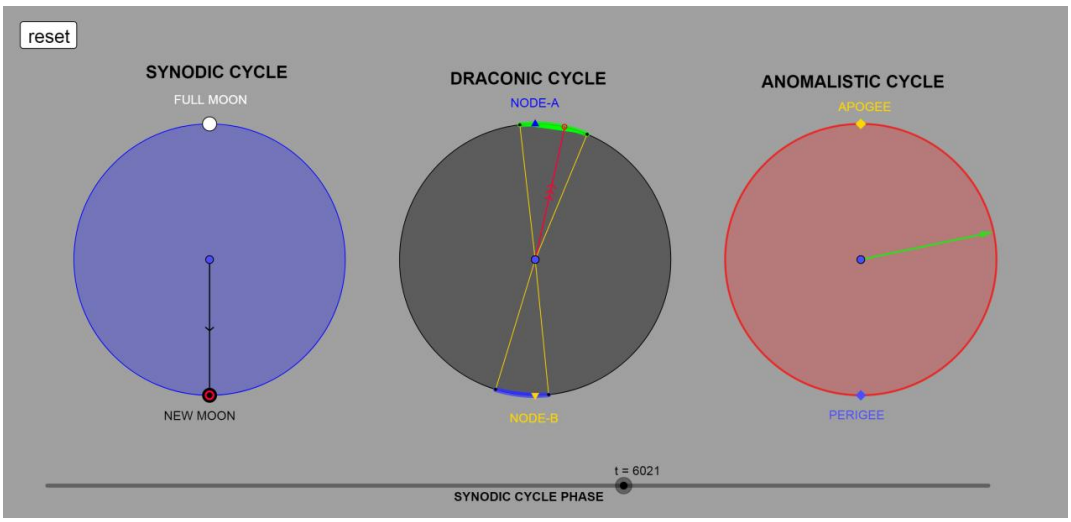

Figure A.89. After 9 Exeligmos/27 Saros.

In every Saros the position of the Moon continuously shifts relative to the Nodes and the Apogee/Perigee position, so the eclipse events are not perfectly repeated at the same geometrical position and the Saros period should be re-calculated during time (https://eclipse.gsfc.nasa.gov/SEsaros/SEsaroscat.html).

References

Anastasiou, M, Bitsakis, Y, Jones, A, Steele, JM & Zafeiropoulou, M 2016, 'The Back Dial and Back Plate Inscriptions' In Special Issue: The Inscriptions of the Antikythera Mechanism, *Almagest* vol. 71, pp. 138-215.

Antikythera Mechanism Research Project, http://www.antikythera-mechanism.gr.

Audacity, multi-track audio editor and recorder, viewed 21 May 2023, https://www.audacityteam.org/.

Bekker, I, Dindorf, L, Vogel, F & Fischer, K (Eds.) 1903-1906, *Diodorus Siculus*, *Bibliotheca Historica*, Teubner, Leipzig.

Bitsakis, Y & Jones, A 2016, 'The Back Cover Inscription' In Special Issue: The Inscriptions of the Antikythera Mechanism, *Almagest*, vol. 71, pp. 216-248.

Carman, C & Evans, J 2014, 'On the Epoch of the Antikythera Mechanism and Its Eclipse Predictor' *AHES*, vol. 68, pp. 693-774.

Espenak, F & Meeus, J 2009, 'Five Millennium Catalog of Solar Eclipses: -1999 to +3000 (2000 BCE to 3000 CE)', revised, NASA Tech. Pub. 2008-214170, NASA Goddard Space Flight Center, Greenbelt, Maryland (2008). Viewed 21 May 2023 https://eclipse.gsfc.nasa.gov/5MCSE/TP2009-214174.pdf.

Edmunds, MG 2011, 'An Initial Assessment of the Accuracy of the Gear Trains in the Antikythera Mechanism', *Journal for the History of Astronomy*, vol. 42, no. 3, pp.307-320.

Freeth, T 2014, 'Eclipse Prediction on the Ancient Greek Astronomical Calculating Machine Known as the Antikythera Mechanism', *PLoS ONE*, vol. 9, no. 7, e103275.

Freeth, T 2019, 'Revising the eclipse prediction scheme in the Antikythera mechanism' *Palgrave Communications*, vol. 5, pp. 1-12.

Freeth, T, Bitsakis, Y, Moussas, X, Seiradakis, JH, Tselikas, A, Mangou, H, Zafeiropolou, M, Hadland, R, Bate, D, Ramsey, A, Allen, M, Crawley, A, Hockley, P, Malzbender, T, Gelb, D, Ambrisco, W & Edmunds, MG 2006, 'Decoding the Ancient Greek Astronomical Calculator Known as the Antikythera Mechanism', *Nature*, vol. 444, pp. 587-591.

Freeth, T, Jones, A, Steele, JM & Bitsakis, Y 2008, 'Calendars with Olympiad Display and Eclipse Prediction on the Antikythera Mechanism', *Nature*, vol. 454, pp. 614-617 (Supplementary Material).

Gaylard, A, Meyer, A & Landy, C 1995, 'Acoustic evaluation of faults in electrical machines', *Seventh International Conference on Electrical Machines and Drives (Conf. Publ. No. 412)*, Durham, pp. 147-150.

GeoGebra for Teaching and Learning Math, viewed 6 June 2023, https://www.geogebra.org

Green, RM 1985, *Spherical Astronomy*, Cambridge University Press.

Heiberg, JL (ed.) 1898, *C. Ptolemy*, *Syntaxis Mathematica*, Teubner, Lipsiae.

Herrmann, KL 1922, 'Some causes of Gear-tooth errors and their detection', *SAE Transactions*, vol. 17, pp. 660-682.

Hecht, E 2015, *Optics* 5th Ed., Pearson Publications.

Iversen, P & Jones, A 2019, 'The Back Plate Inscription and eclipse scheme of the Antikythera Mechanism revisited', *Archive for History of Exact Sciences*, vol. 73, pp. 469-511.

Jones, A 1990, 'Ptolemy's First Commentator', *Transactions of the American Philosophical Society*, vol. 80, pp. i-vi+1-61.

Jones, A 2020, 'The Epoch Dates of the Antikythera Mechanism', *ISAW Papers*, vol. 17.

Kennard, T 1923. 'A Simple Explanation of Eclipses', *Pomona College Astronomical Society*, vol. 8, pp.4-6.

Kircher, A 1646, '*Ars Magna Lucis et Umbrae in Decem Libros Digesta'*, Sumptibus Hermanni Scheus ; Ex typographia Ludouici Grignani, Romæ, viewed 4 June 2023, https://ia600100.us.archive.org/16/items/athanasiikirche00kirc/athanasiikirche00kirc.pdf

Korpel, A 1968, 'Acoustic imaging and holography', *IEEE Spectrum*, vol. 5, pp. 45-52.

Manitius, C (ed.) 1898, *Gemini Elementa Astronomiae*, Teubner, Leipzig.

Mommsen, T (ed.) 1864, *Pindari Carmina*. Apud Weidmannos, Berolini.

Muffly, G 1923, 'Gear grinding and Tooth-forms', *SAE Transactions*, vol. 18, pp. 568-612.

NASA Eclipse Web Site, 'Index to catalog of Saros series of solar eclipses', by Fred Espenak, NASA GSFC Emeritus, viewed 29 May 2023, https://eclipse.gsfc.nasa.gov/SEsaros/SEsaroscat.html,

NASA Eclipse Web Site, Lunar Eclipses 'Eclipse Predictions', by Fred Espenak, NASA GSFC Emeritus, viewed 6 June 2023 https://eclipse.gsfc.nasa.gov/LEplot/LEplot2001/LE2020Jan10N.pdf

NASA Eclipse catalogue, Catalogue of solar eclipses, viewed 6 June 2023, https://eclipse.gsfc.nasa.gov/SEsaros/SEperiodicity.html#section106 https://eclipse.gsfc.nasa.gov/SEcatmax/SE-3999-6000MaxA.html https://eclipse.gsfc.nasa.gov/SEcat5/SEcatalog.html, https://eclipse.gsfc.nasa.gov/SEcat5/SE-0199--0100.html, https://eclipse.gsfc.nasa.gov/SEcat5/SE-0099-0000.html, https://eclipse.gsfc.nasa.gov/SEsaros/SEsaros058.html, https://eclipse.gsfc.nasa.gov/SEgoogle/SEgoogle2001/SE2027Aug02Tgoogle.html,

NASA Eclipse catalogue World Atlas of Solar Eclipse Paths, viewed 6 June 2023, https://eclipse.gsfc.nasa.gov/SEatlas/SEatlas-1/SEatlas-0179.GIF

NASA, Solar Eclipse page, glossary of solar eclipse terms, viewed 6 June 2023, https://eclipse.gsfc.nasa.gov/SEhelp/SEglossary.html

NASA, Eclipses and the Saros, viewed 6 June 2023, https://eclipse.gsfc.nasa.gov/SEsaros/SEsaros.html

NASA eclipse page, Periodicity of solar eclipses, by Fred Espenak, NASA's GSFC, § 1.10 Secular Variations in the Saros and Inex, viewed 6 June 2023, https://eclipse.gsfc.nasa.gov/SEsaros/SEperiodicity.html#section106

Neugebauer, O 1975, *A History of Ancient Mathematical Astronomy*, Springer-Verlag, Berlin, New York.

Pasachoff, JM, Lockwood, C, Meadors, E, Yu, R, Perez, C, Peñaloza-Murillo, MP, Seaton, DB, Voulgaris, A, Dantowitz, R, Rušin, V, Economou, T 2018, 'Images and Spectra of the 2017 Total Solar Eclipse Corona From Our Oregon Site', *Frontiers in Astronomy and Space Sciences*, vol. 5, pp. 1-6.

PHD2 Guiding Project, guiding software for telescopes, viewed 21 May 2023, https://openphdguiding.org/

PHD2 Log Viewer, visualization of the guiding performance, viewed 21 May 2023, https://openphdguiding.org/phd2-log-viewer/

Perrottet, T 2004, *The Naked Olympics: The True Story of the Ancient Games*, Random House Digital, Inc.

Python, programming language, viewed 6 June 2023, https://www.python.org/about/

Radio Sky Pipe, An Internet Enabled Strip Chart Recorder, viewed 21 May 2023, https://www.radiosky.com/skypipeishere.html

Robertson, N 2010, *Religion and Reconciliation in Greek Cities: The Sacred Laws of Selinus and Cyrene*, Society for Classical Studies American Classical Studies, Vol. 54.

Smart, WM 1949, *Textbook on Spherical Astronomy*, Cambridge University Press.

Spandagos, E (ed.) 2002, *Gemini Elementa Astronomiae*, (in Greek), Aithra, Athens.

Spectrum Lab, Audio Spectrum Analyzer, viewed 21 May 2023, https://www.qsl.net/dl4yhf/spectra1.html

Stephenson, FR, Morrison, LV & Hohenkerk, CY 2020, 'Astronomical dating of seven Classical Greek eclipses', *Journal of Astronomical History and Heritage*, vol. 23, no. 1, pp. 47-62.

Tavner, PJ 2008, 'Review of condition monitoring of rotating electrical machines', *IET Electrical Power Applications*, vol. 2, pp. 215-247.

Toomer, GJ 1984, *Ptolemy's Almagest*, Duckworth Classical, Medieval and Renaissance Editions, London.

Vanidhis, E 2022, *Optics Lessons: Geometrical Optics* (in Greek), Thessaloniki, Personal Edition, viewed 6 June 2023,
http://users.auth.gr/vanidhis/books.html

van Riesen, D, Schlensok, C, Henrotte, F & Hameyer, K, 2006 'Acoustic measurement for detecting manufacturing faults in electrical machines', *17th International Conference on Electrical Machines ICEM*.

Vaughan, V 2002, *The Origin of the Olympics: Ancient Calendars and the Race Against Time*, One Reed Publications, Massachusetts, viewed 4 June 2023,
https://www.onereed.com/articles/vvf/olympics.html.

Voulgaris, A, Vossinakis, A & Mouratidis C 2018a, 'The New Findings from the Antikythera Mechanism Front Plate Astronomical Dial and its Reconstruction' *Archeomatica International*, Special Issue vol. 3 pp. 6-18, viewed 21 May 2023,

https://www.yumpu.com/en/document/view/59846561/archeomatica-international-2017.

Voulgaris, A, Mouratidis, C & Vossinakis, A 2018b, 'Conclusions from the Functional Reconstruction of the Antikythera Mechanism', *Journal for the History of Astronomy*, vol. 49, pp. 216-238.

Voulgaris, A, Vossinakis, A & Mouratidis, C 2018c, 'The Dark Shades of the Antikythera Mechanism', *Journal of Radioanalytical and Nuclear Chemistry*, vol. 318, pp. 1881-1891.

Voulgaris, A, Mouratidis, C & Vossinakis, A 2019a, 'Ancient Machine Tools for the Construction of the Antikythera Mechanism parts', *Digital Applications in Archaeology and Cultural Heritages Journal*, vol. 13, pp. 1-12.

Voulgaris, A, Mouratidis, C & Vossinakis, A 2019b, 'Simulation and Analysis of Natural Seawater Chemical Reactions on the Antikythera Mechanism', *Journal of Coastal Research*, vol. 35, pp. 959-972.

Voulgaris, A, Mouratidis, C, Vossinakis A & Bokovos, G 2021, 'Renumbering of the Antikythera Mechanism Saros cells, resulting from the Saros spiral Mechanical Apokatastasis', *Mediterranean Archaeology and Archaeometry*, vol. 21, pp. 107-128.

Voulgaris, A, Mouratidis, C & Vossinakis, A 2022, 'The Draconic gearing of the Antikythera Mechanism: Assembling the Fragment D, its role and operation', *Mediterranean Archaeology and Archaeometry*, vol. 22, pp. 103-131.

Voulgaris, A, Mouratidis, C & Vossinakis, A 2023a, 'The Initial Calibration Date of the Antikythera Mechanism after the Saros spiral mechanical Apokatastasis', *Almagest* (in press).

Voulgaris, A, Mouratidis, C & Vossinakis, A *, 'The Antikythera Mechanism Eclipse events classification, applying the Draconic gearing', under writing.

Wright, MT 2006, 'The Antikythera Mechanism and the Early History of the Moon-Phase Display', *Antiquarian Horology*, vol. 29(3), 319-329.